



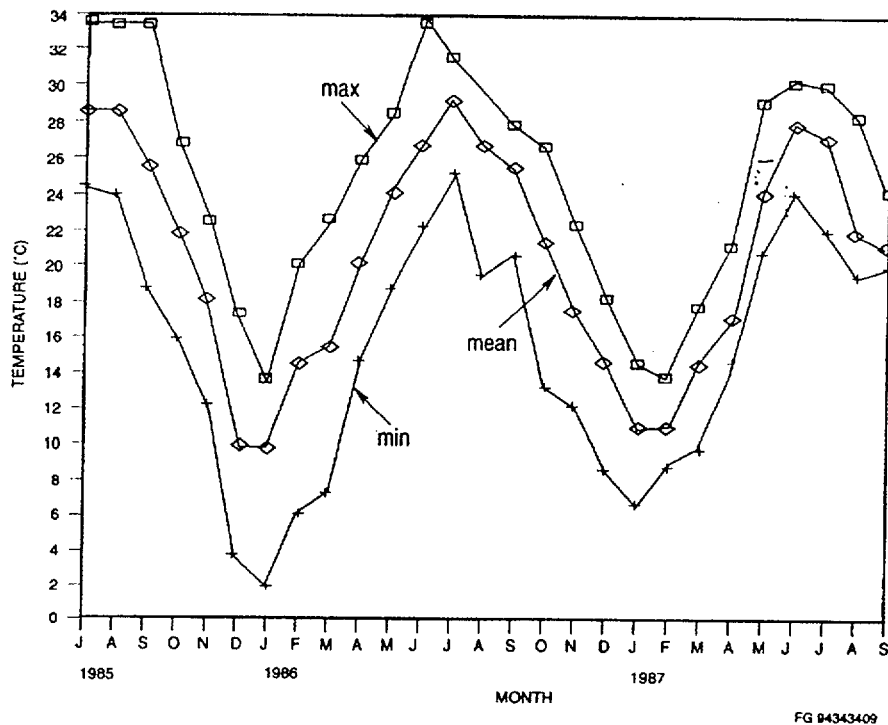
Figure 1.4-14 Savannah River Basin

001



Figure 1.4-15 Savannah River Basin Dams Upstream of SRS

COJ



FG 94343409

(Note: Figure 1.4-17 is intentionally omitted.)

Figure 1.4-16 Monthly Range and Mean Water Temperature of Fourmile Branch for June 1985 Through September 1987

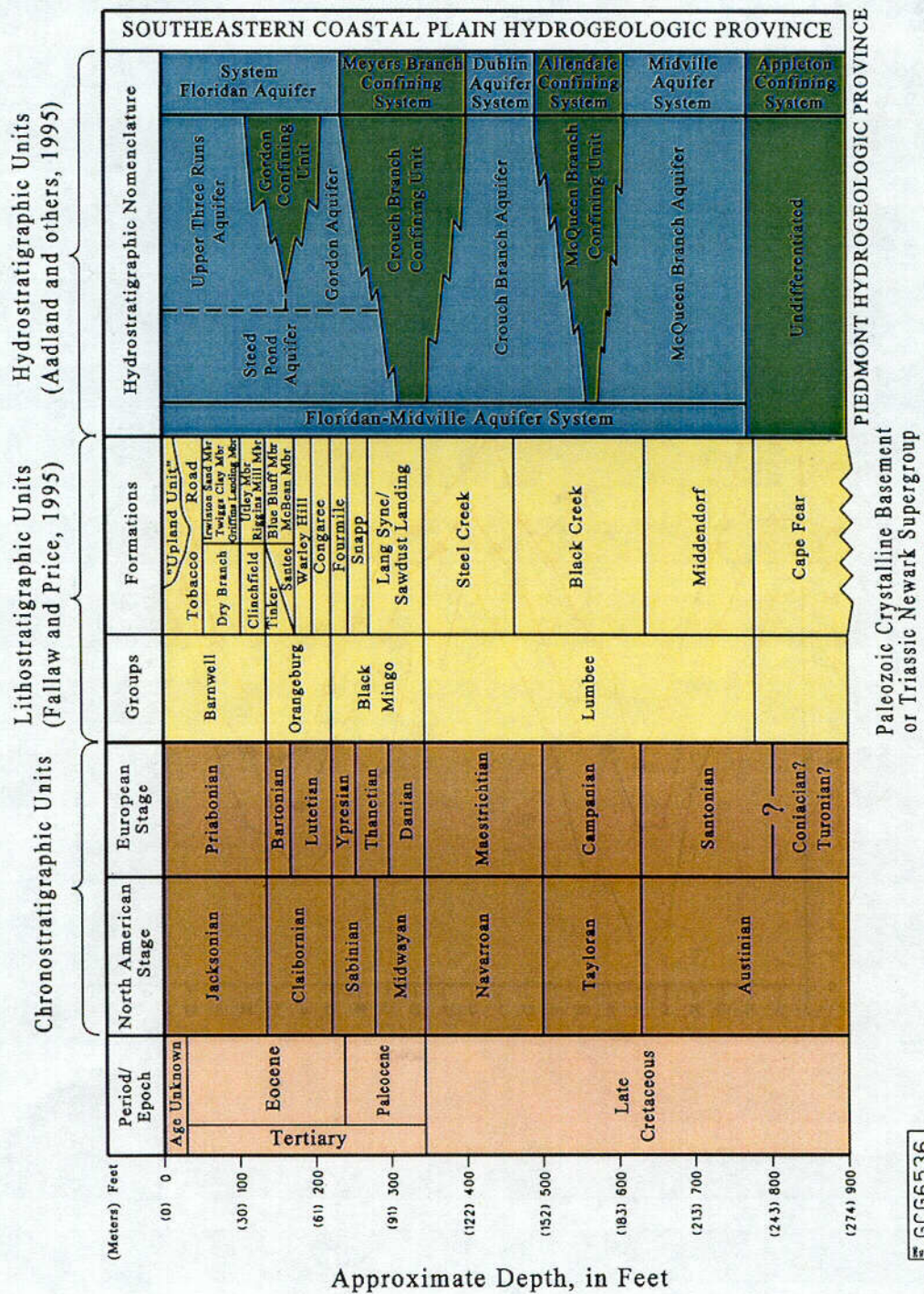


Figure 1.4-18. Comparison of chronostratigraphic, lithostratigraphic, and hydrostratigraphic units in the SRS region.

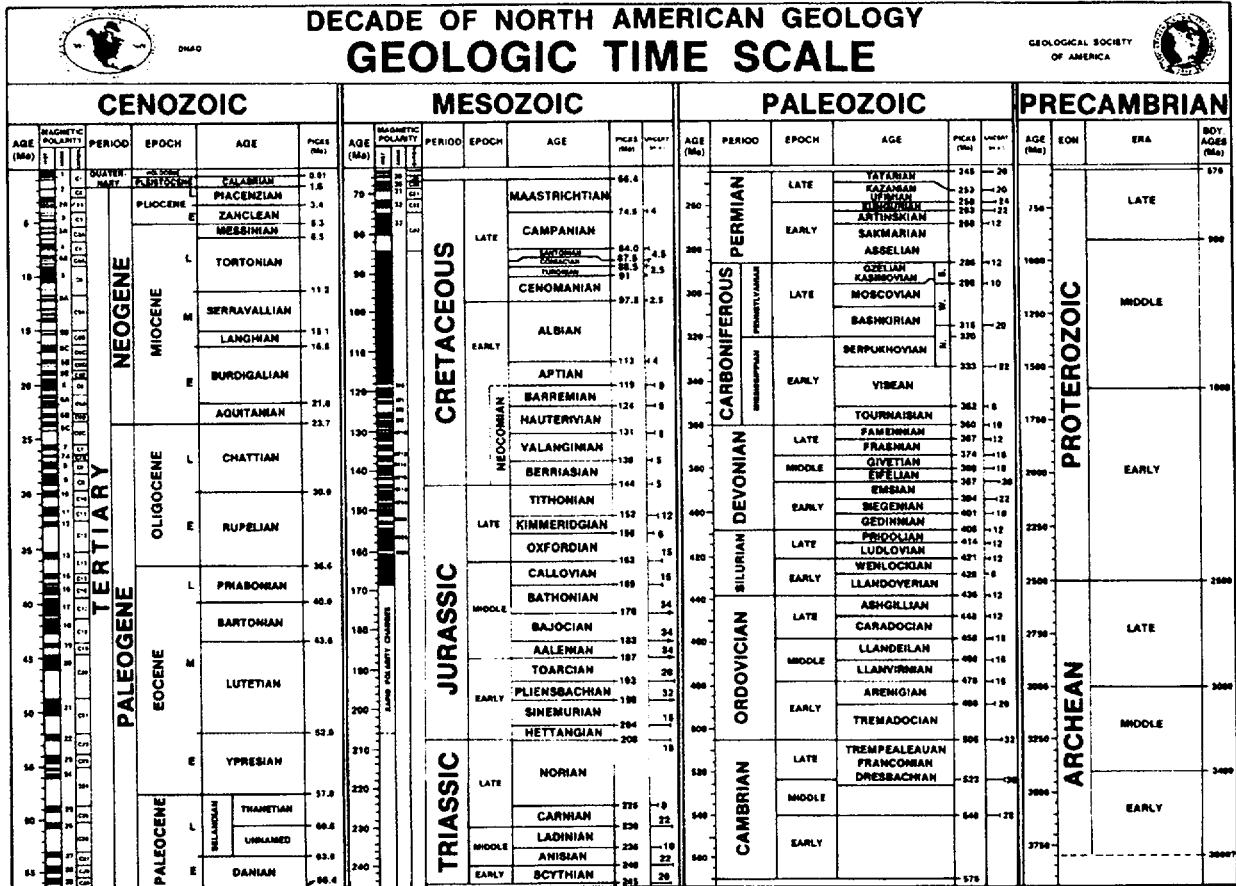


Figure 1.4-19. Geologic time scale. Decade of North American Geology, (1998).

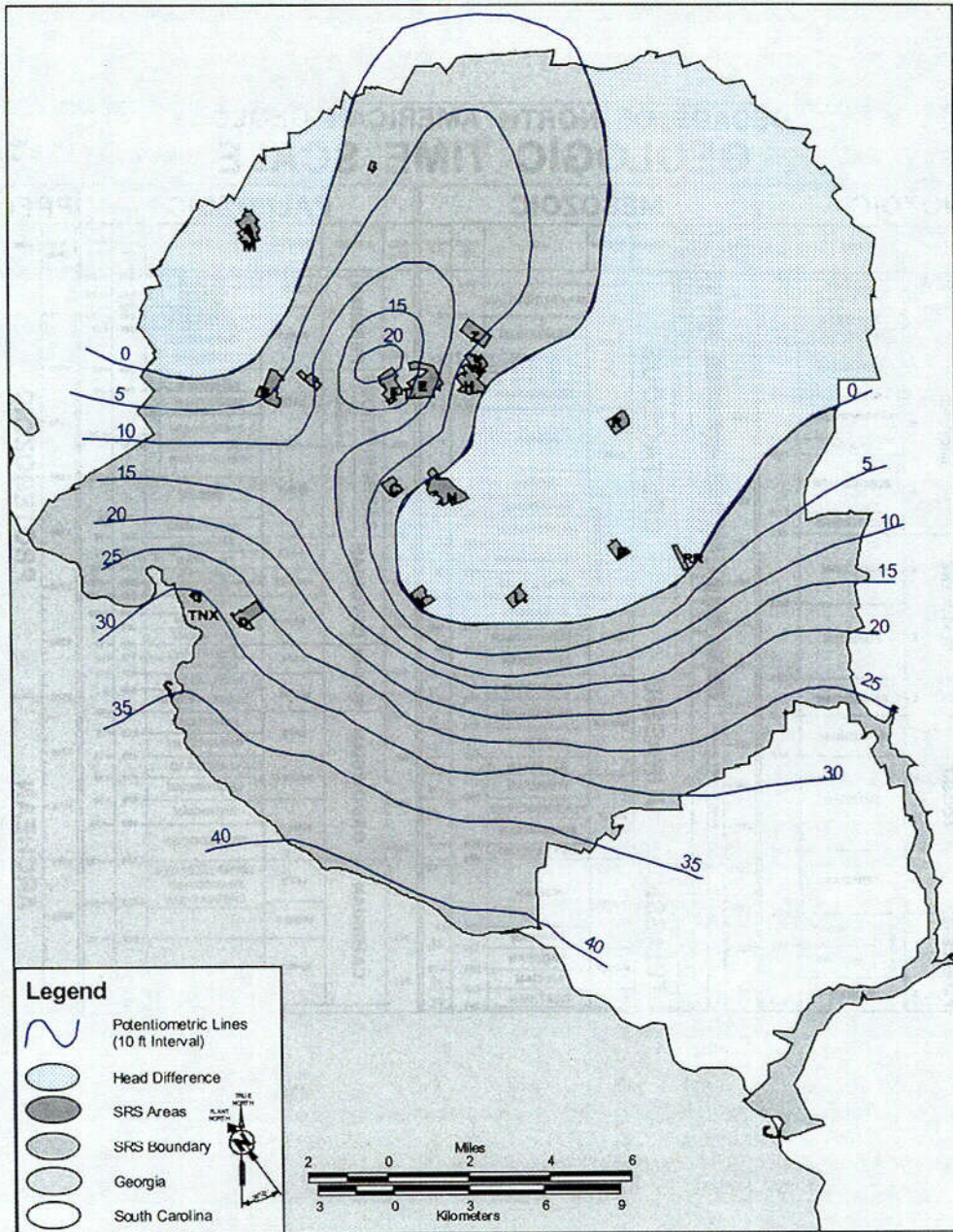


Figure 1.4-20. Hydraulic head difference across the Crouch Branch confining unit, July 1990 (modified from Bledsoe et al., 1990).

C04

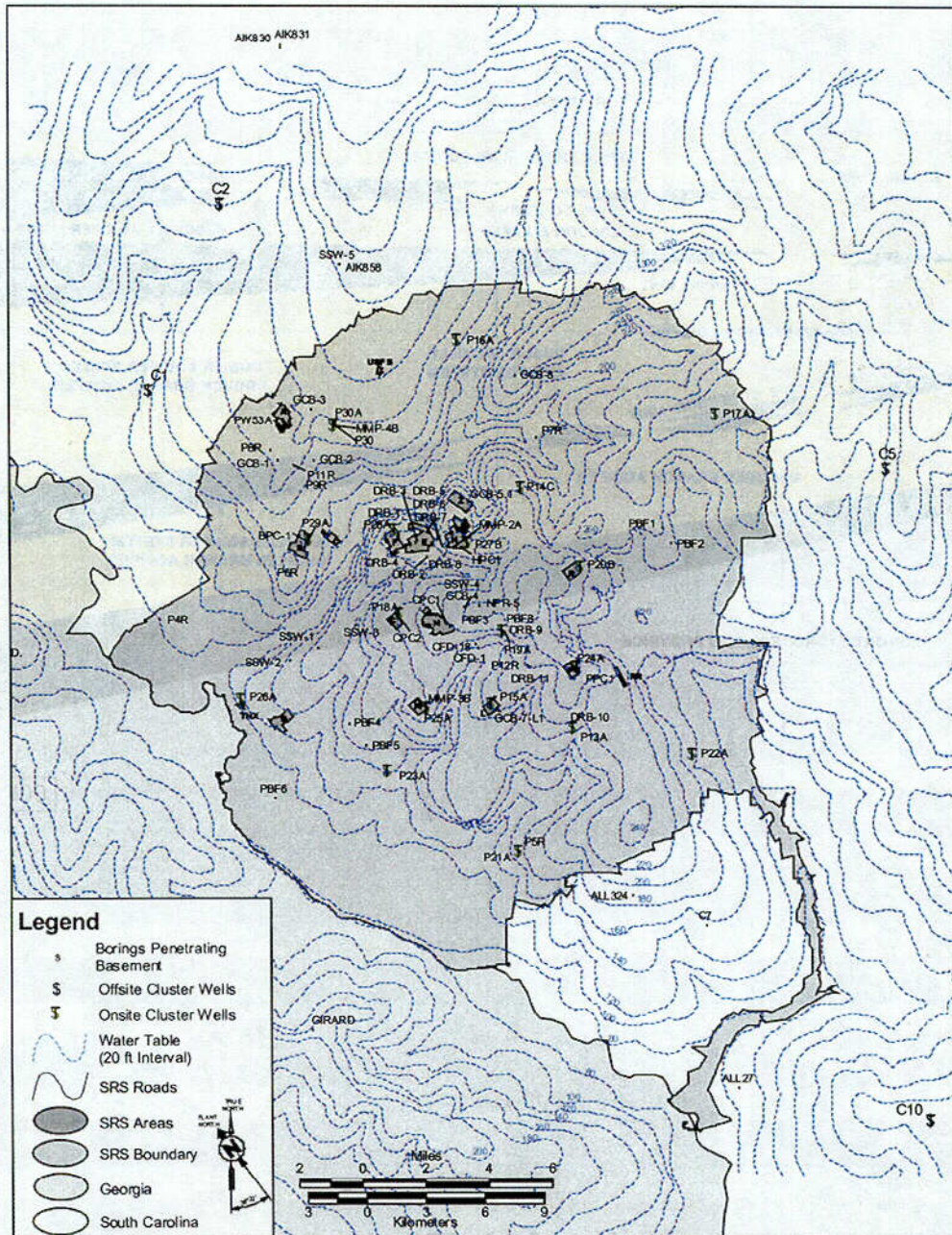


Figure 1.4-21. Location of type and reference wells for hydrostratigraphic units at SRS.

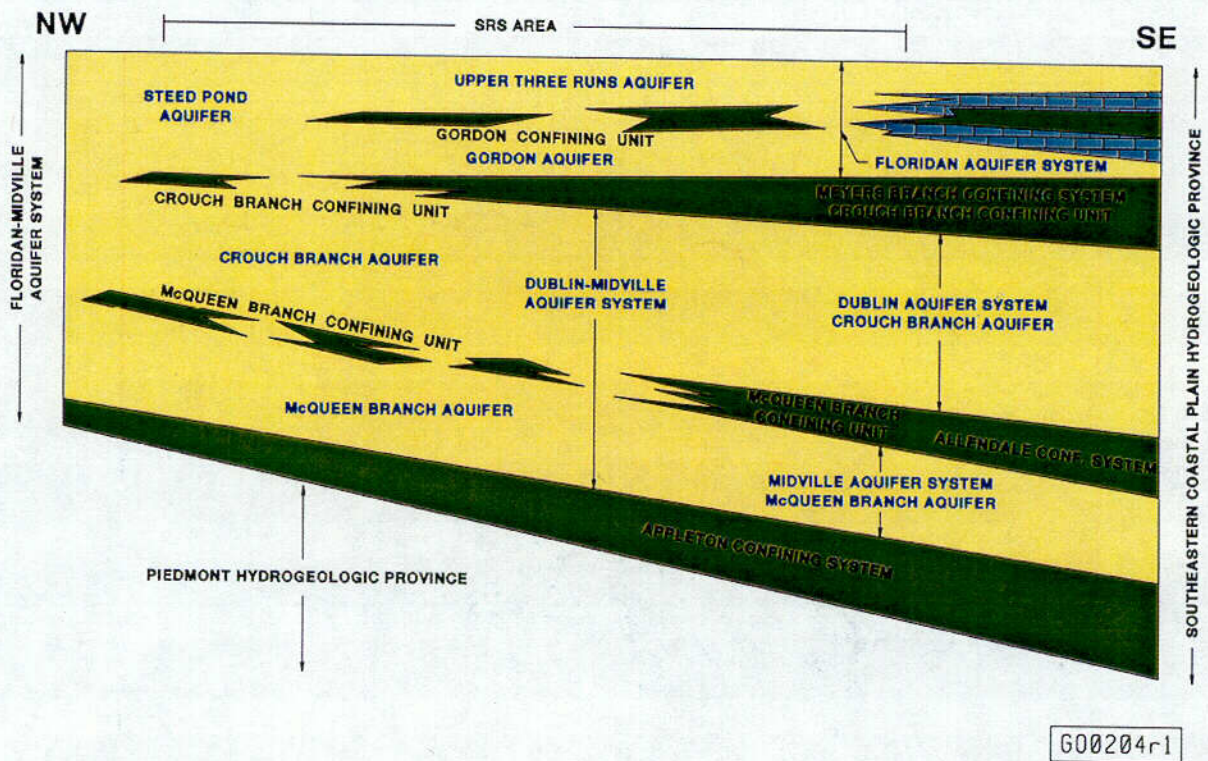


Figure 1.4-22. Hydrogeologic nomenclature for the SRS region.

Cole

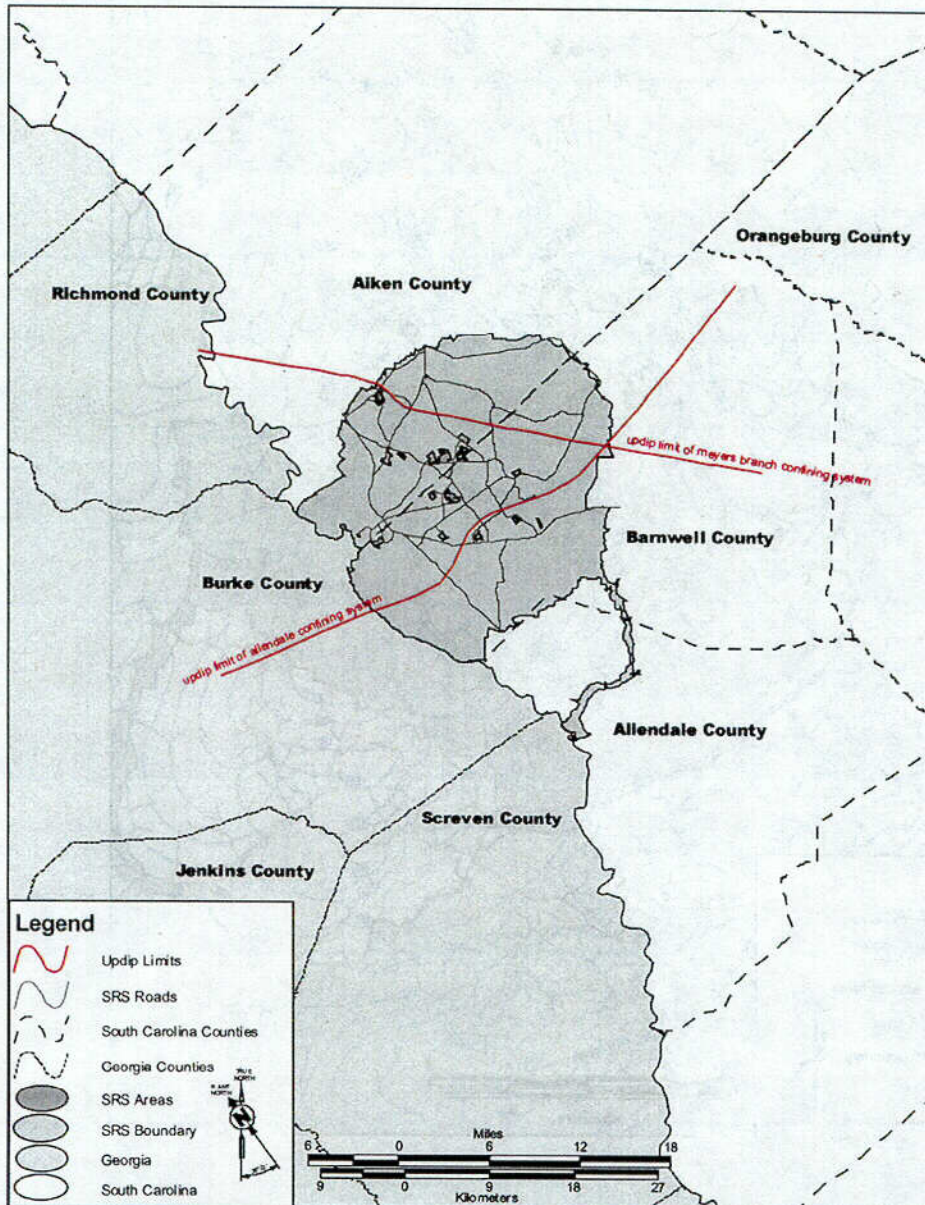


Figure 1.4-23. Location of aquifer and confining systems in the SRS region.

C07

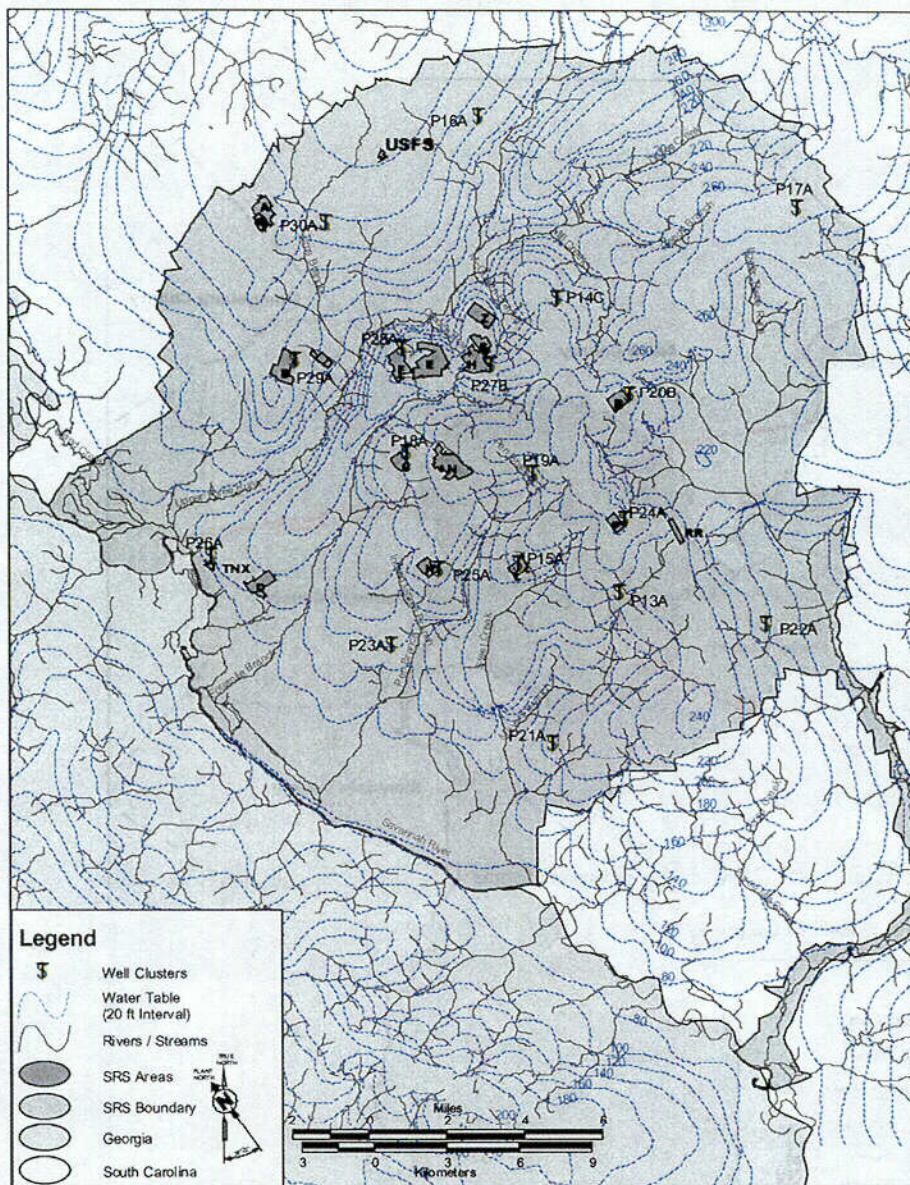


Figure 1.4-24. Potentiometric surface of the Upper Three Runs/Steed Pond aquifers, 1998 (water table map).

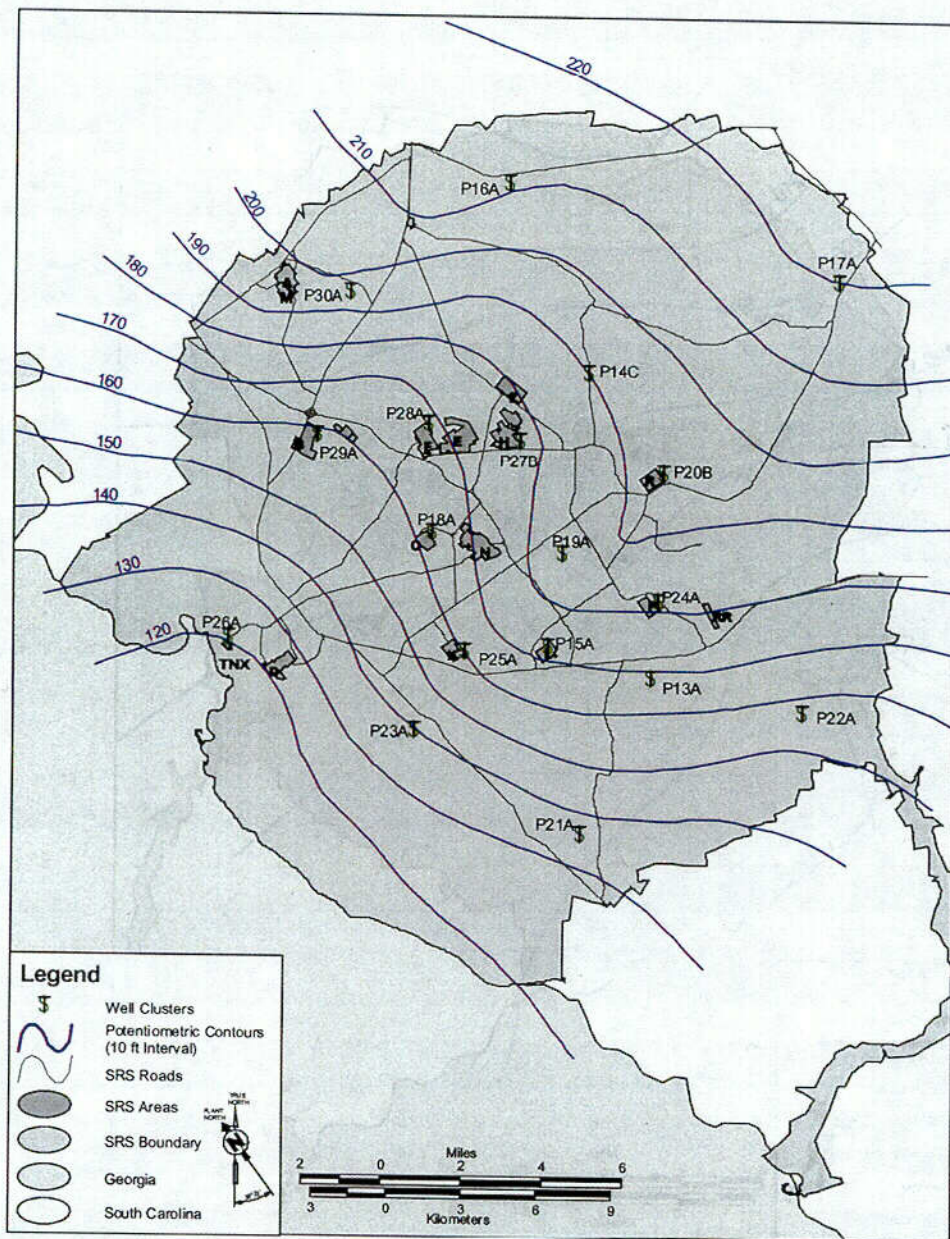


Figure 1.4-25. Potentiometric surface of the Gordon aquifer.

009

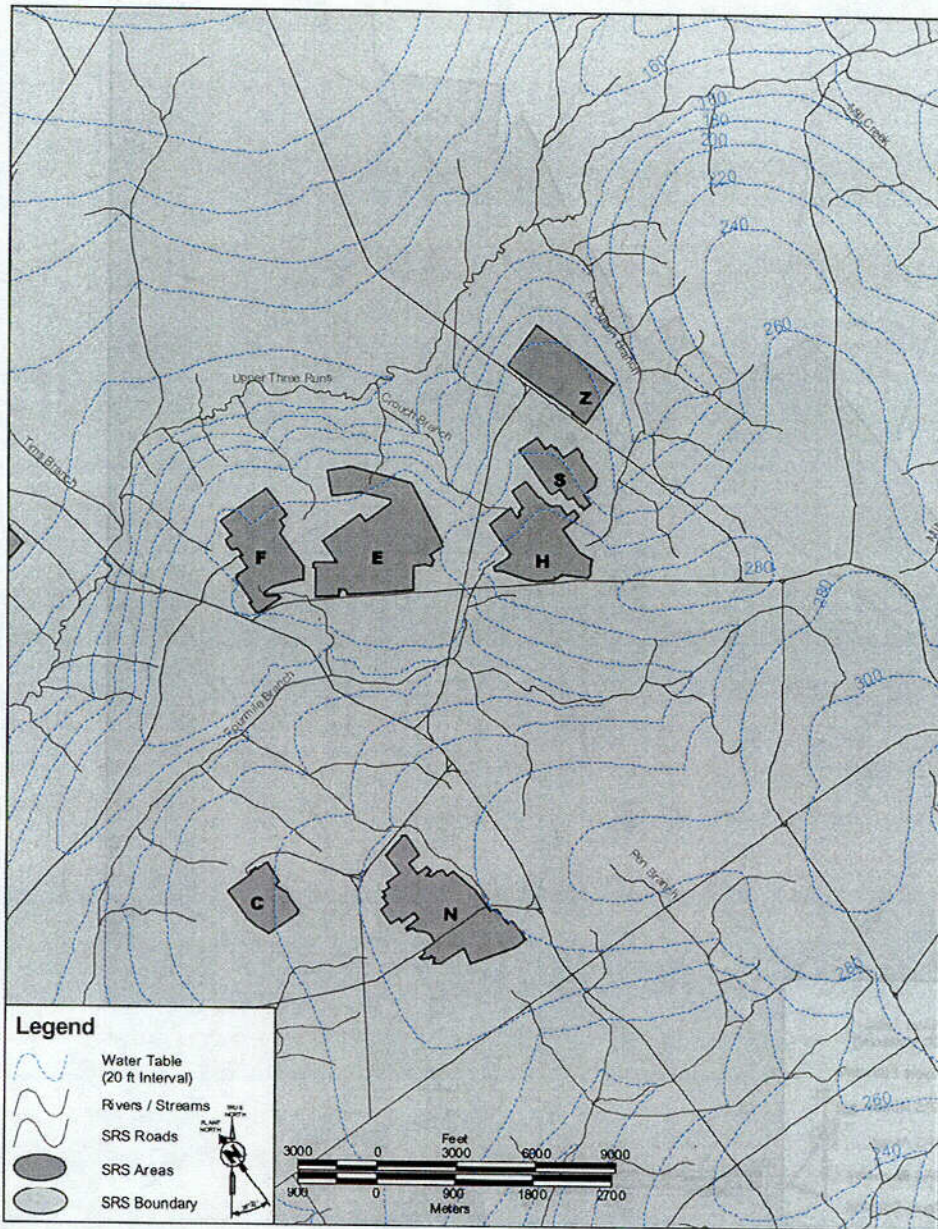


Figure 1.4-27. Potentiometric surface of the Upper Three Runs Creek aquifer (water table) for the General Separations Area.

C11

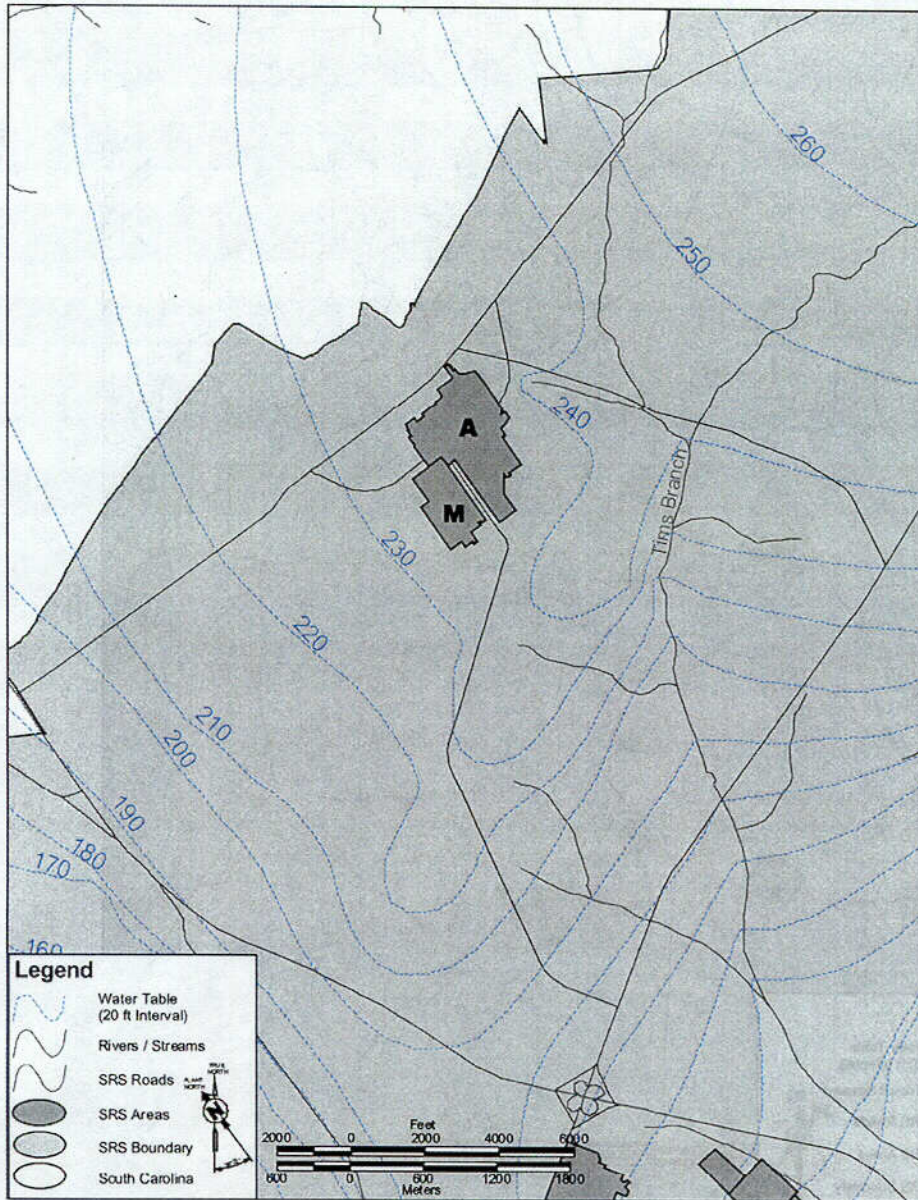


Figure 1.4-28. Potentiometric surface of the Steed Pond aquifer (water table) for the A/M Area.

C12

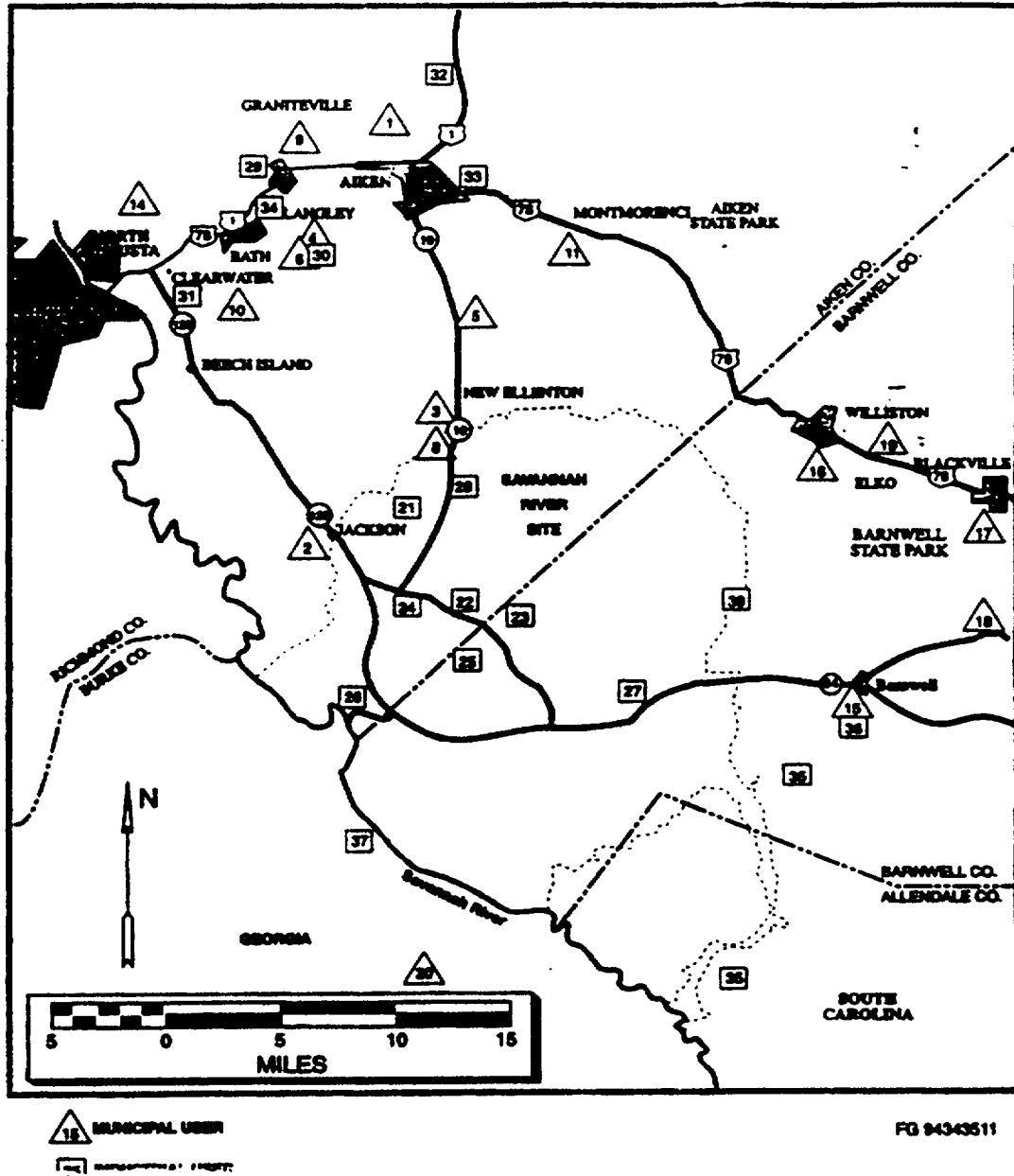


Figure 1.4-29. The location of industrial and municipal groundwater users near SRS.

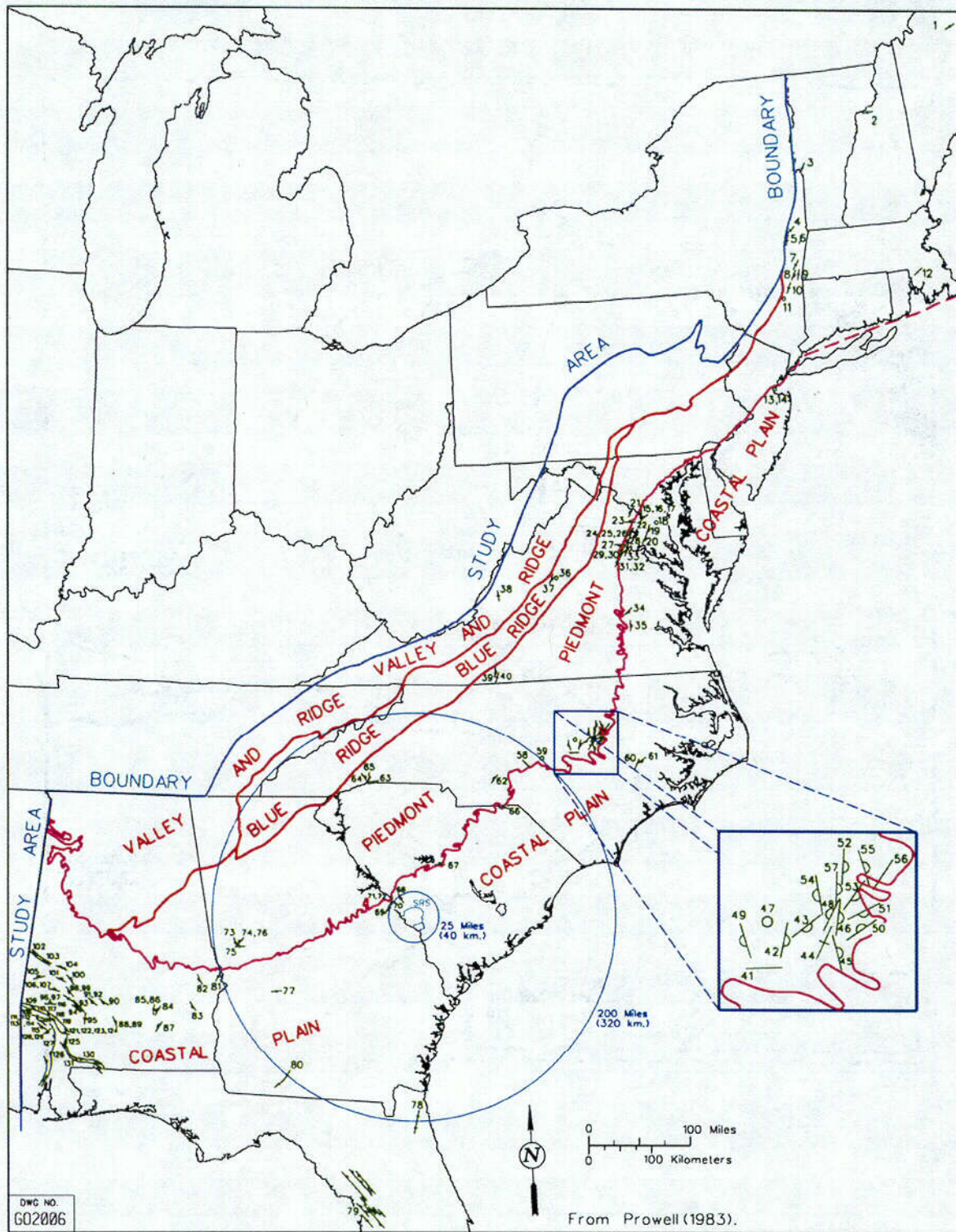


Figure 1.4-30. Relationship of SRS to regional geological provinces and terranes.

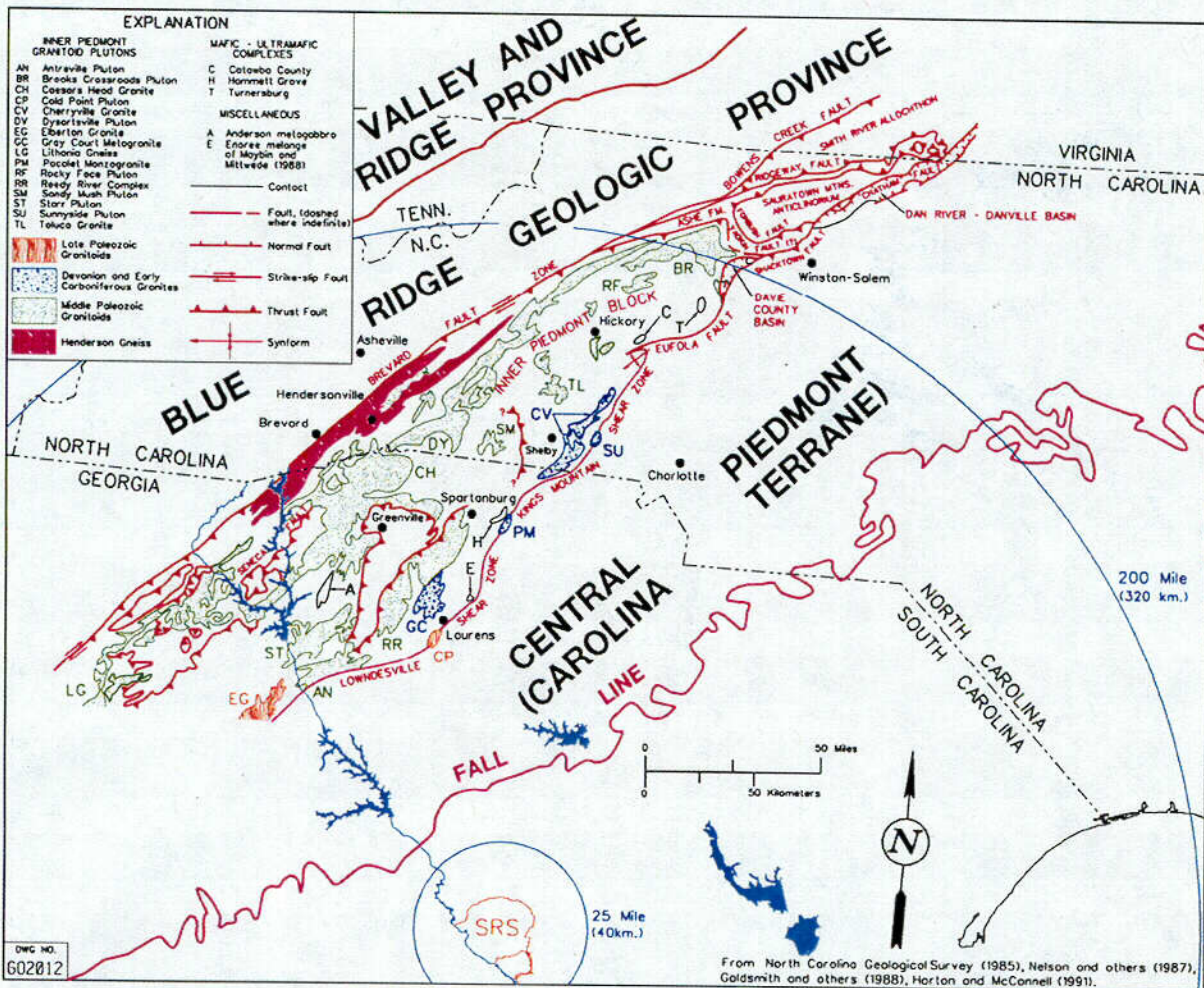


Figure 1.4-31. Piedmont Terrane.

C14

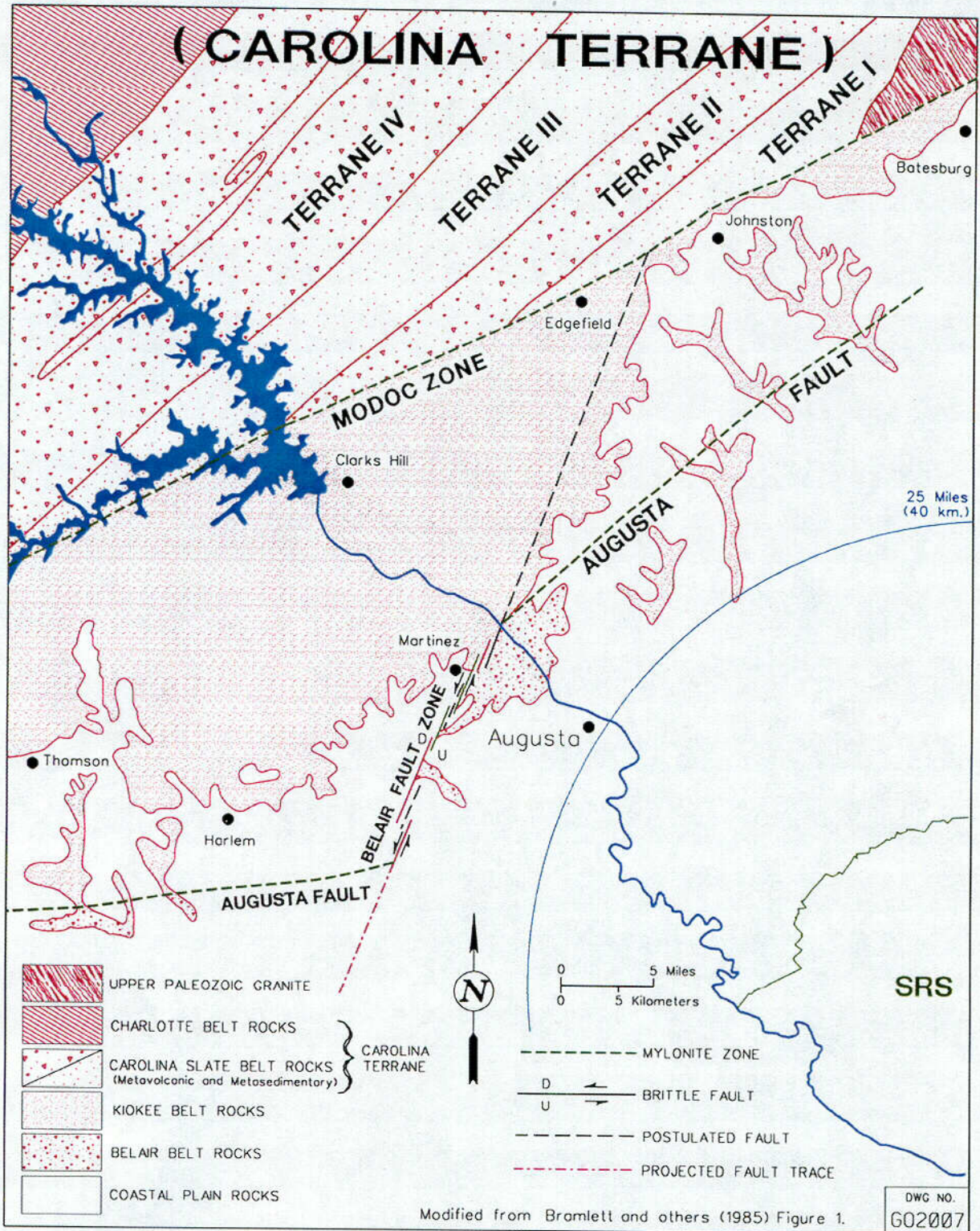


Figure 1.4-32. Carolina Terrane.

C15

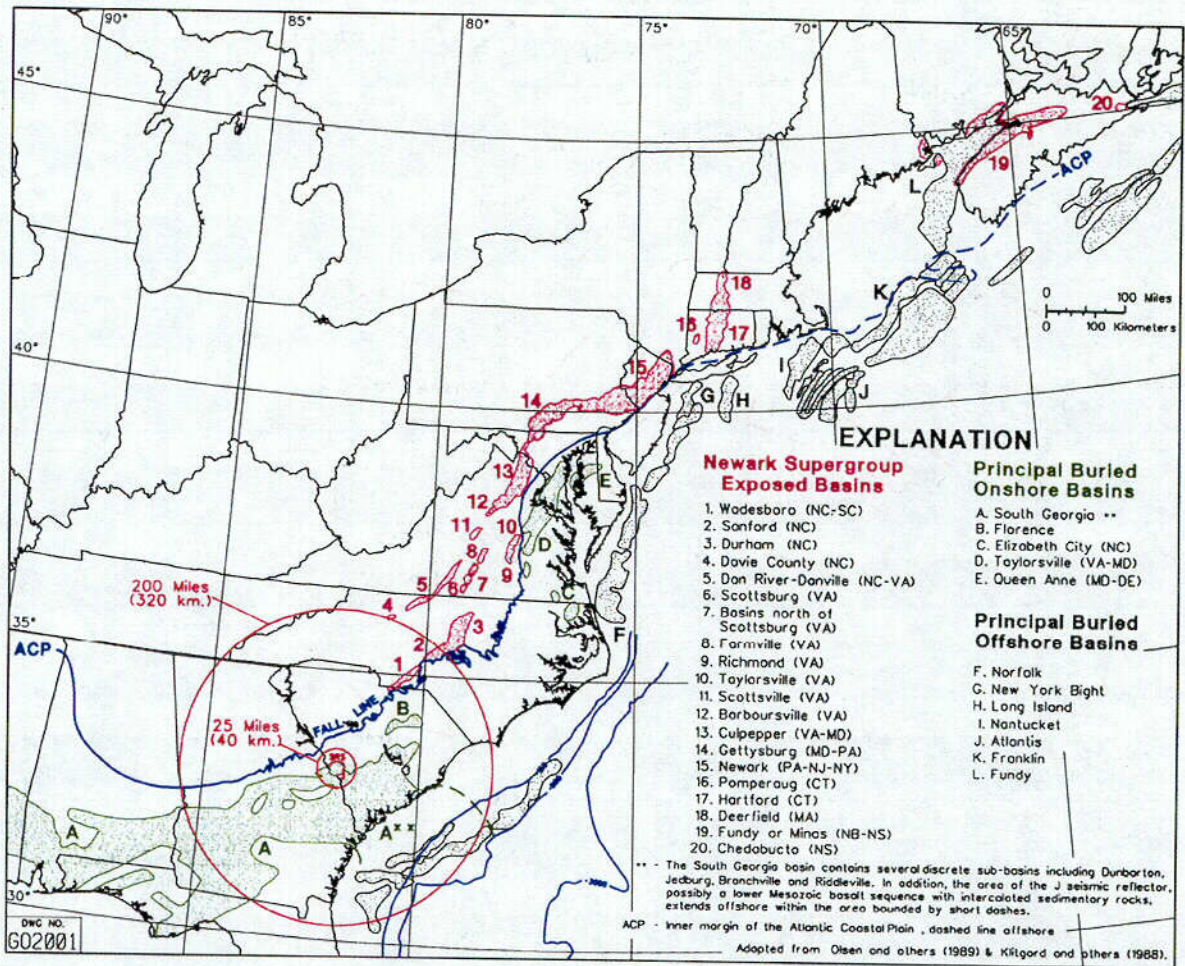


Figure 1.4-33. Location of Mesozoic rift basins along the entire eastern continental margin of North America from the gulf coast through Nova Scotia.

C16

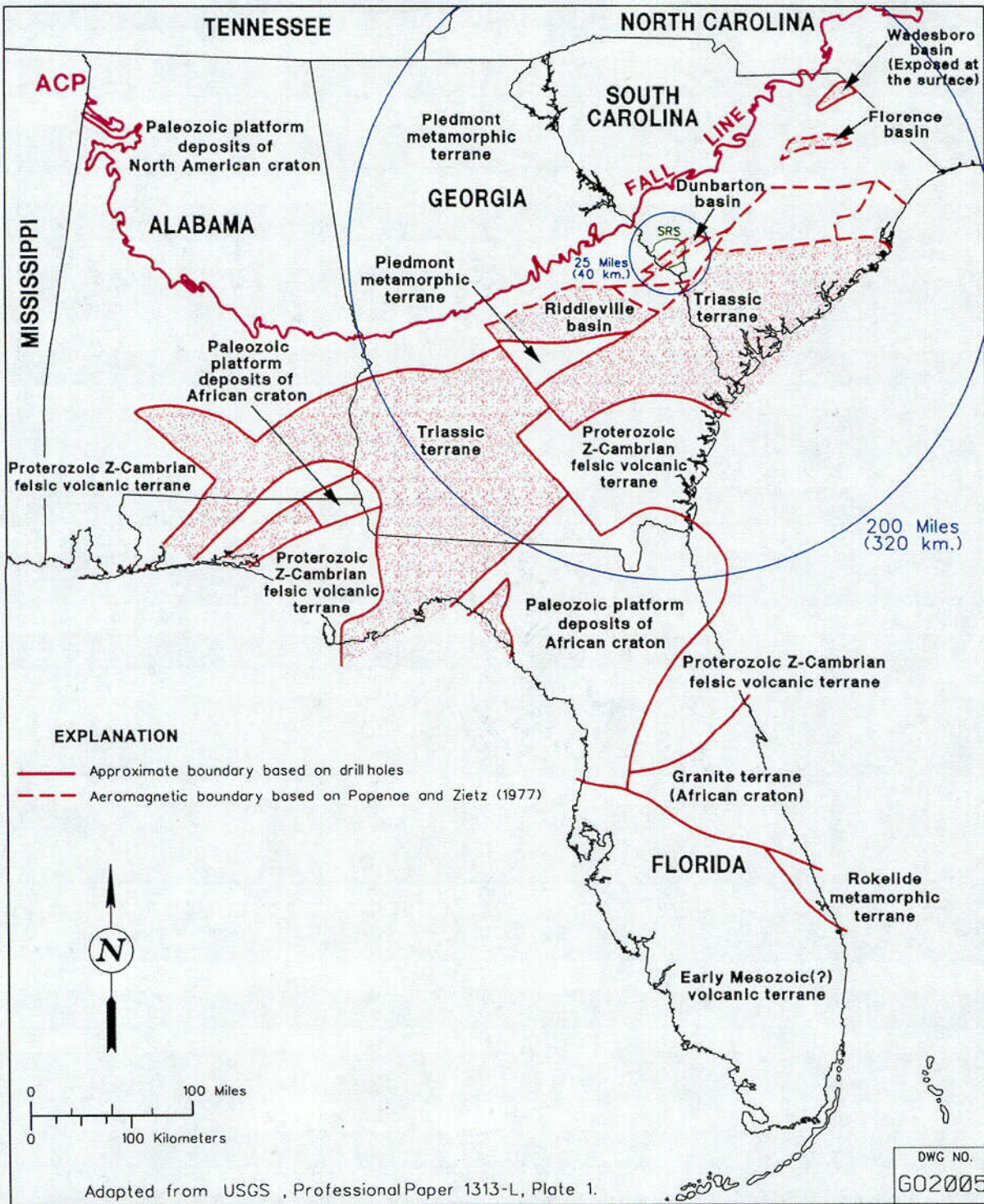


Figure 1.4-34. The Triassic basins beneath the Alabama, Florida, Georgia South Carolina coastal Plain.

C17

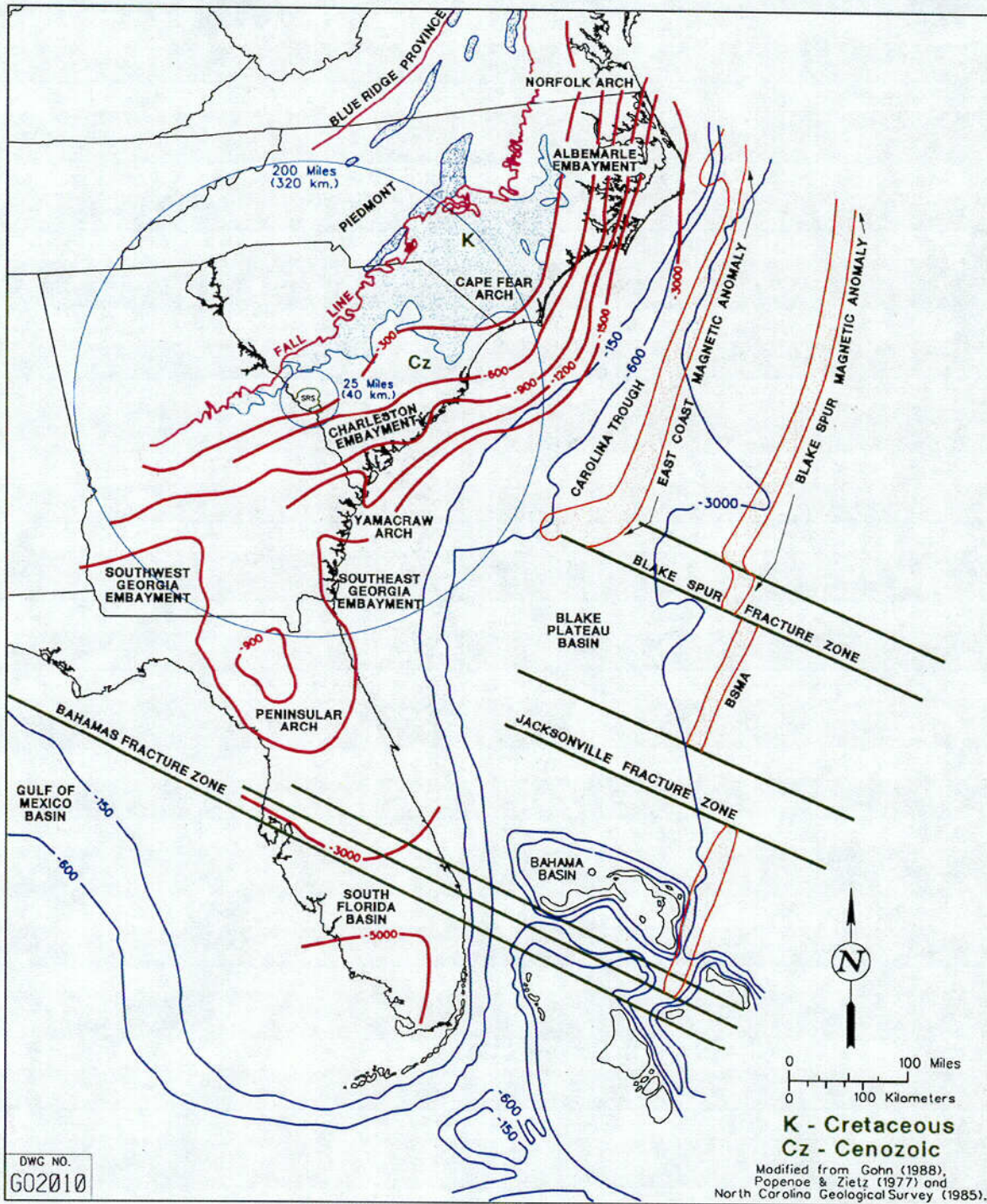


Figure 1.4-35. Structural configuration of the Atlantic continental margin.

C18

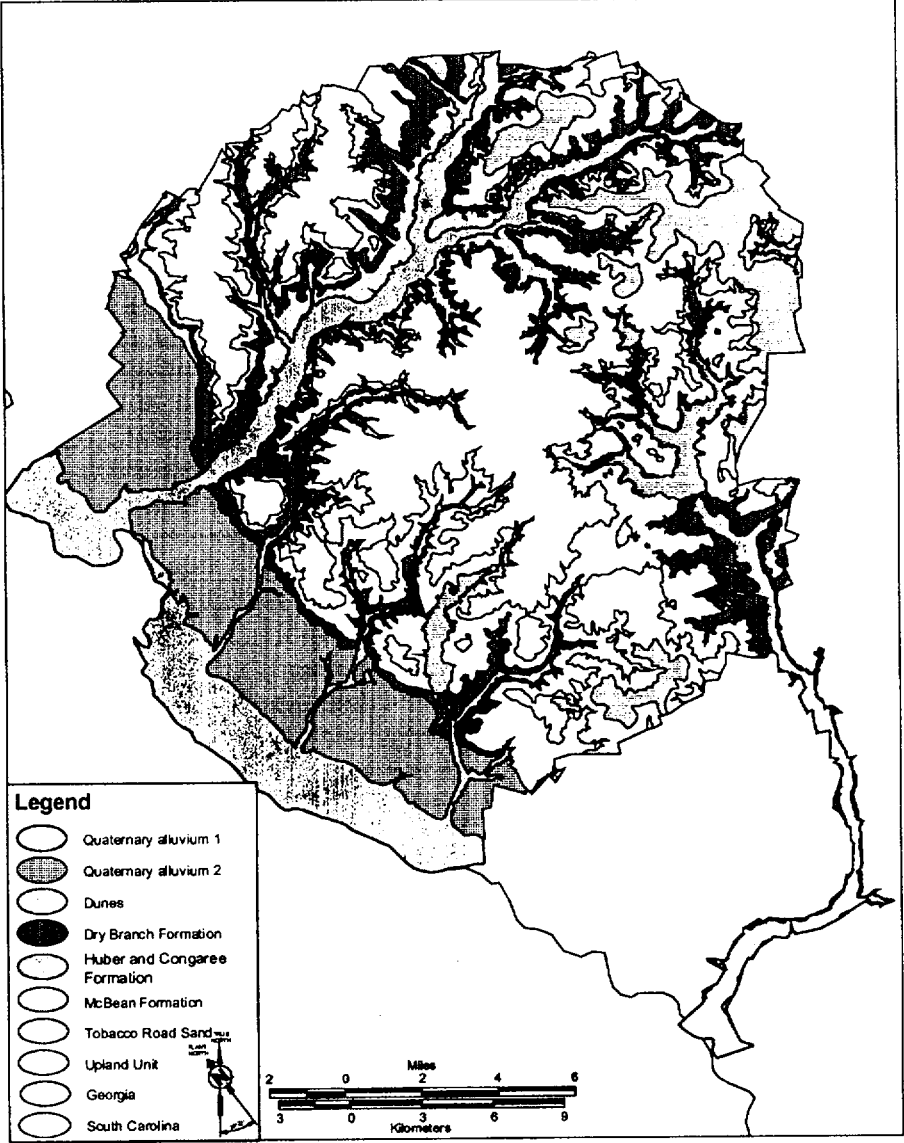
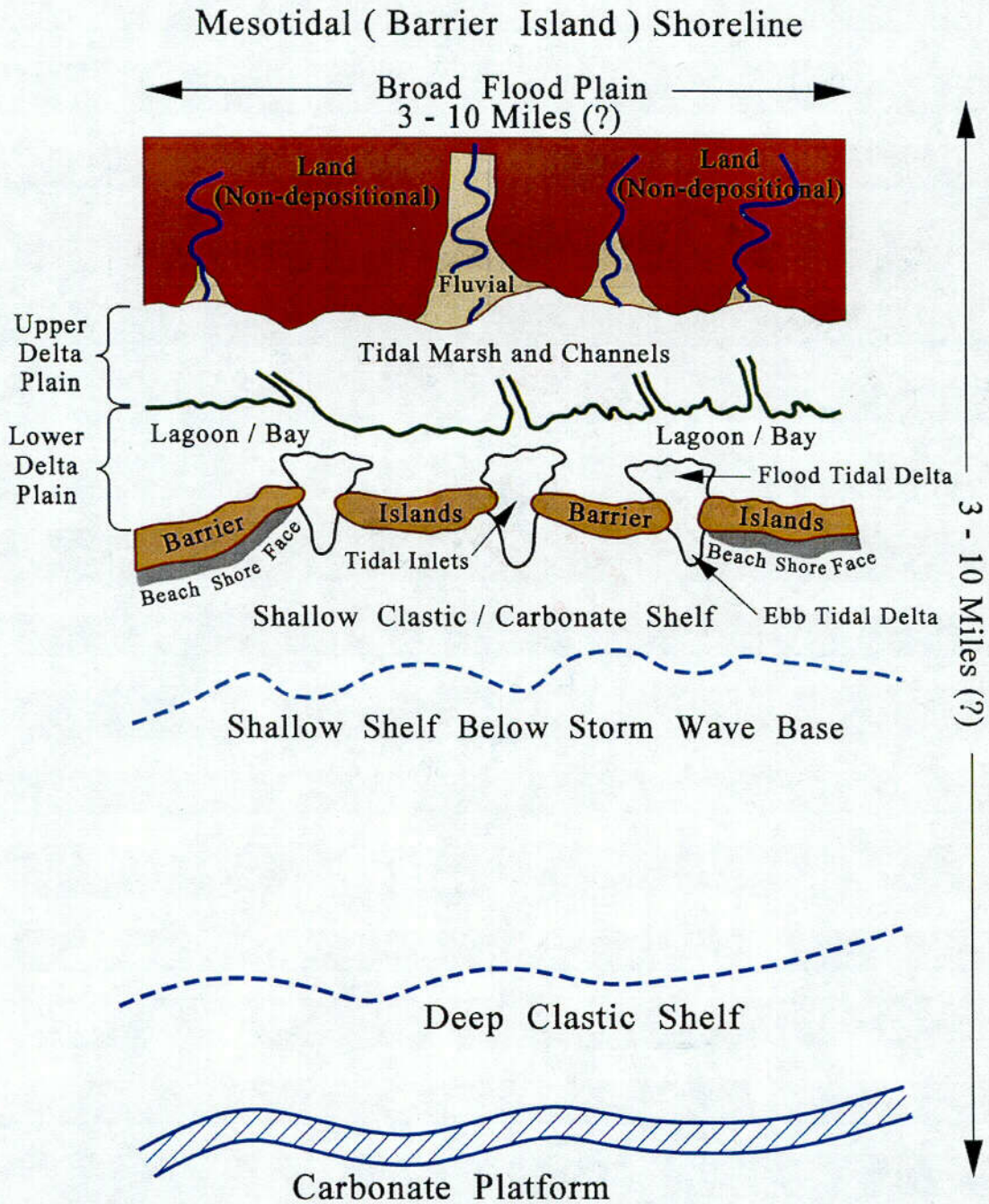


Figure 1.4-36. Geologic map of the SRS.



GC65767

Figure 1.4-37. Spatial relationships of depositional environments typical of the Tertiary sediments at the SRS.

C19

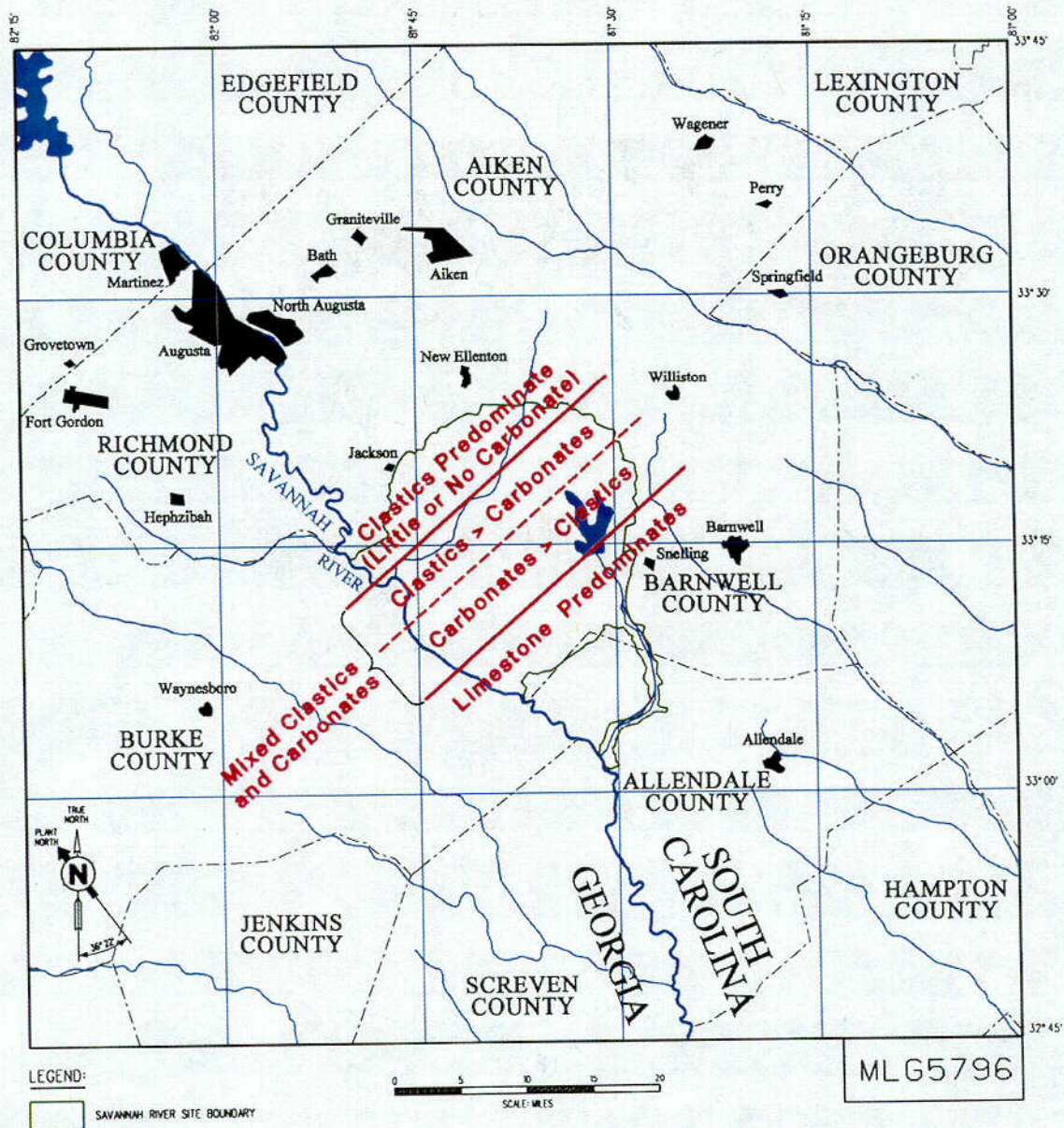


Figure 1.4-38. Regional distribution of carbonate in the Santee/Utley-Dry Branch sequence.

C20

HSB-TB

GROUND ELEV. = 267 FEET

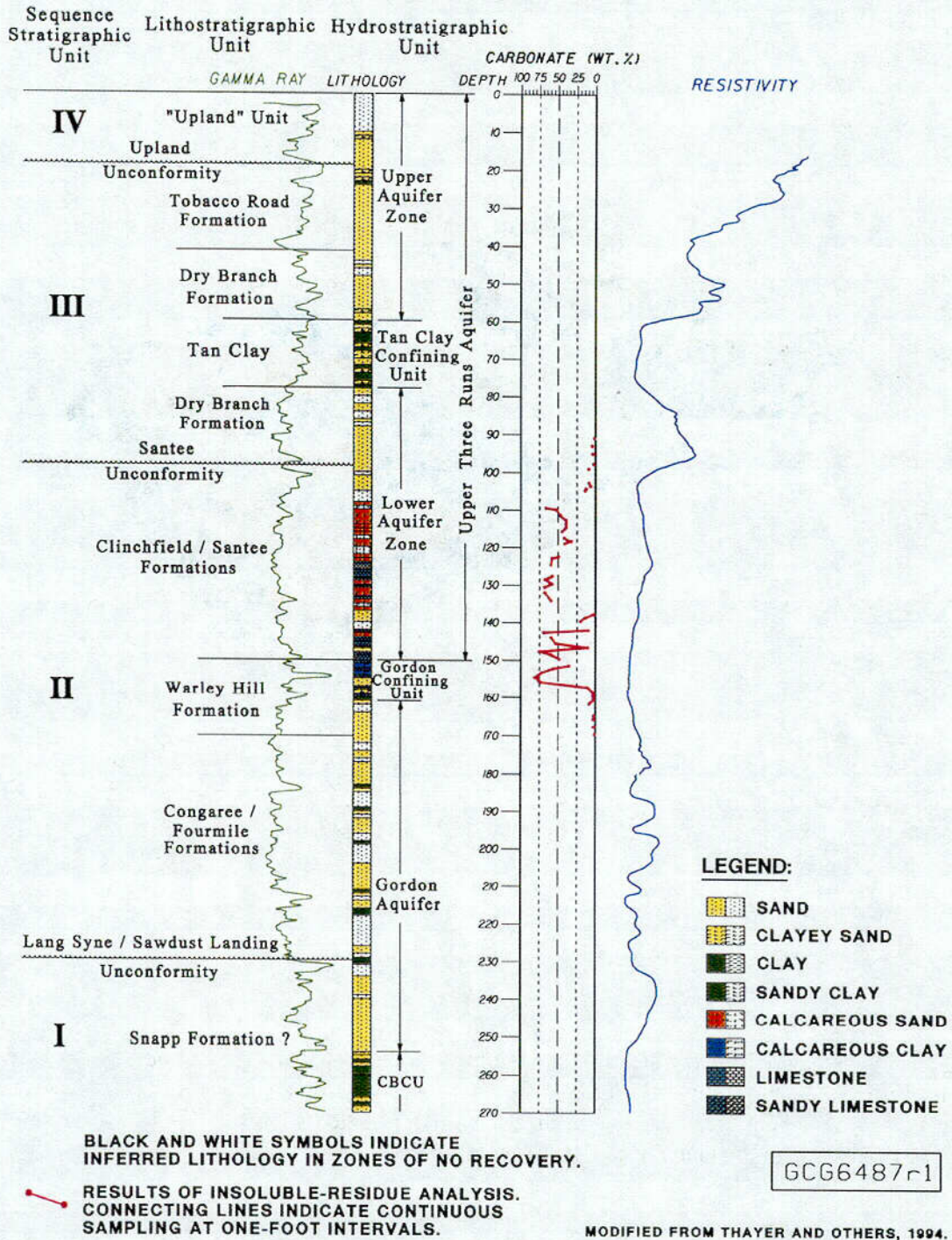


Figure 1.4-39. Lithologic and geophysical signature typical of the Tertiary section in the General Separations Area, Savannah River Site.

C21

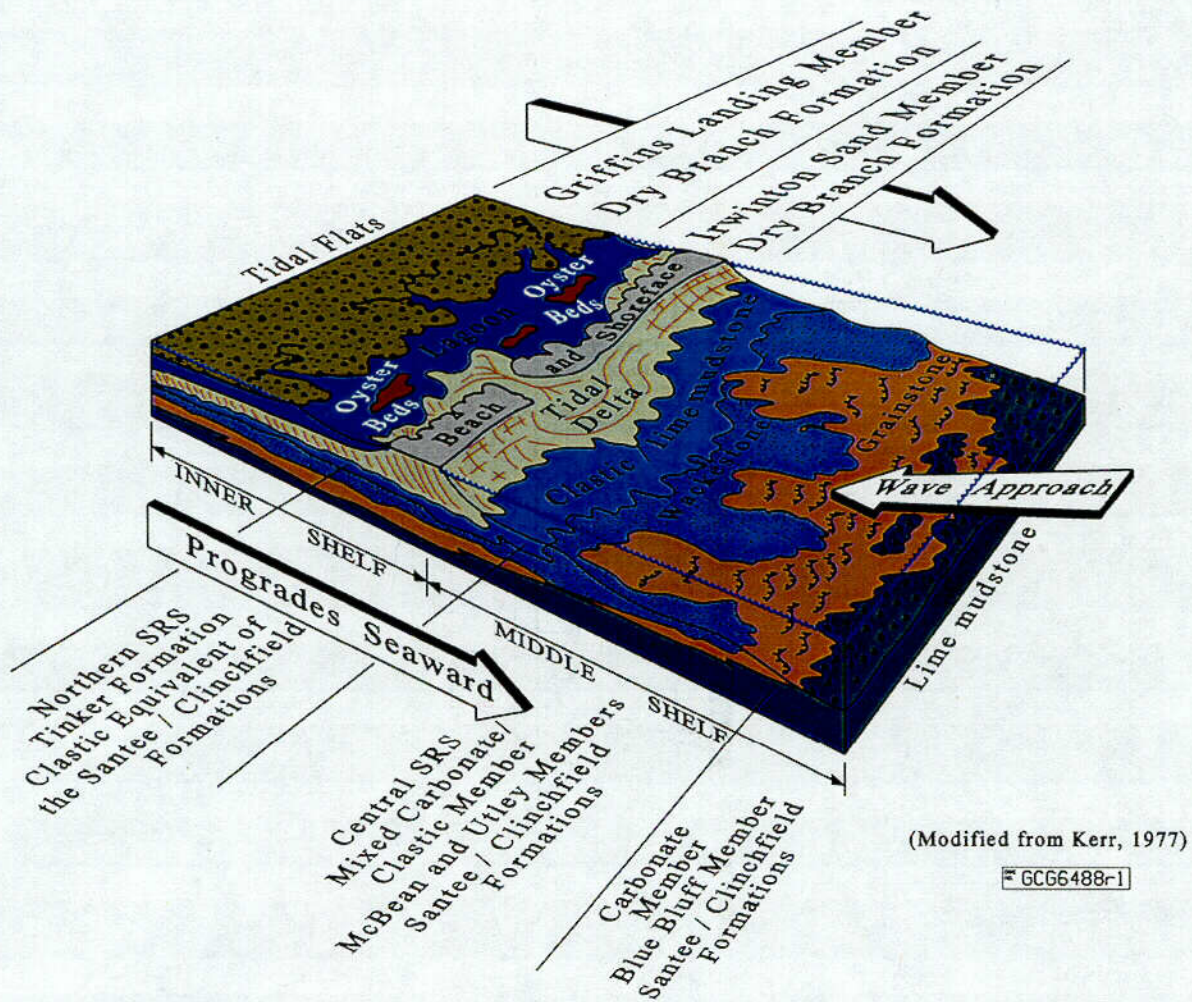


Figure 1.4-40. Spatial relationships of depositional environments typical of the Dry Branch and Tinker/Santee (Utley) sediments at SRS. Progradation seaward pus the tidal flat/marsh/shoreline (inner shelf) sediments of the Dry Branch Formation over the middle shelf sediments typical f the Santee Formation in the General Separations area, SRS.

C22

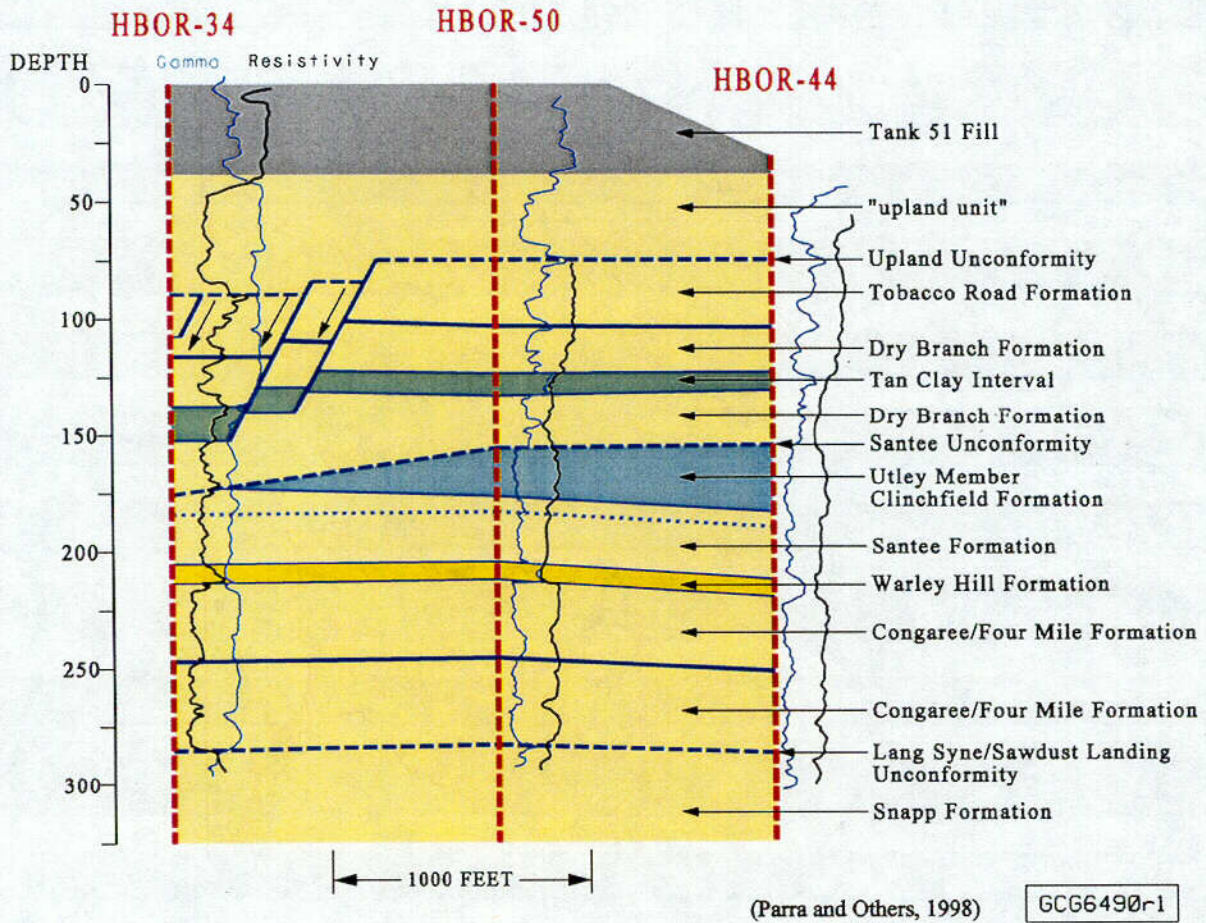


Figure 1.4-41. Carbonate dissolution in the Tinker/Santee (Utley) interval resulting in consolidation and slumping of the overlying sediments of the Tobacco Road and Dry Branch Formations into the resulting lows.

C23

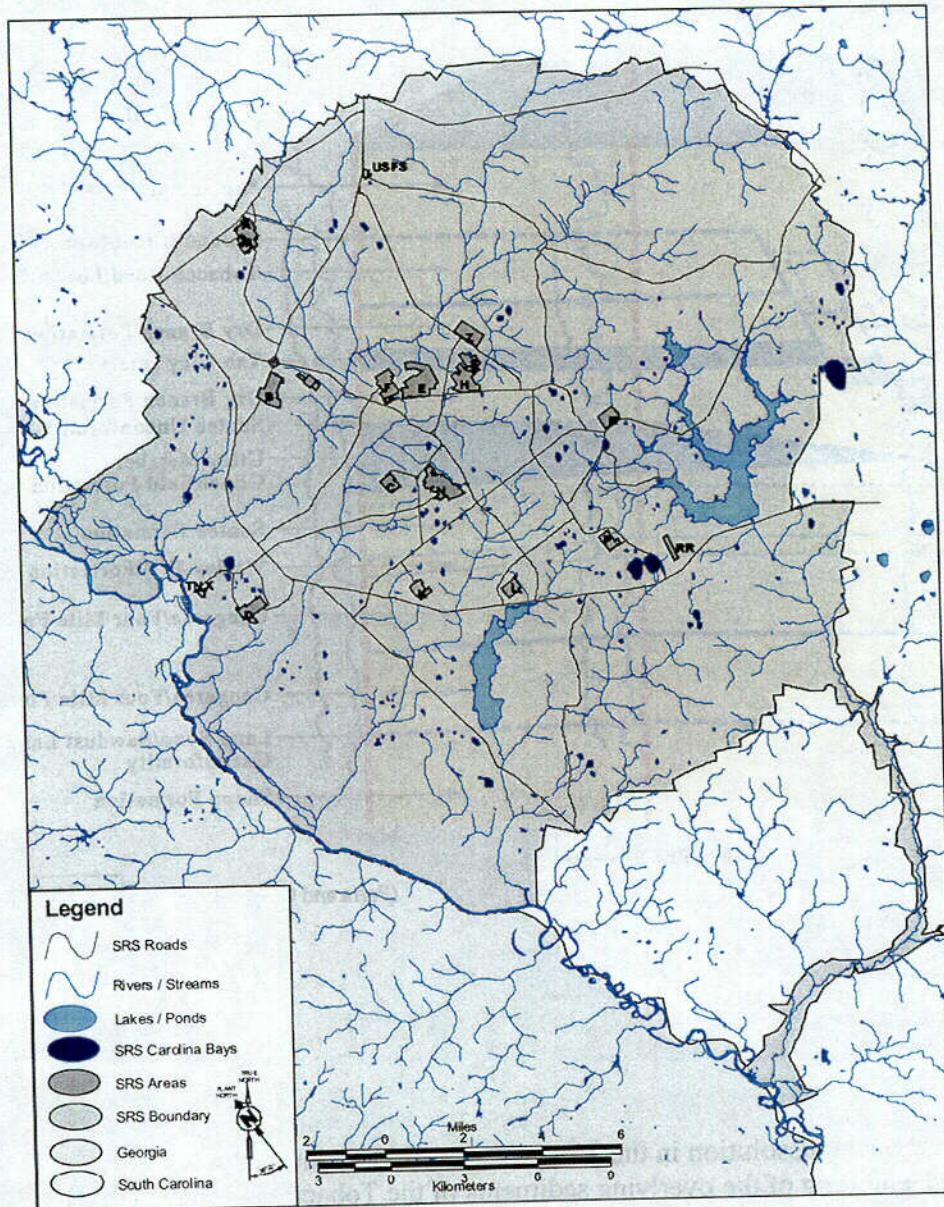


Figure 1.4-42. Distribution of Carolina Bays within the SRS.

024

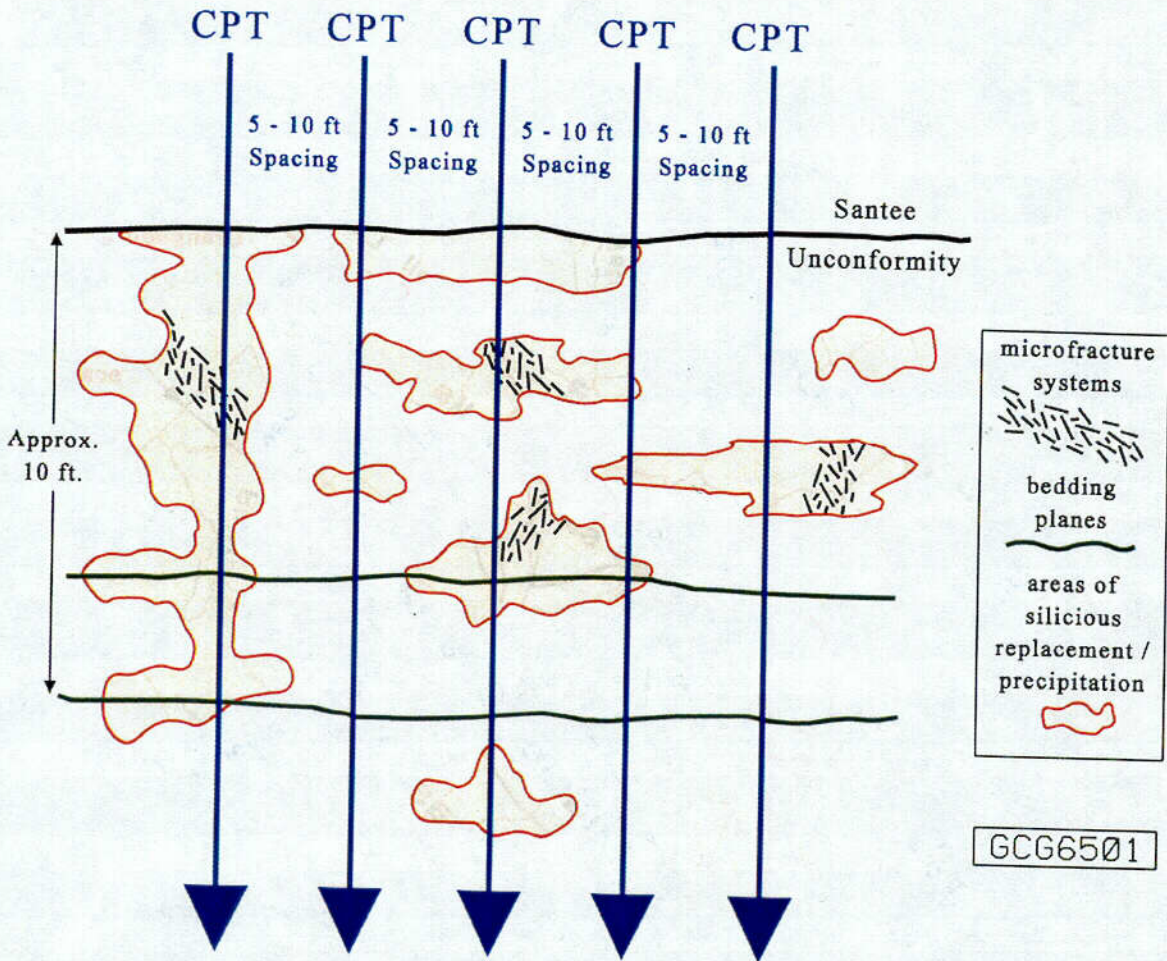


Figure 1.4-43. Diagram illustrating the stratigraphic and lateral distribution of soft zones due to silica replacement of carbonate in the GSA. Replacement/precipitation occurs along bedding planes, microfracture systems, and zones of enhanced permeability resulting in highly irregular pods, stringers, and sheets of silica replaced carbonate (i.e., soft zones).

C25

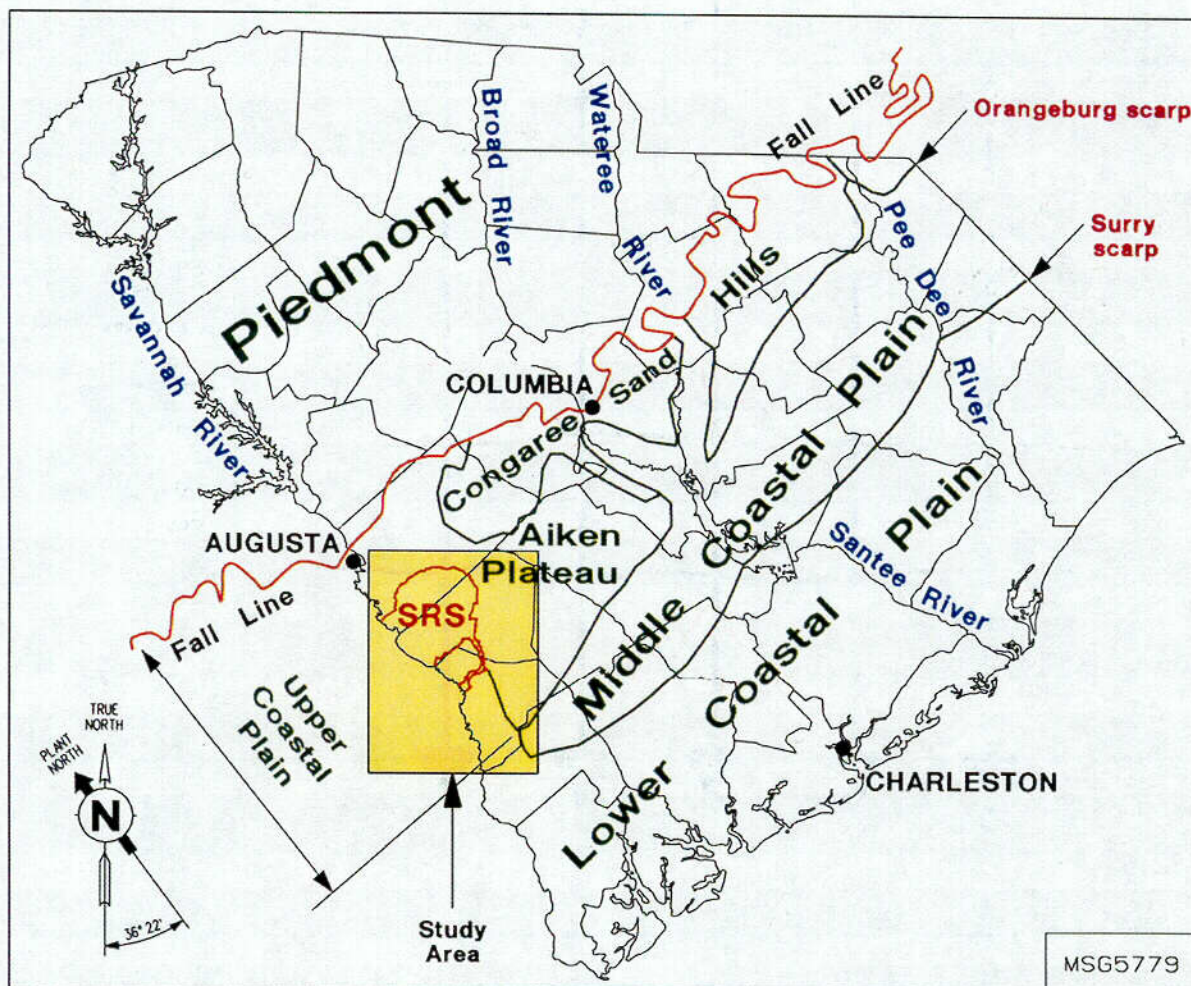


Figure 1.4-44. Regional physiographic provinces of South Carolina.

C26

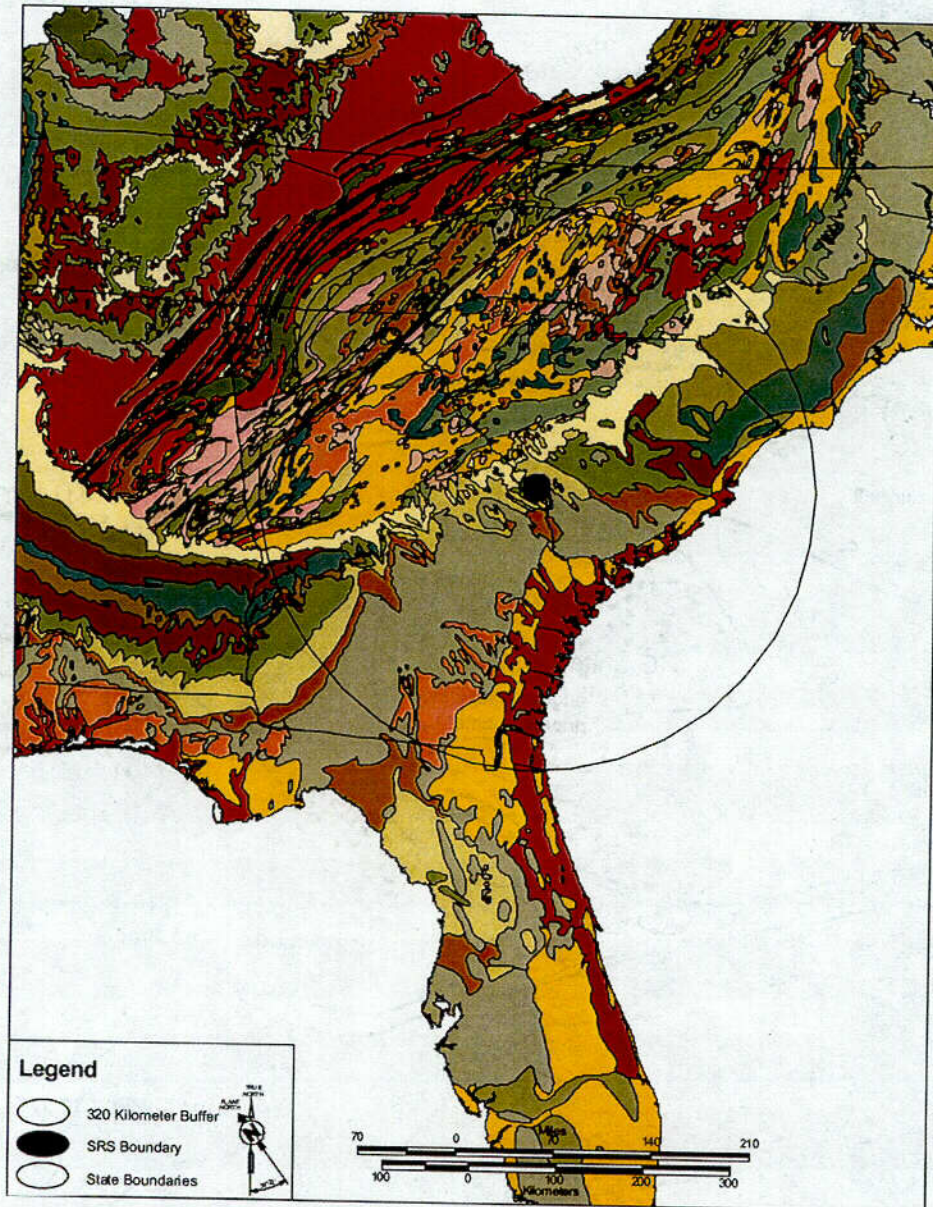


Figure 1.4-45. Regional geologic map of the southeastern US.

027

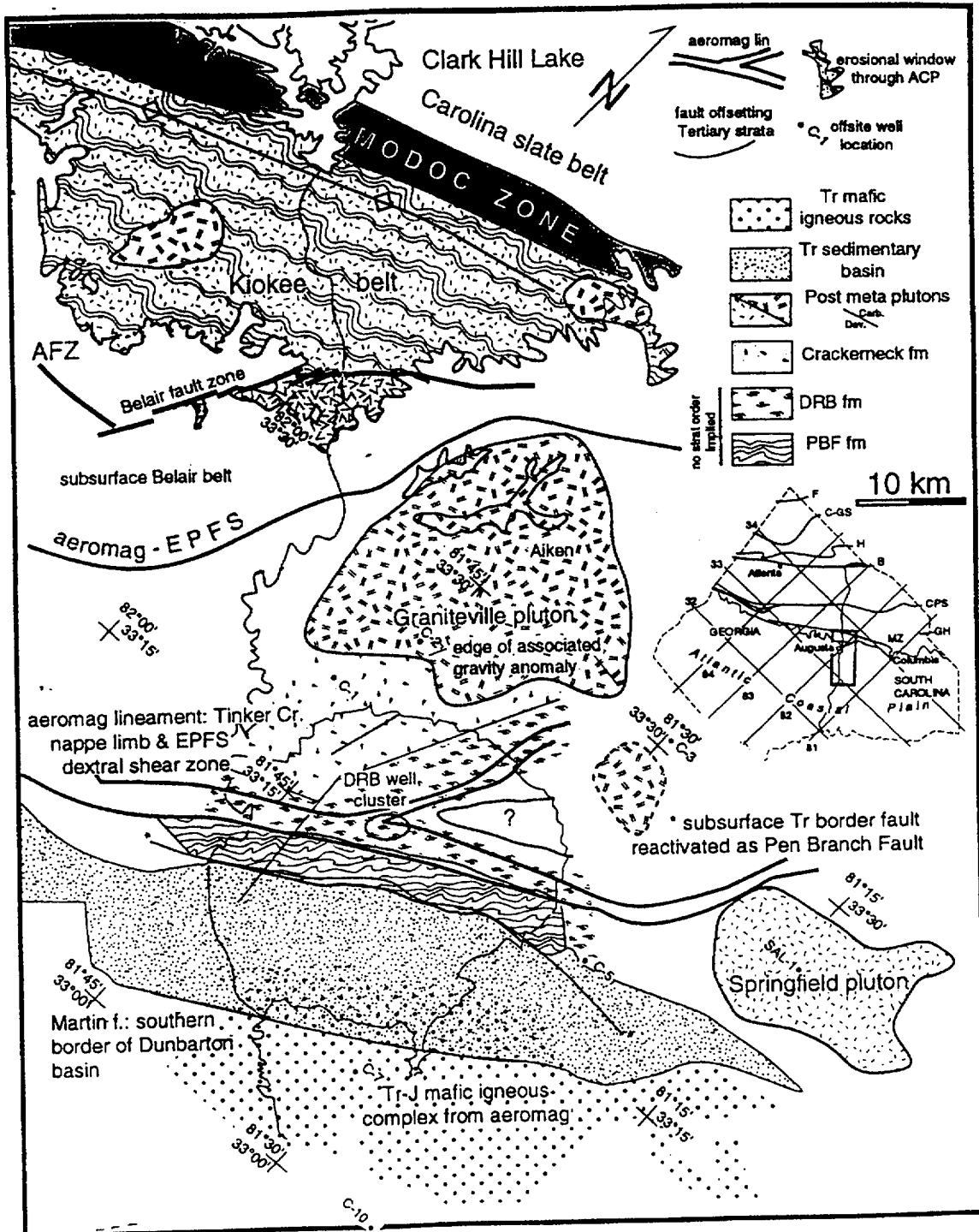


Figure 1.4-46. Geologic map of basement lithologies beneath the Savannah River Site and vicinity with adjacent piedmont (from Dennis et al. 1997).

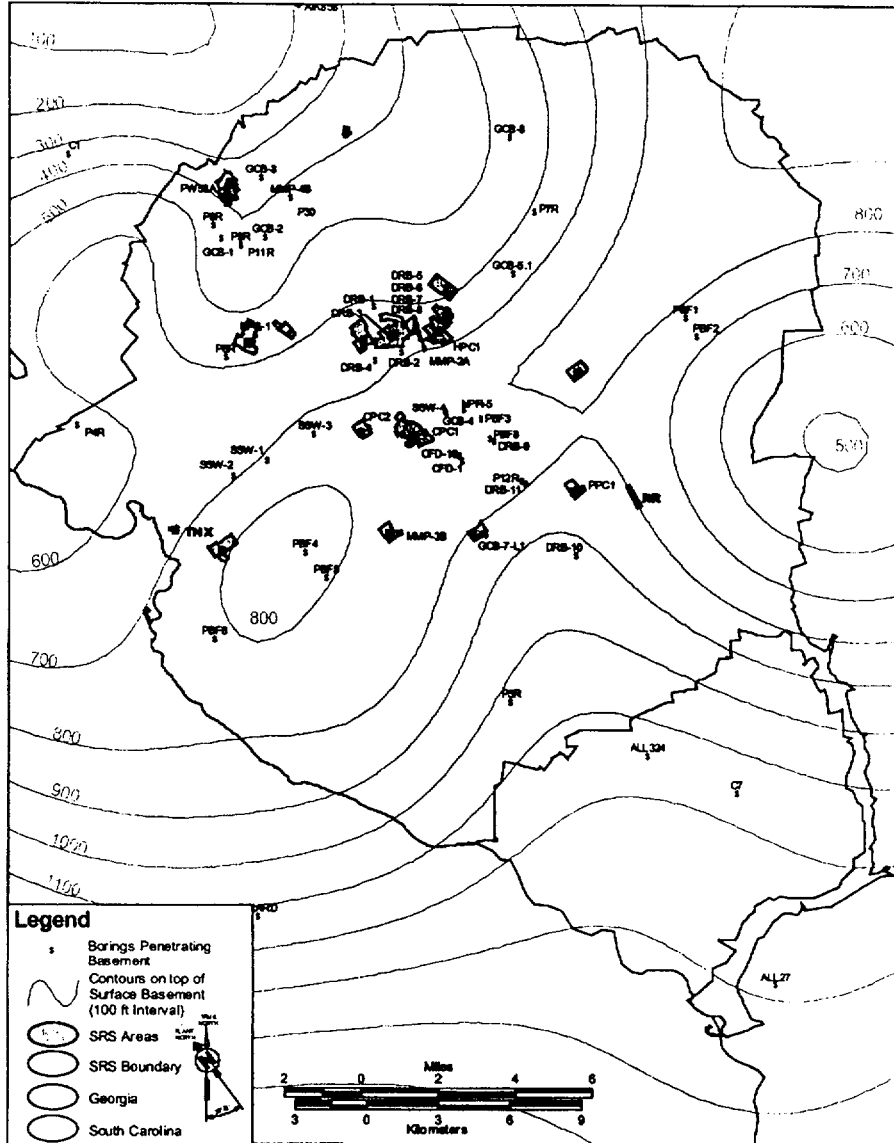


Figure 1.4-47. Map of the basement surface at the SRS.

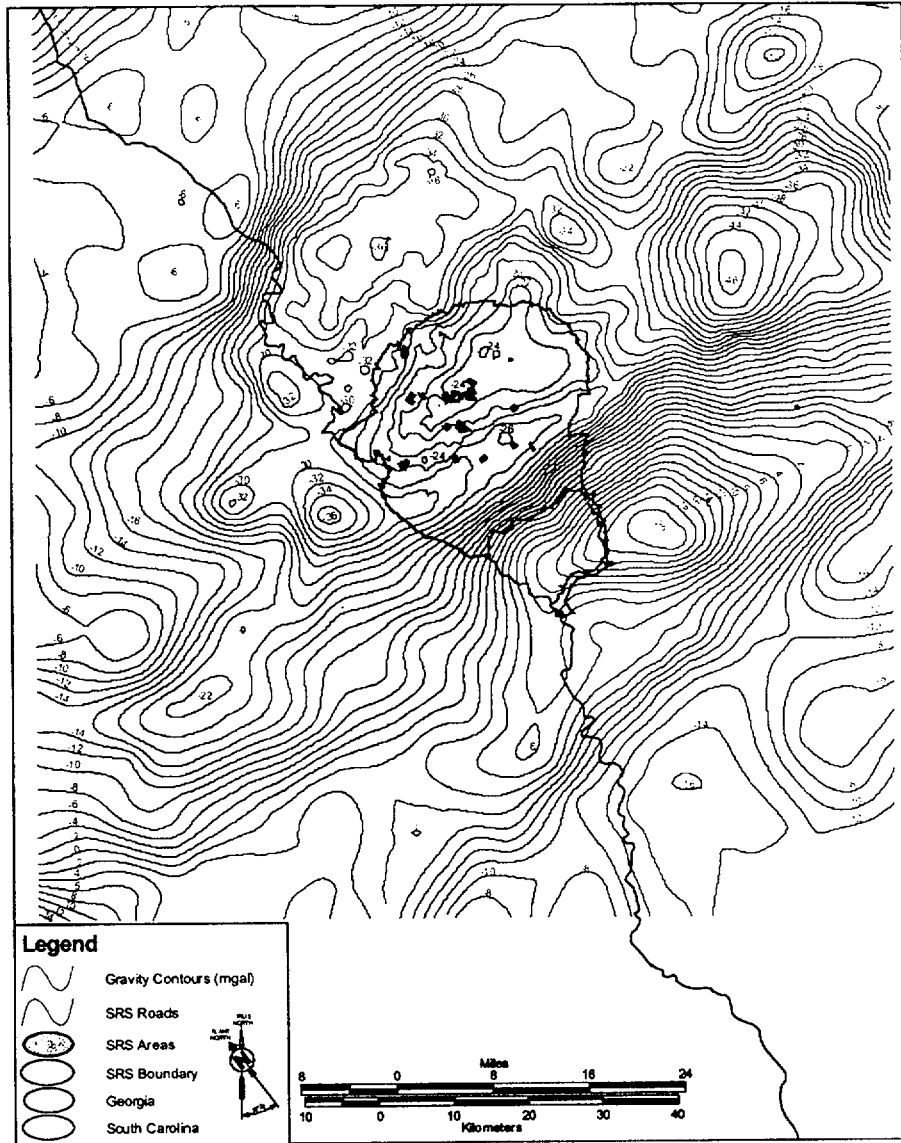


Figure 1.4-48. Free air gravity anomaly map for SRS and vicinity (40 km radius). Based on data from Domoracki (1994).

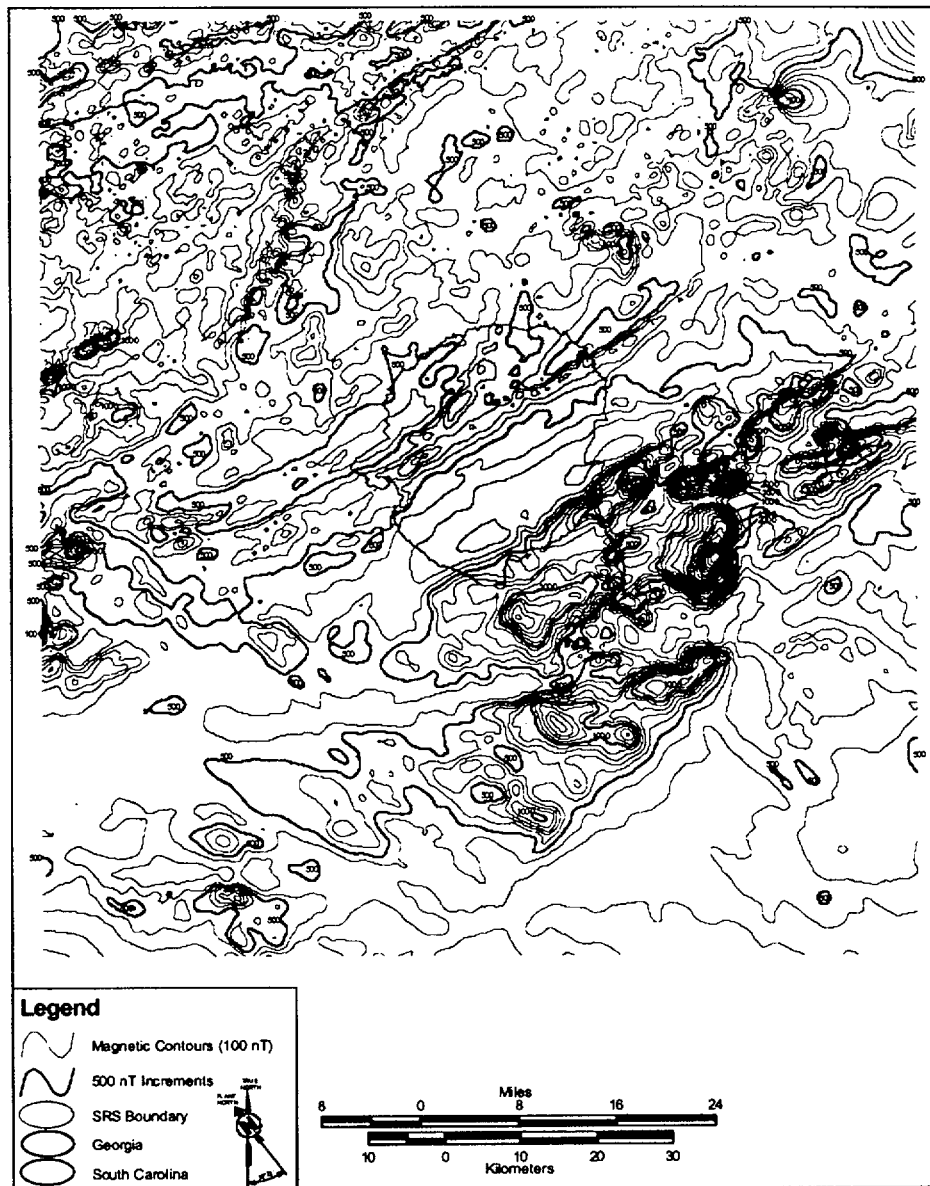


Figure 1.4-49. Aeromagnetic anomaly map for SRS and vicinity (40 km radius) Based on Petty et al., (1965).

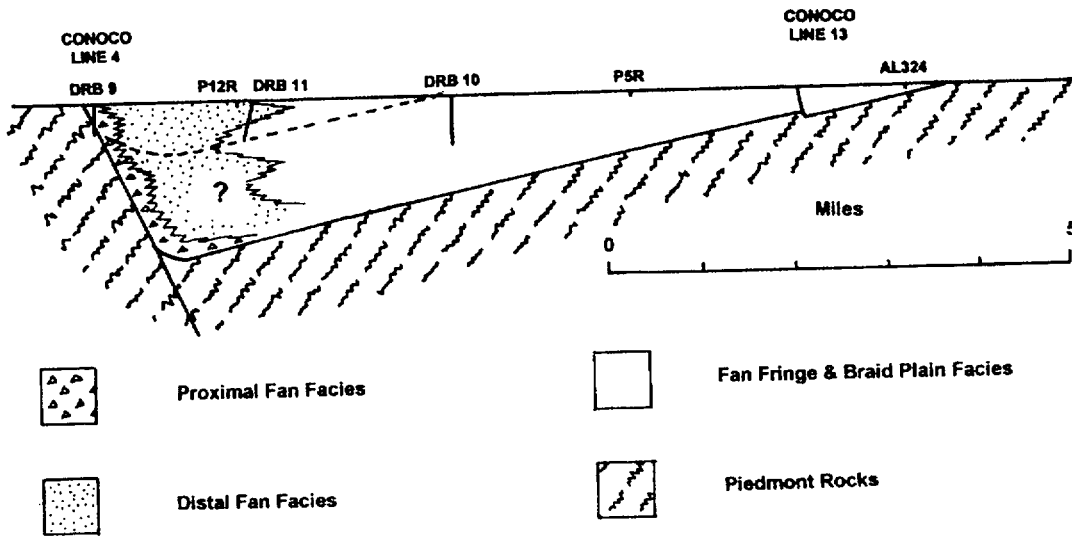


Figure 1.4-50. Generalized geologic cross-section of the Dunbarton Basin (from Chowns e a., 1996).

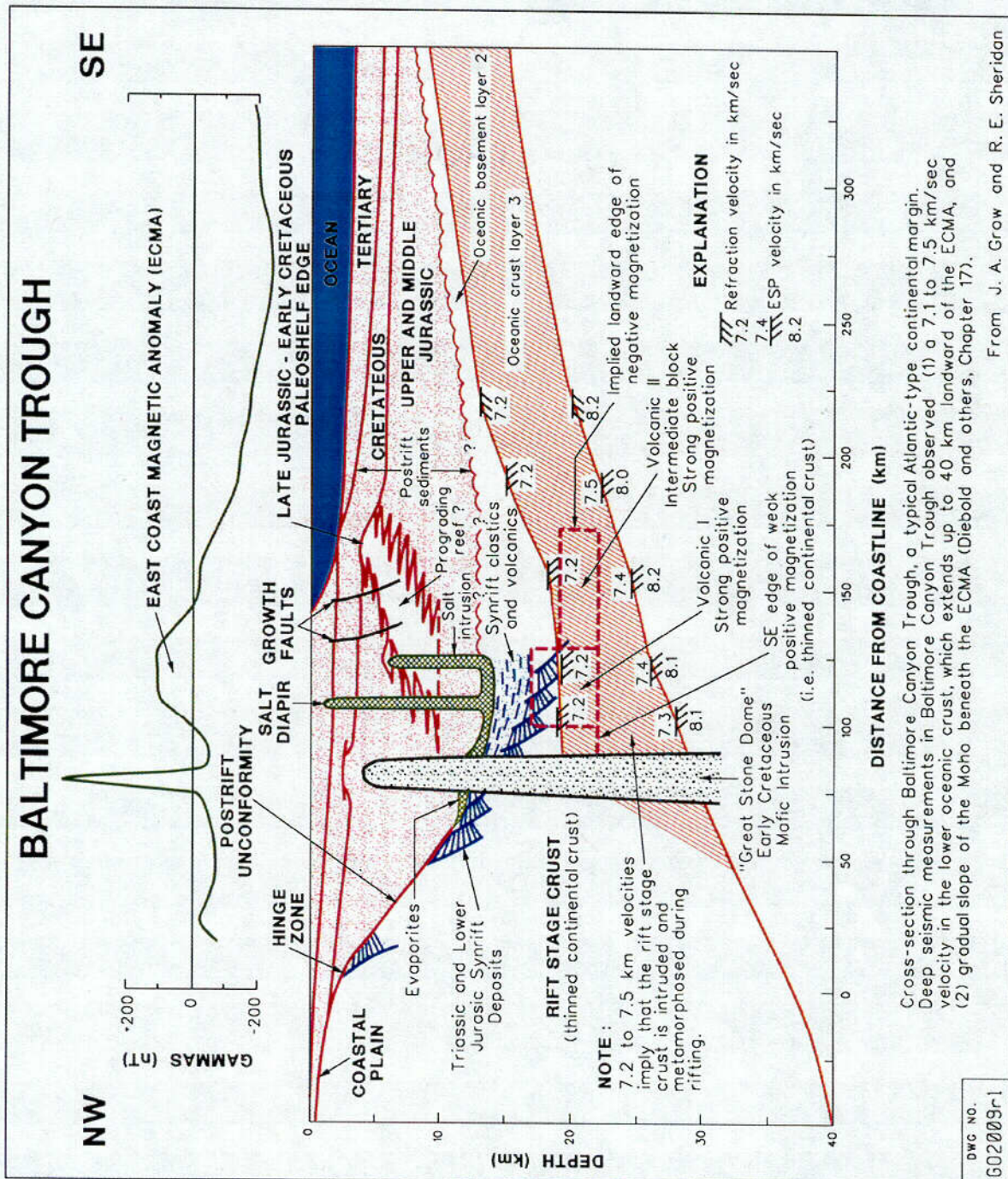


Figure 1.4-51. A cross-section through the continental margin and Baltimore trough (offshore New Jersey). This is a typical Atlantic-type margin showing the geometry of oceanic crust to the east and continental crust to the west. After Sheridan and Grow (1988).

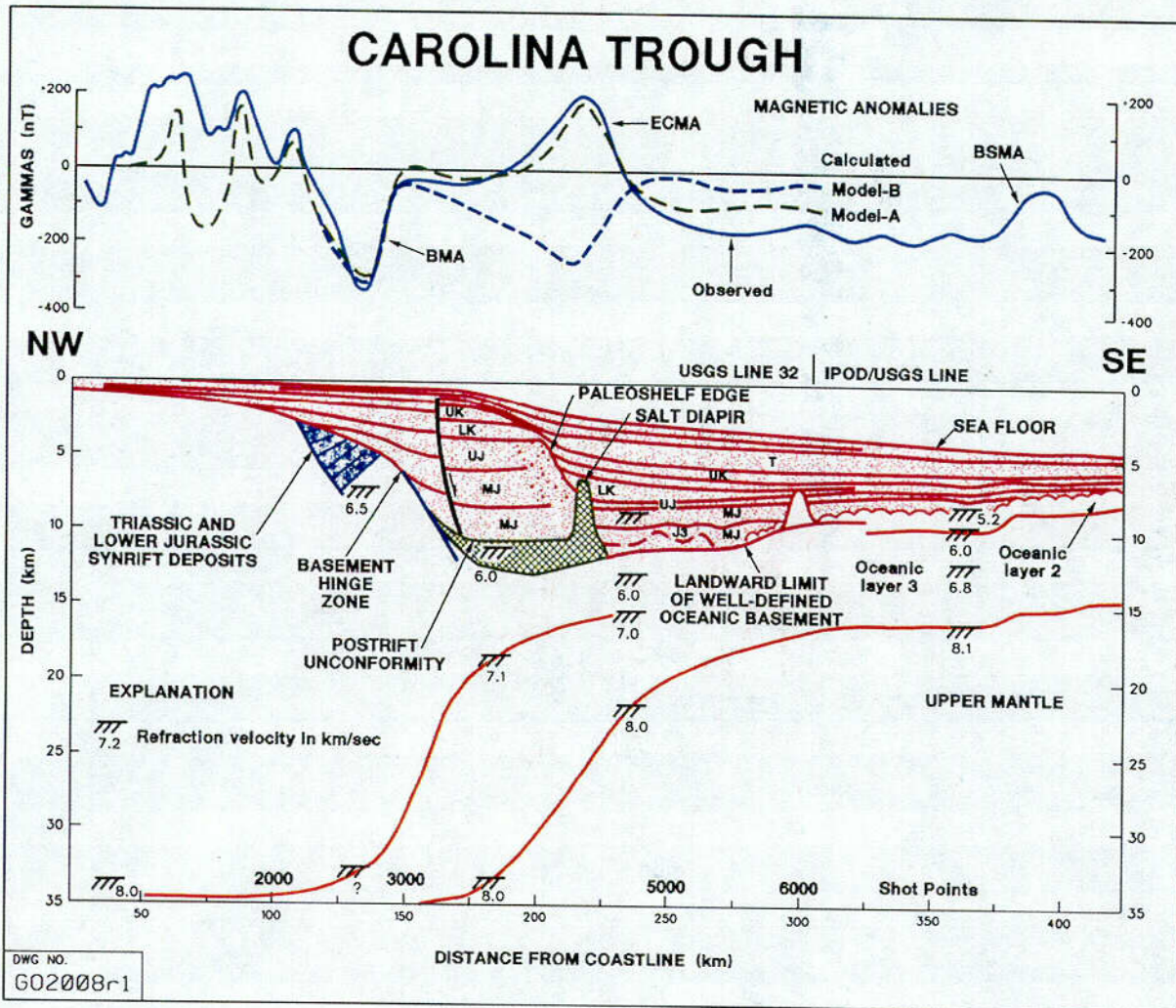


Figure 1.4-52. Crustal geometry for offshore South and North Carolina show a geometry of thinning crust (Klitgord et al; 1988).

C29

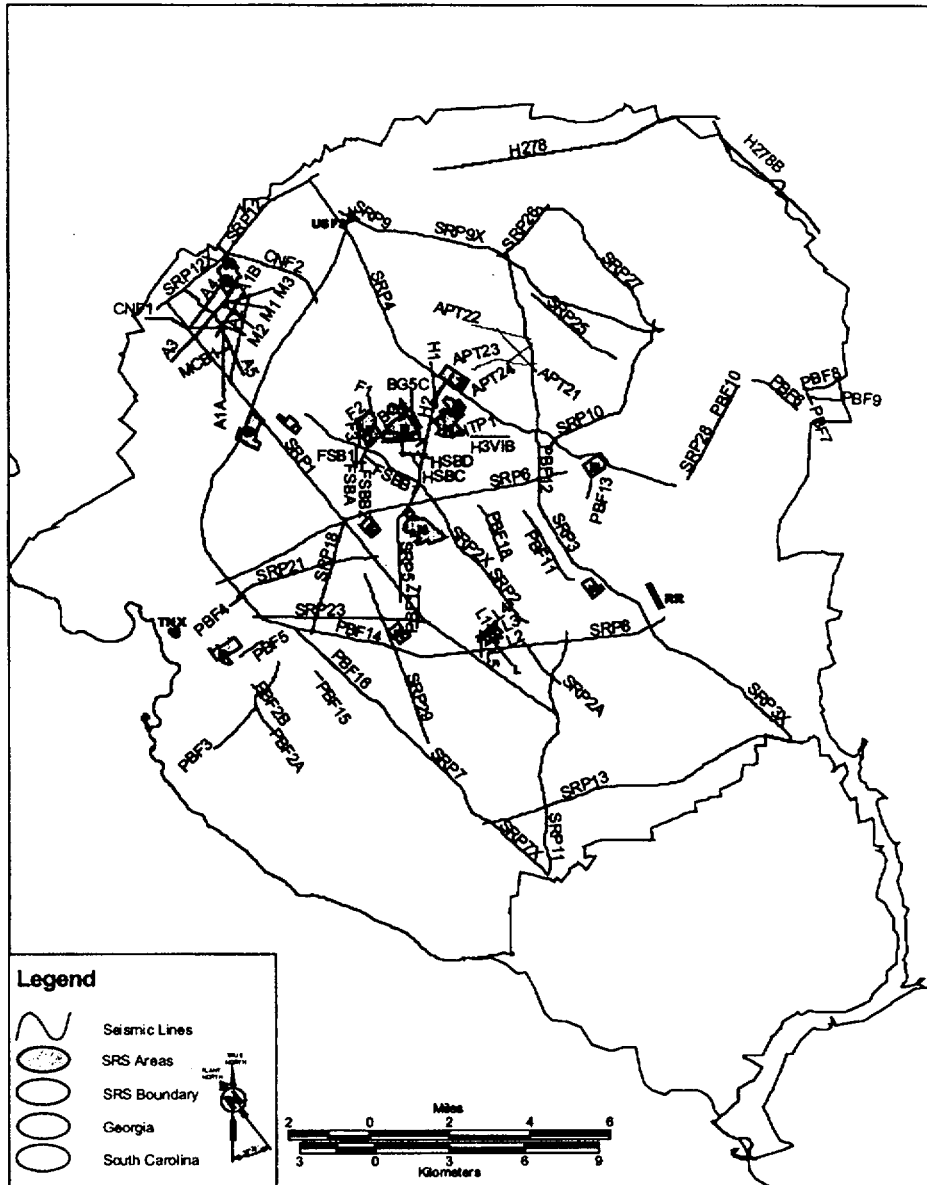
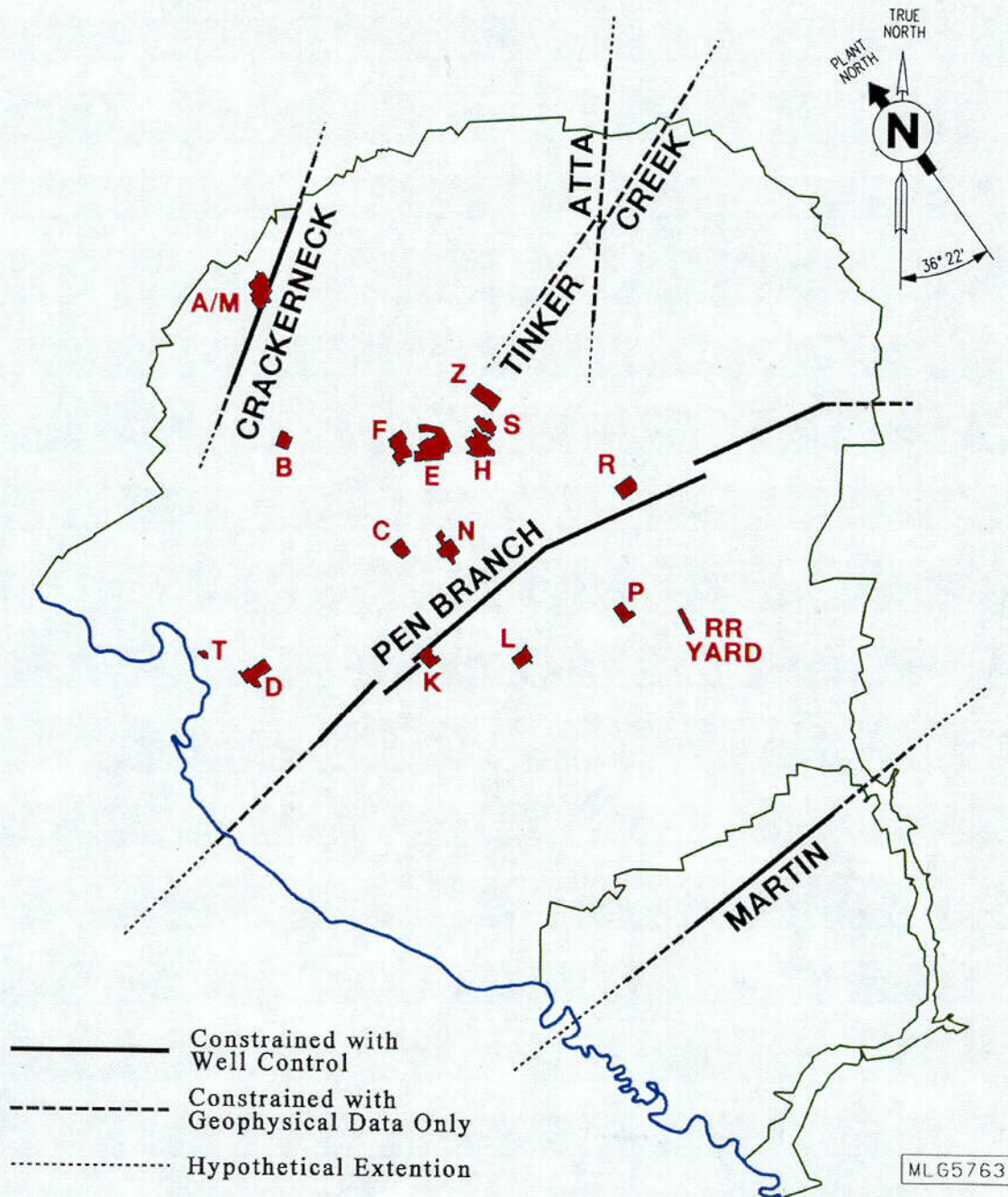


Figure 1.4-53. Seismic line coverage (location of seismic reflection data) for the SRS.



Regional Scale Faults for SRS and Vicinity

Figure 1.4-54. Faults that involve Coastal Plain sediments that are considered regionally significant based on their extent and amounts of offset.

C30

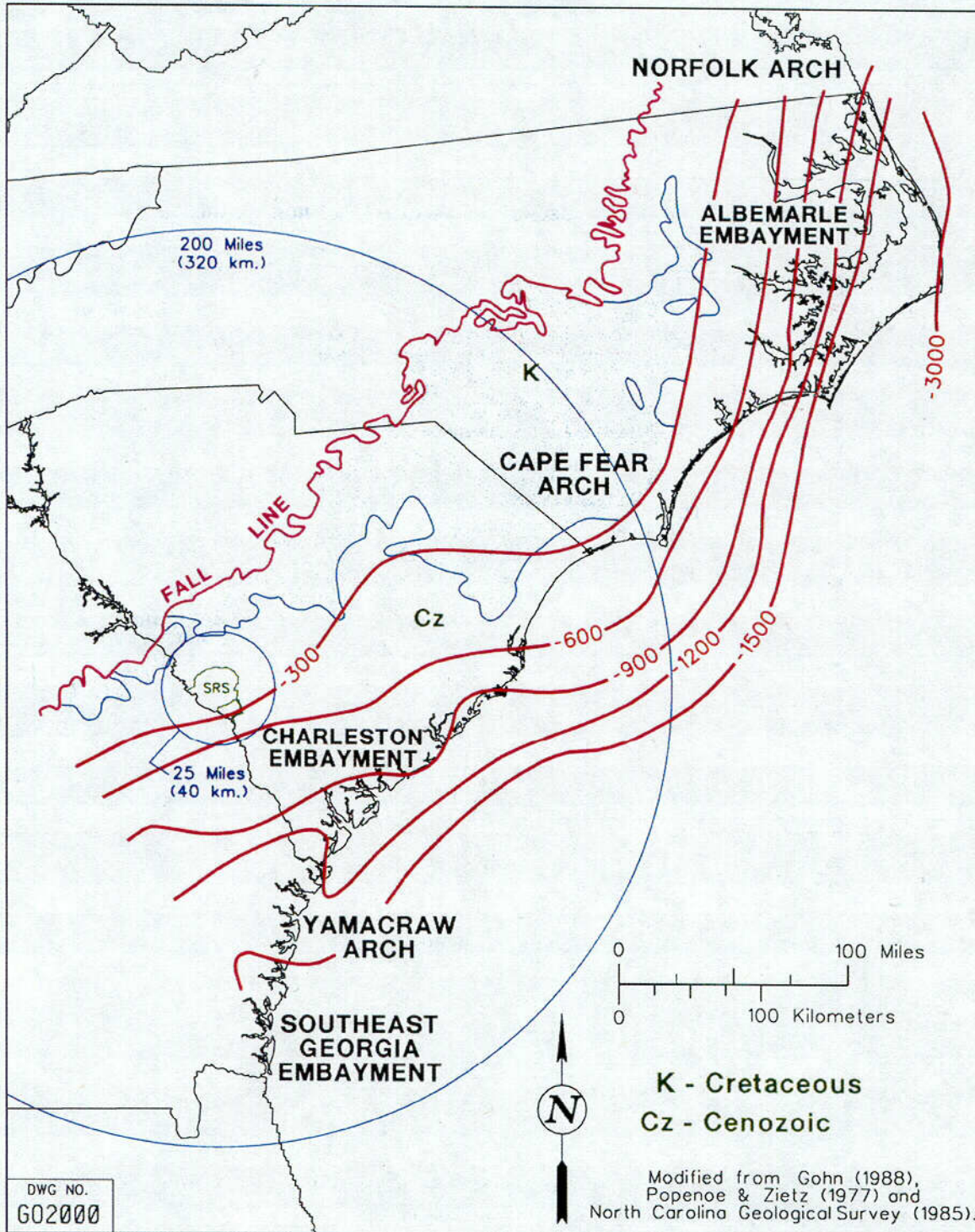


Figure 1.4-55. The Cape Fear arch near the North Carolina-South Carolina border.

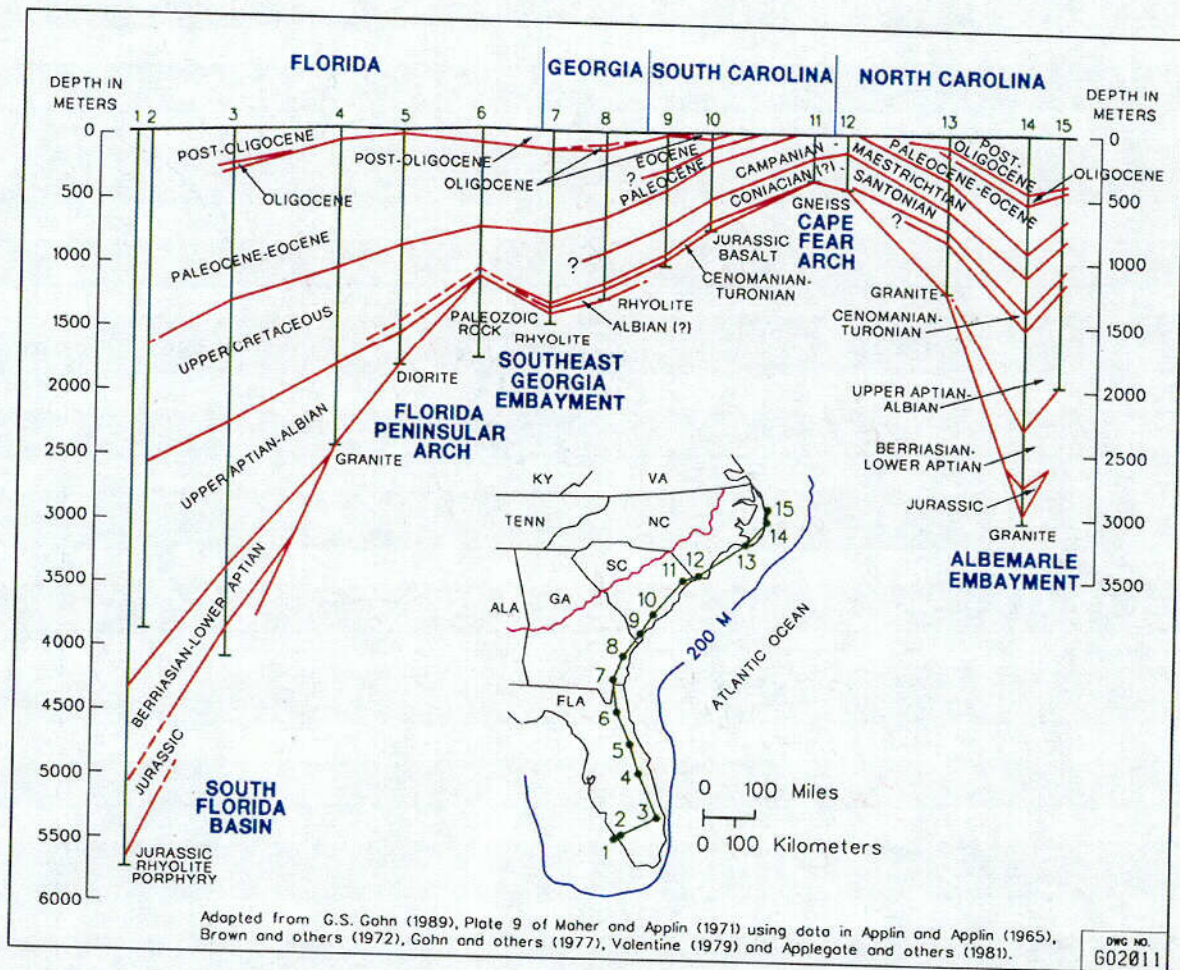


Figure 1.4-56. Other arches in the region include the Norfolk arch near the North Carolina-Virginia border, and the Yamacraw arch near the South Carolina-Georgia border.

C32

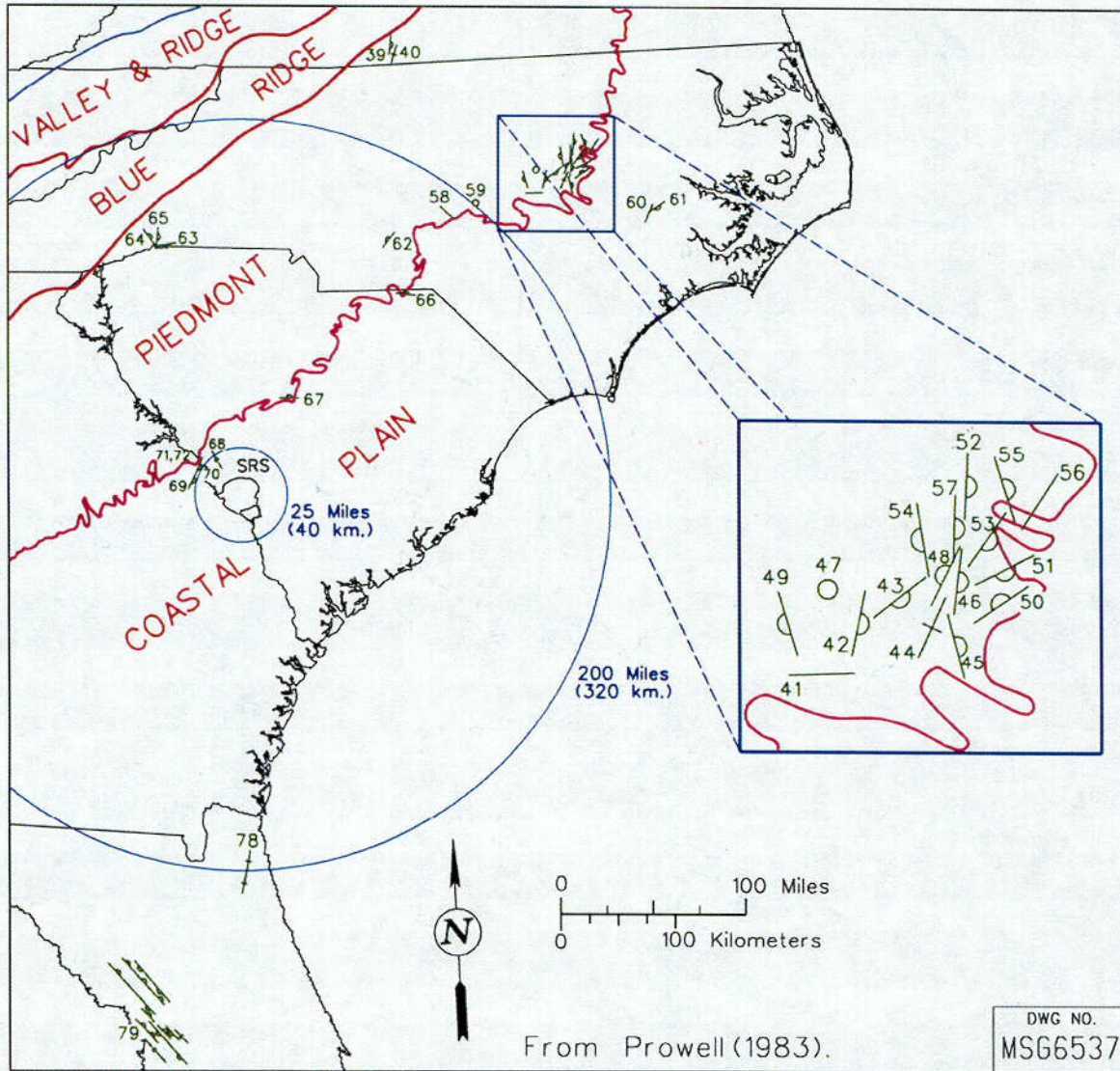


Figure 1.4-57. Previously unrecognized Cretaceous and Cenozoic fault zones found by Prowell, (1983). Of 131 fault localities cited, 26 are within North and South Carolina.

233

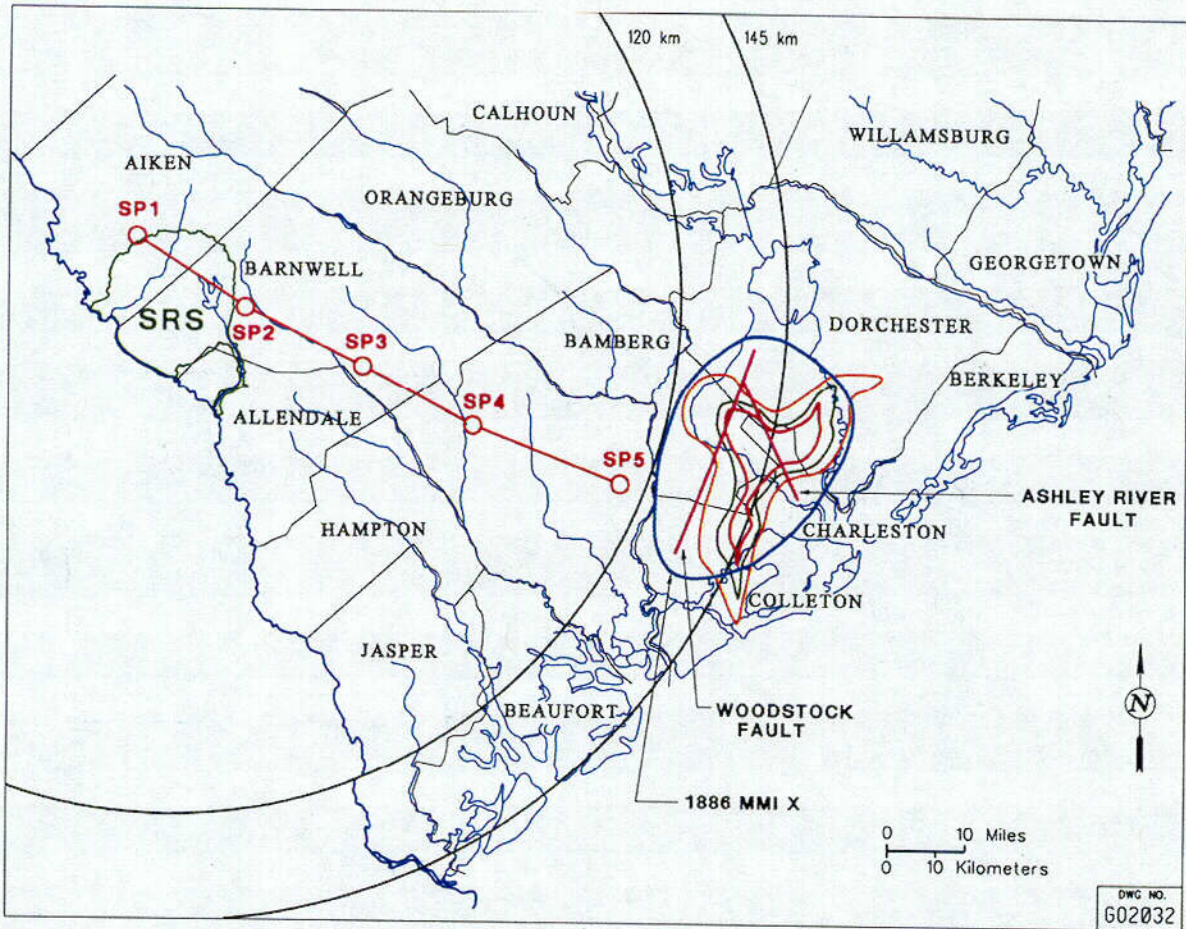


Figure 1.4-58. Ashley River/Woodstock Faults.

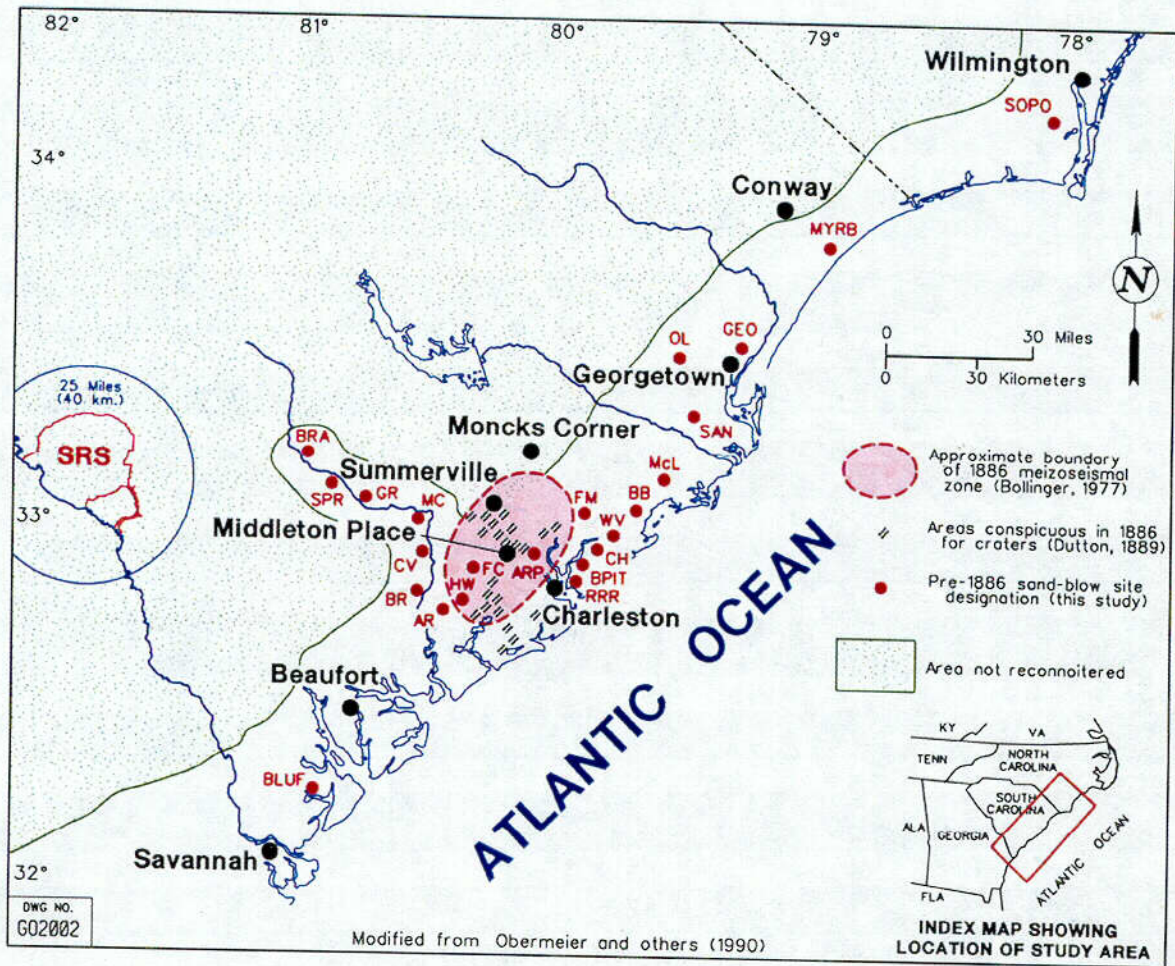


Figure 1.4-59. . Location of sand blows.

C 35

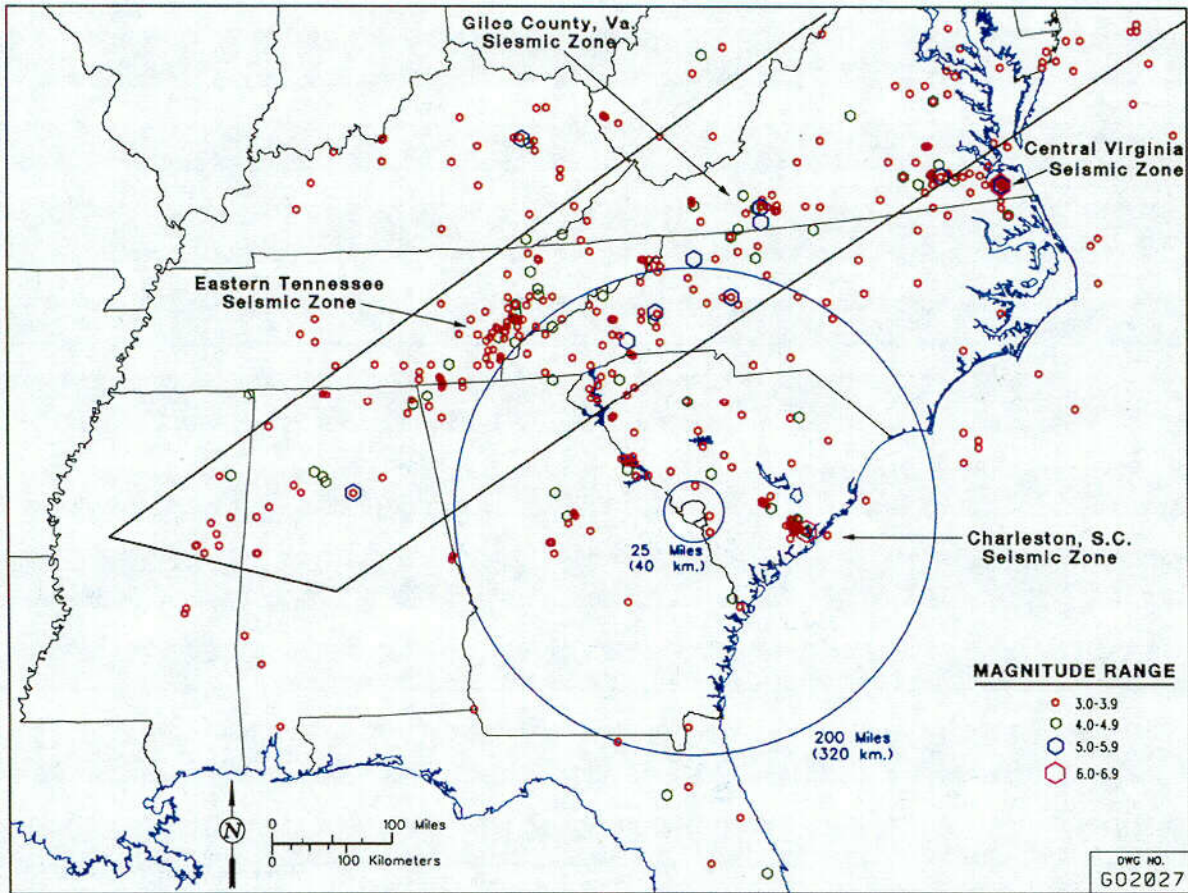


Figure 1.4-60. Location of historical seismic events, 1568 – 1993.

C36

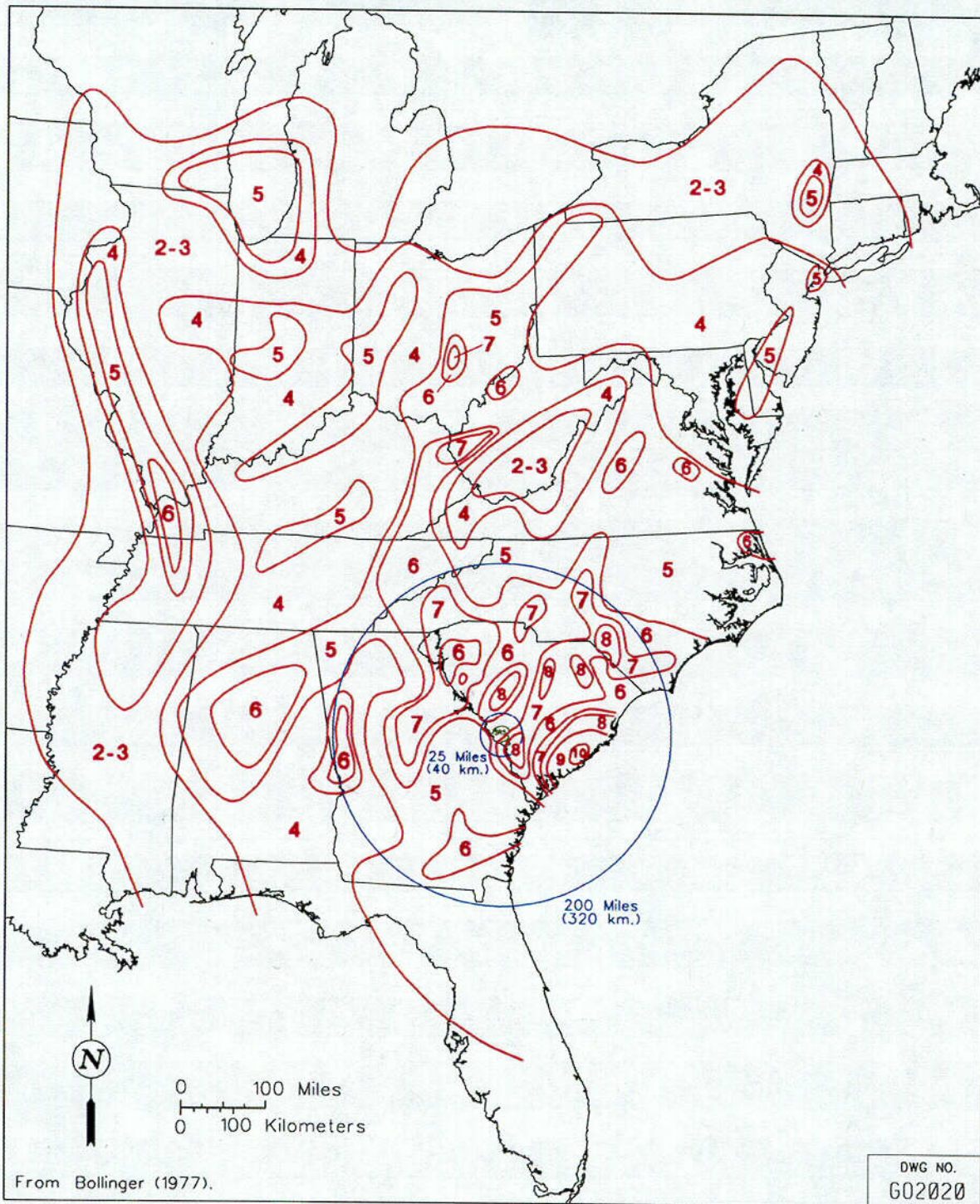


Figure 1.4-61. MMI intensity isoseismals for the Charleston event.

C37

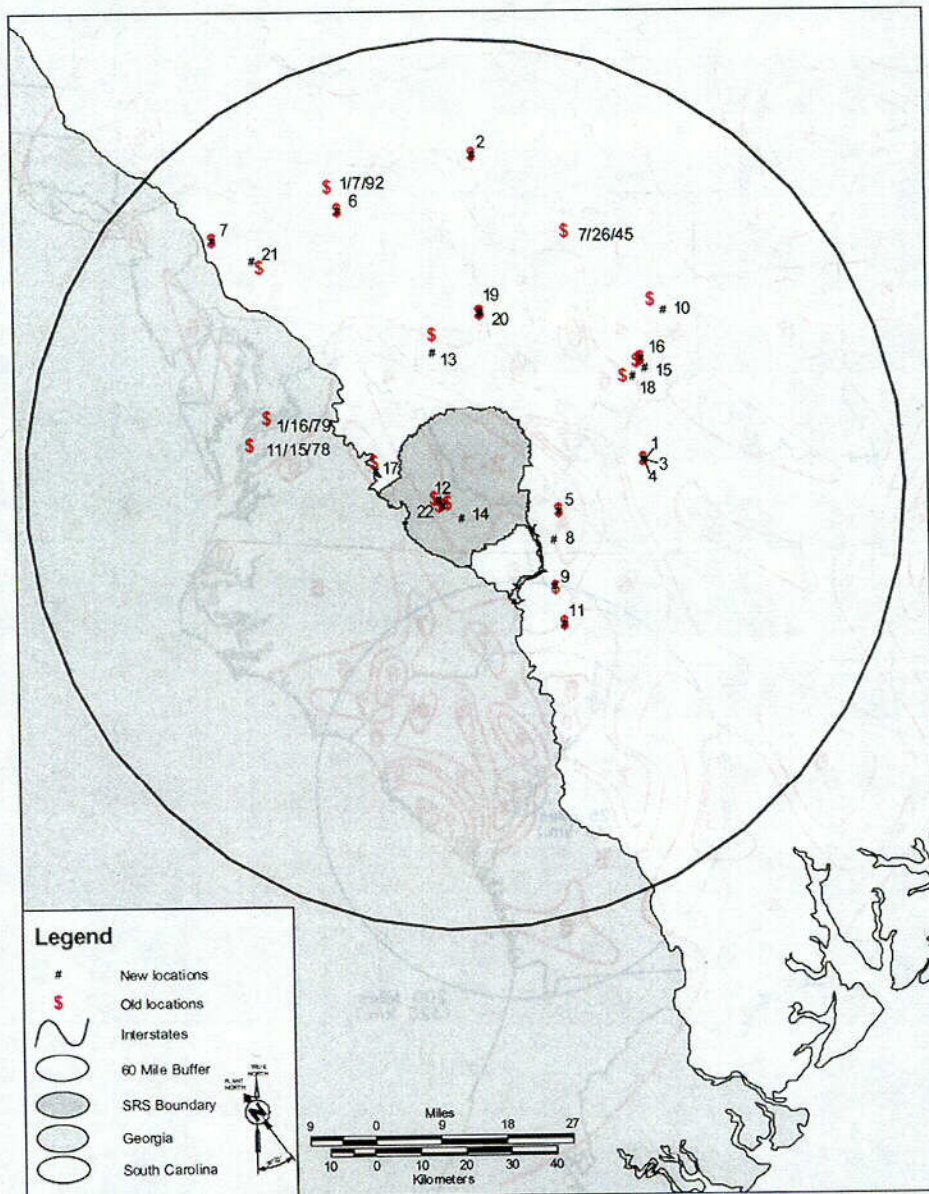


Figure 1.4-62. Historical seismic events. Triangles with date are historically mis-located.

C38

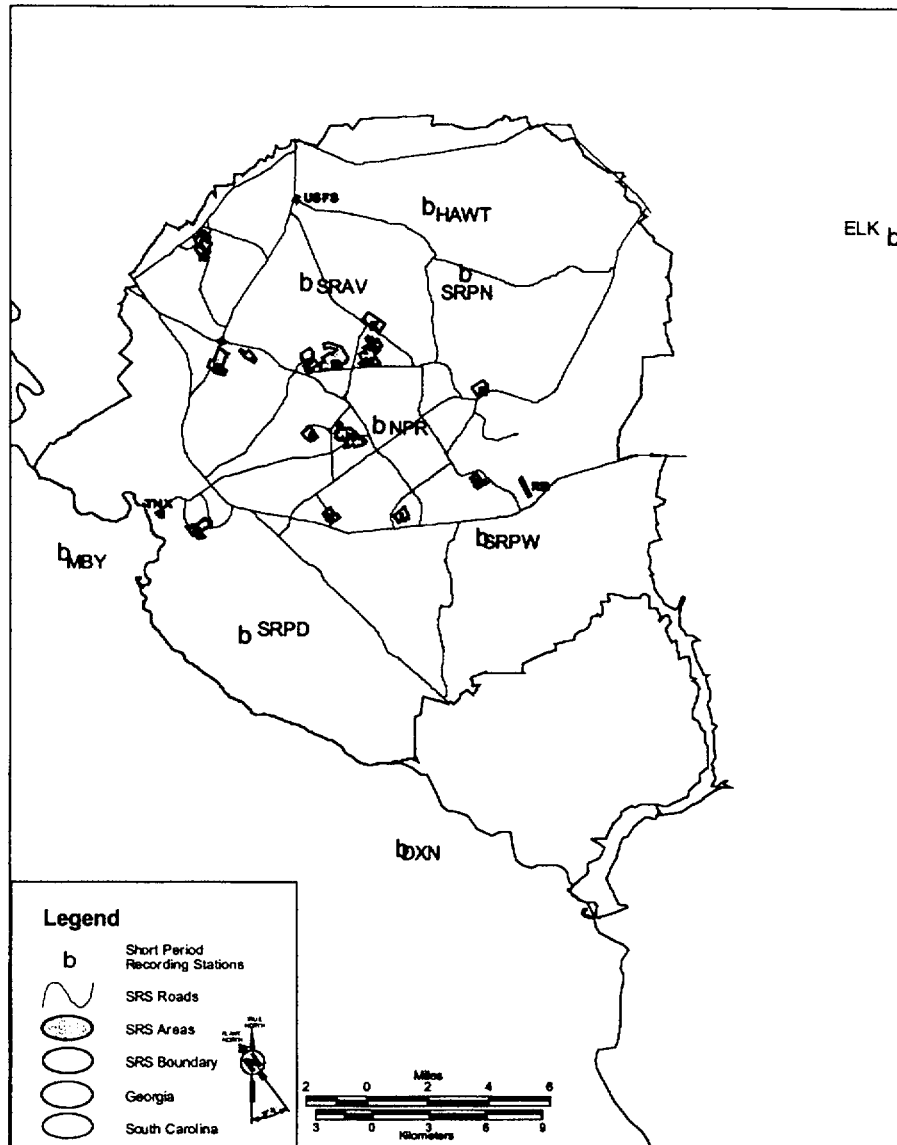


Figure 1.4-63. SRS short period recording stations.

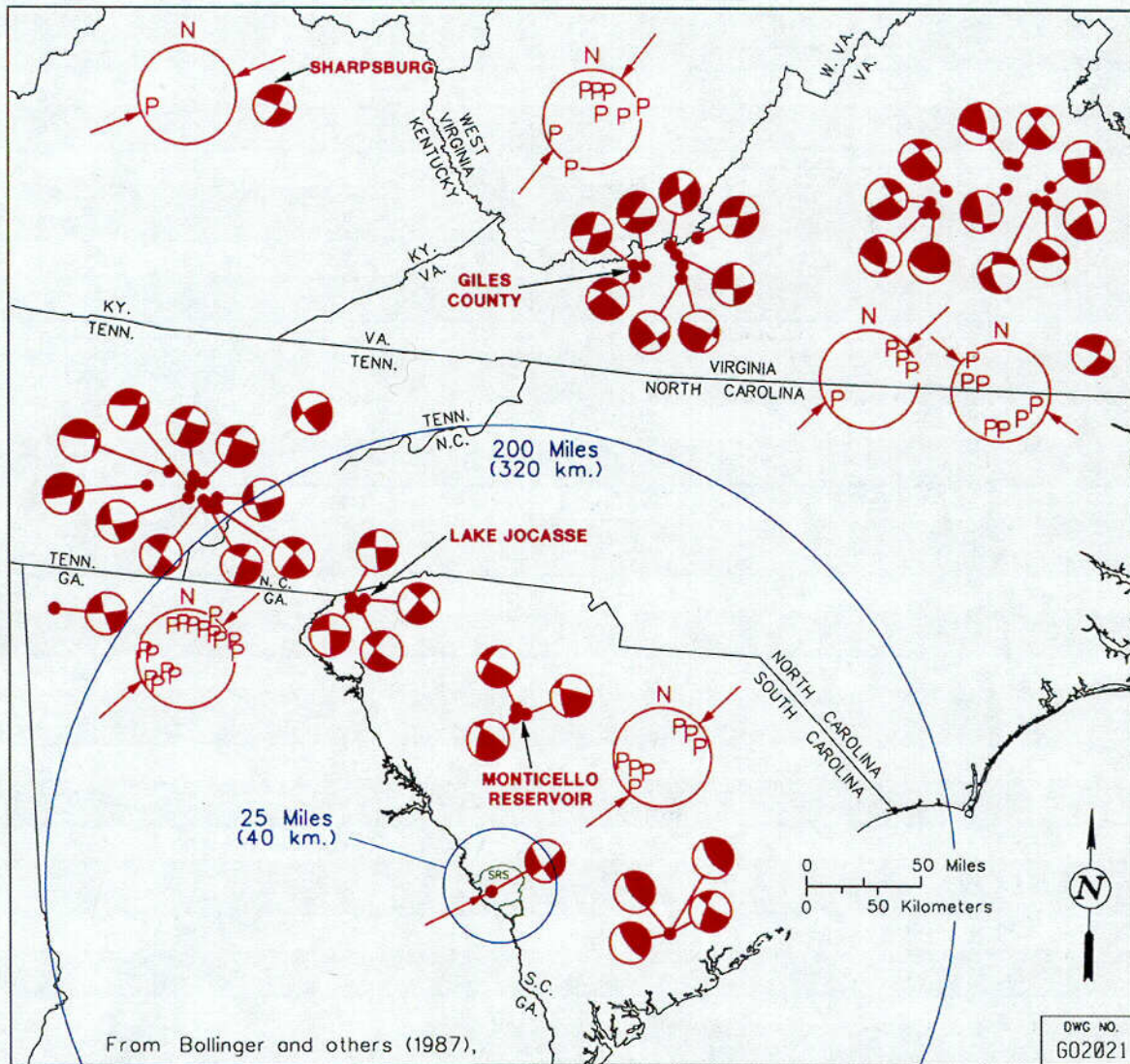


Figure 1.4-64. Summary fault plane solutions for southeastern United States.

C39

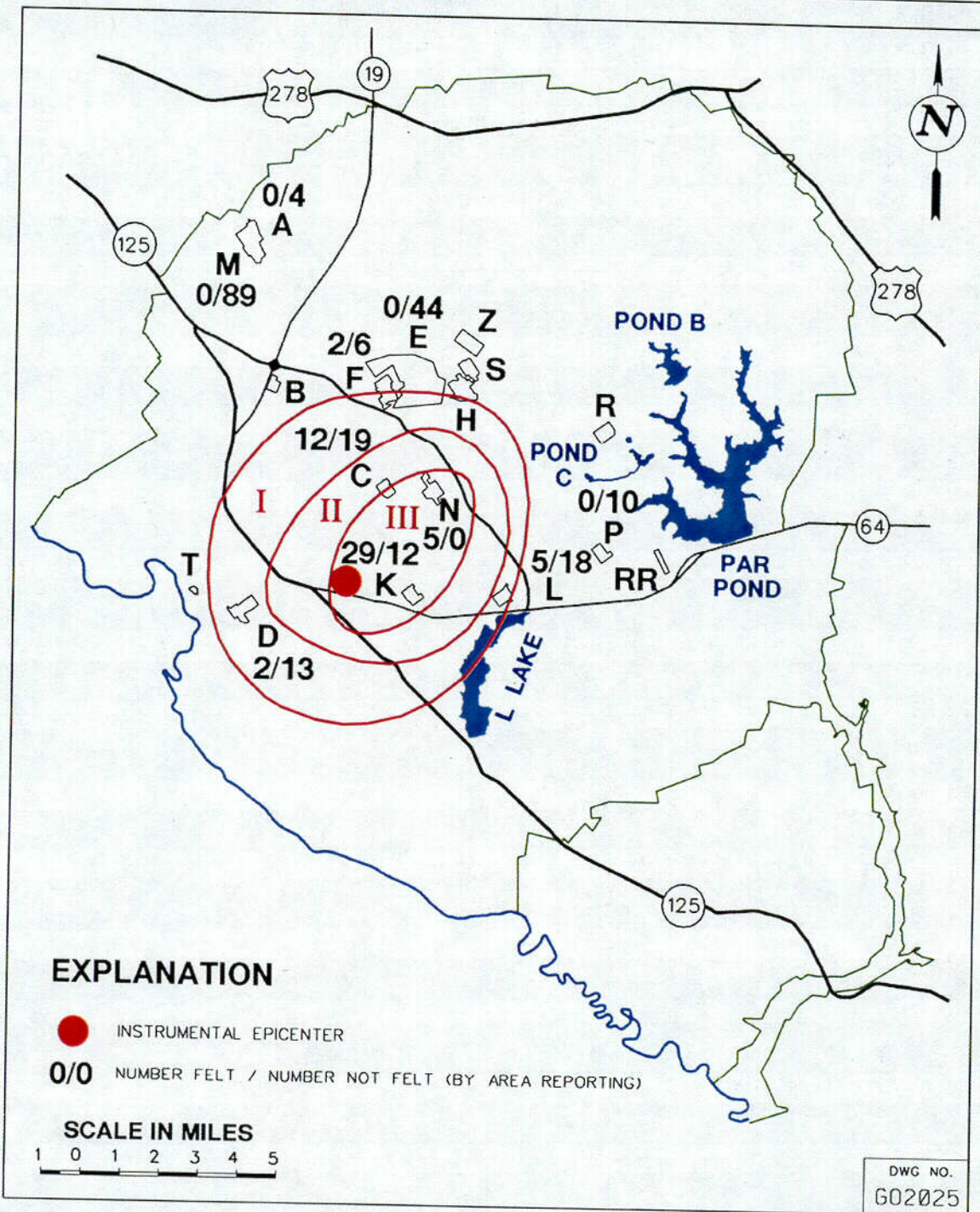


Figure 1.4-65. Isoseismal map for the June, 1985 earthquake.

C 40

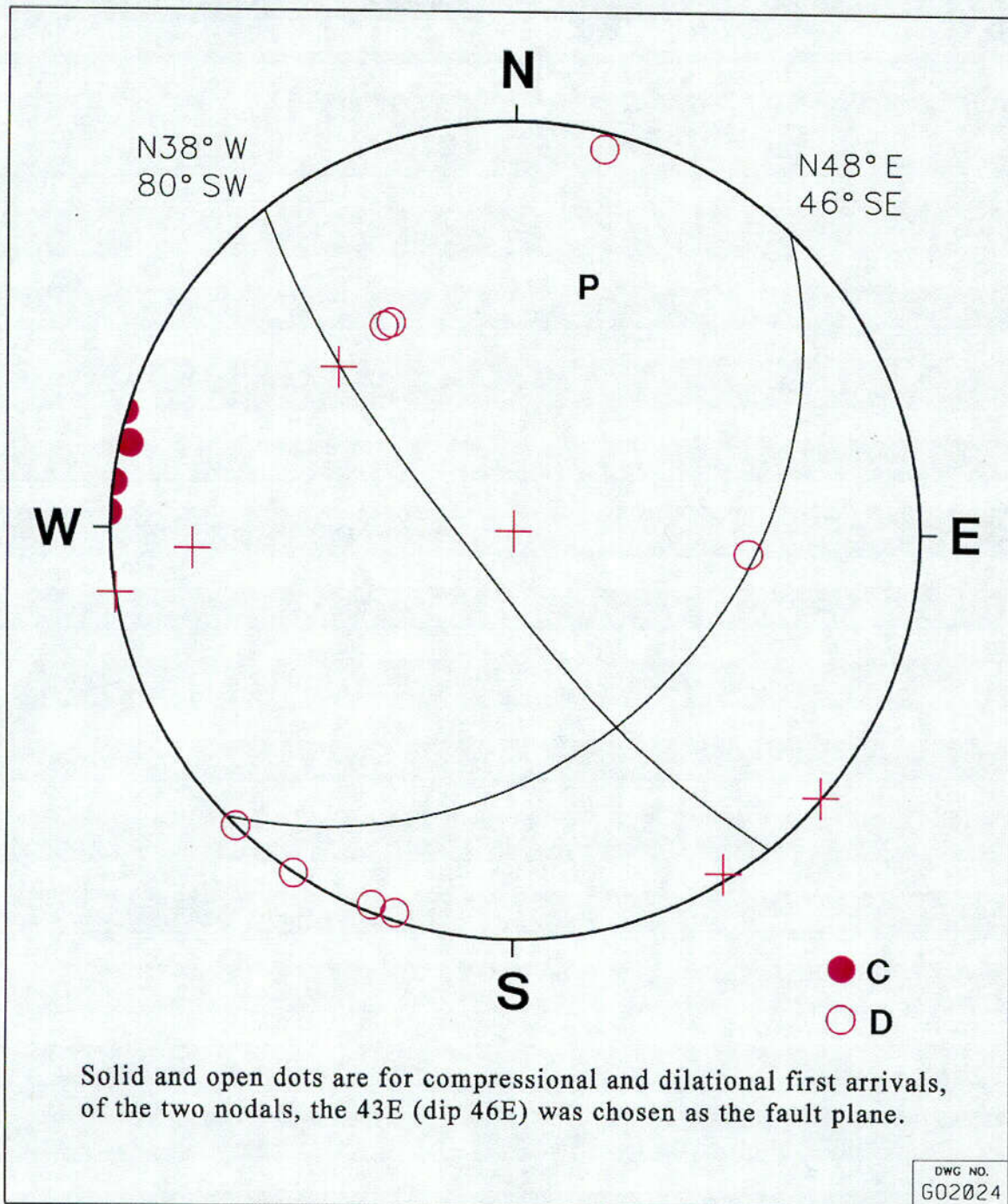


Figure 1.4-66. Fault plane solution for the June, 1985 earthquake..

C41

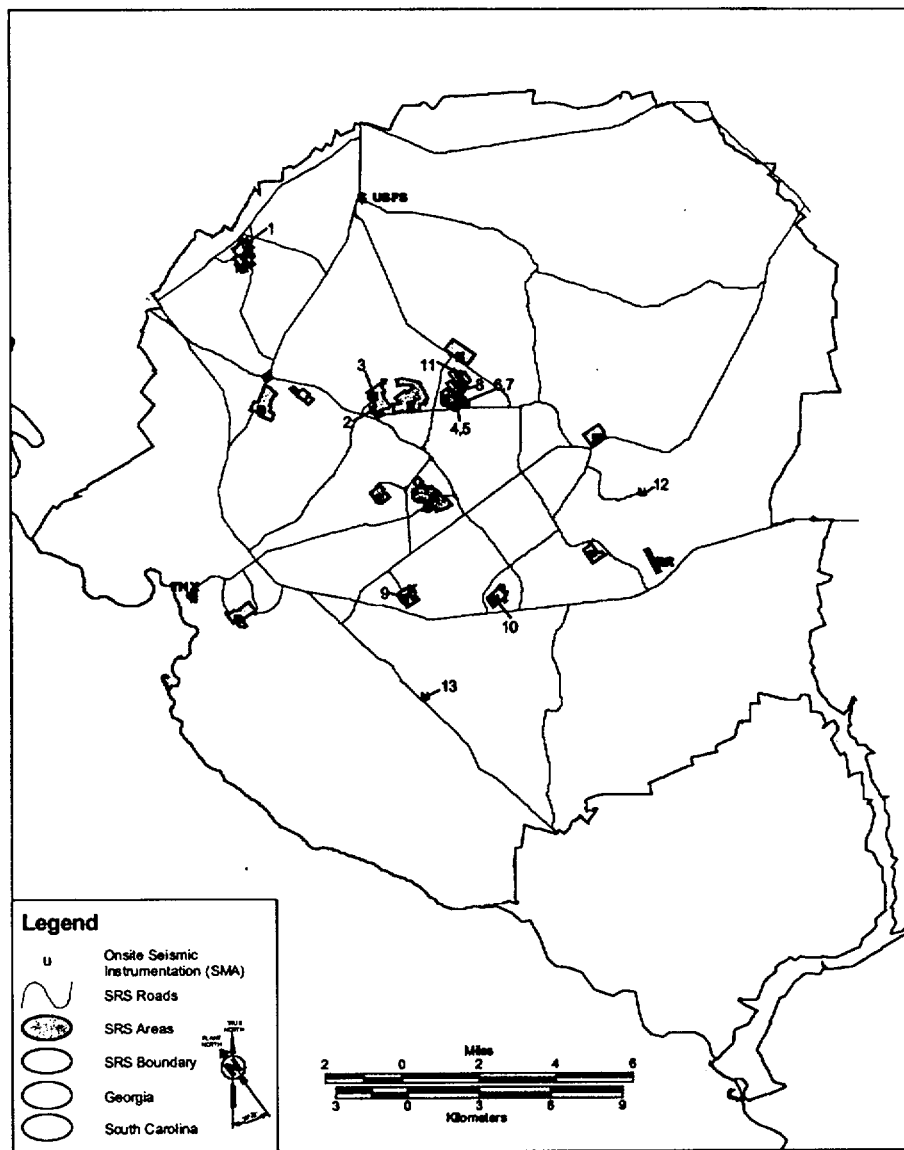


Figure 1.4-67. Location of strong motion accelerographs.

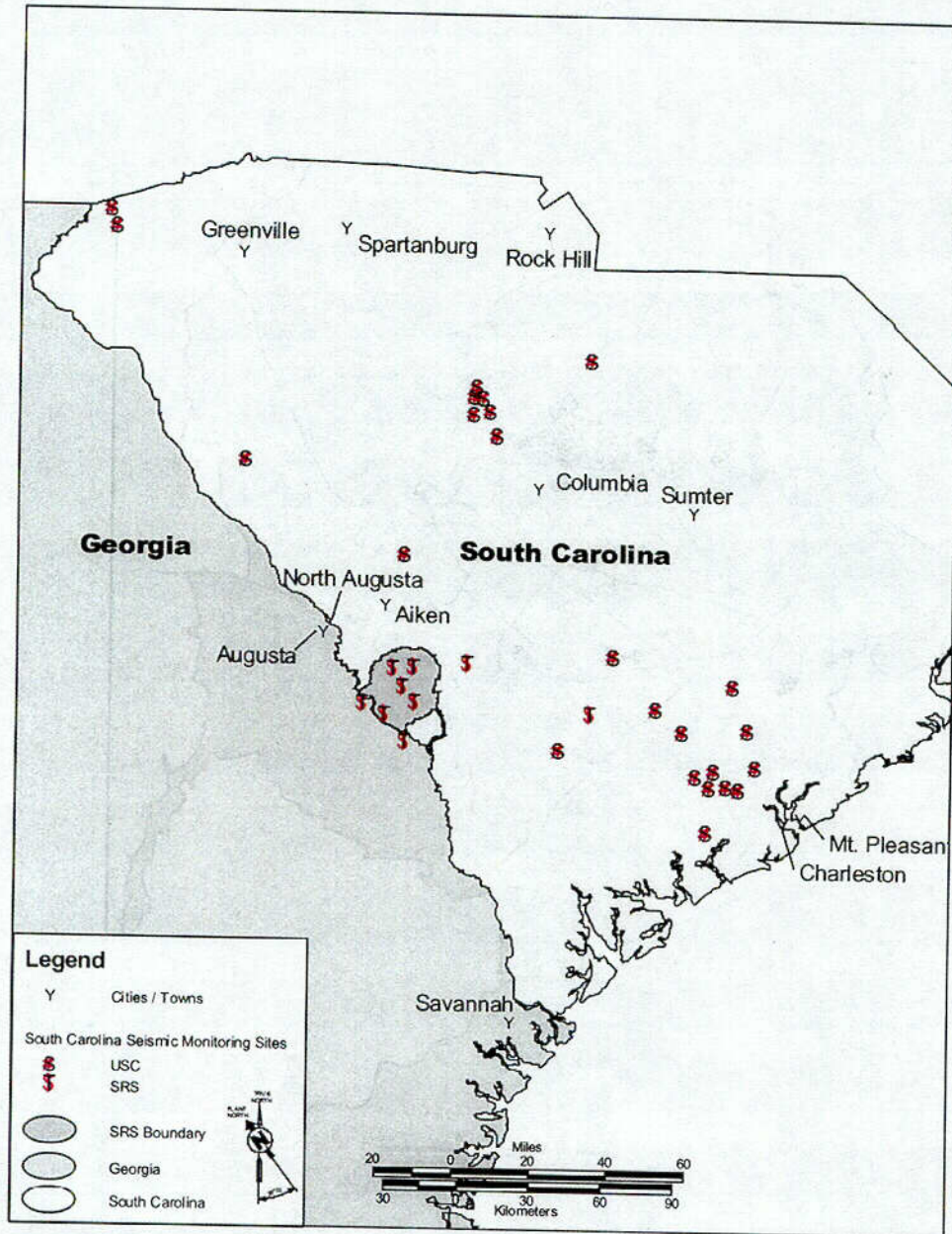


Figure 1.4-68. Seismic network for SRS and the surrounding region.

C42

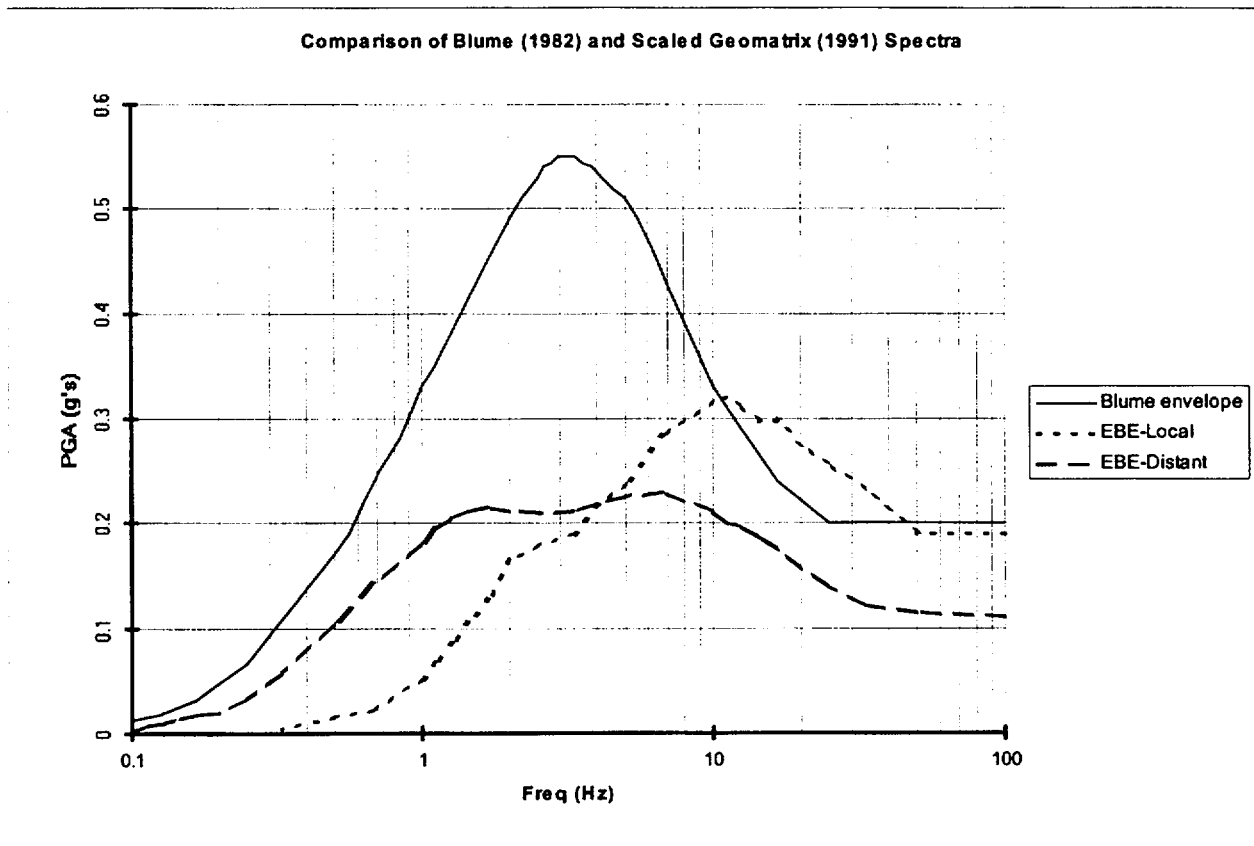


Figure 1.4-69. Response spectrum envelope developed by URS/Blume (1982).

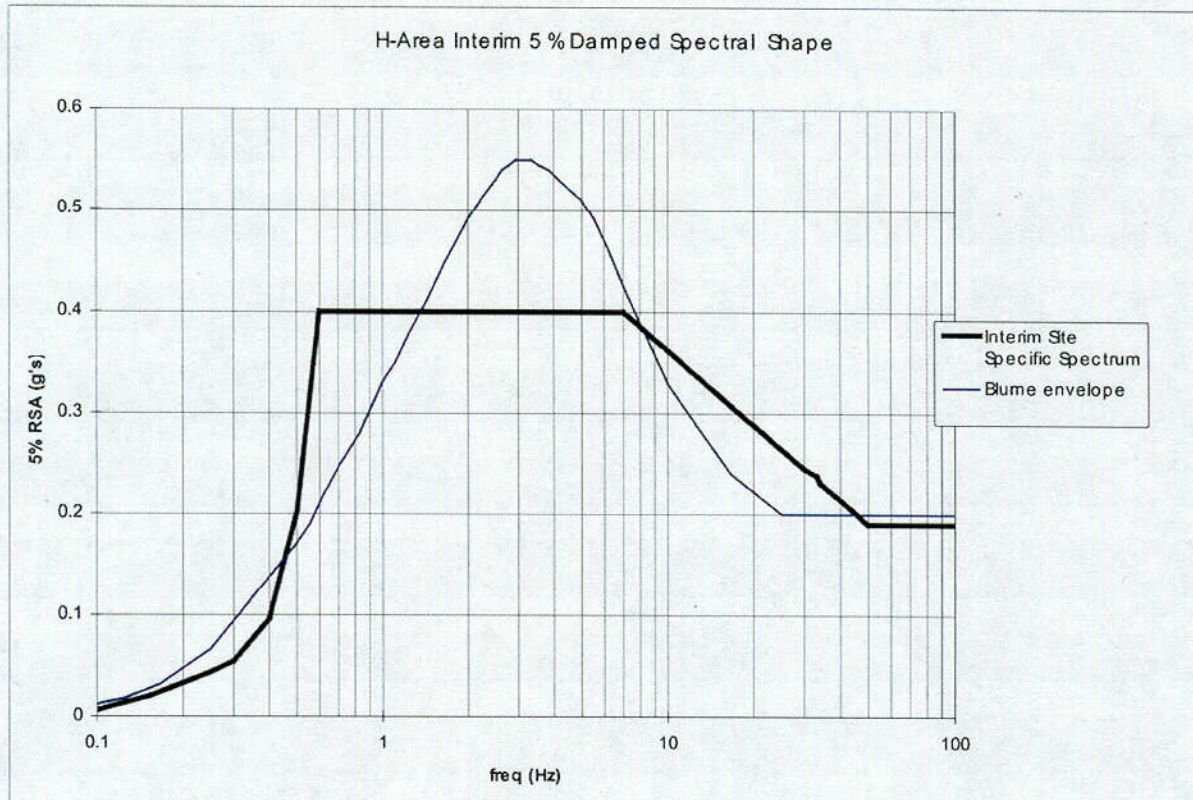


Figure 1.4-70. Interim site spectrum versus Blume envelope.

043

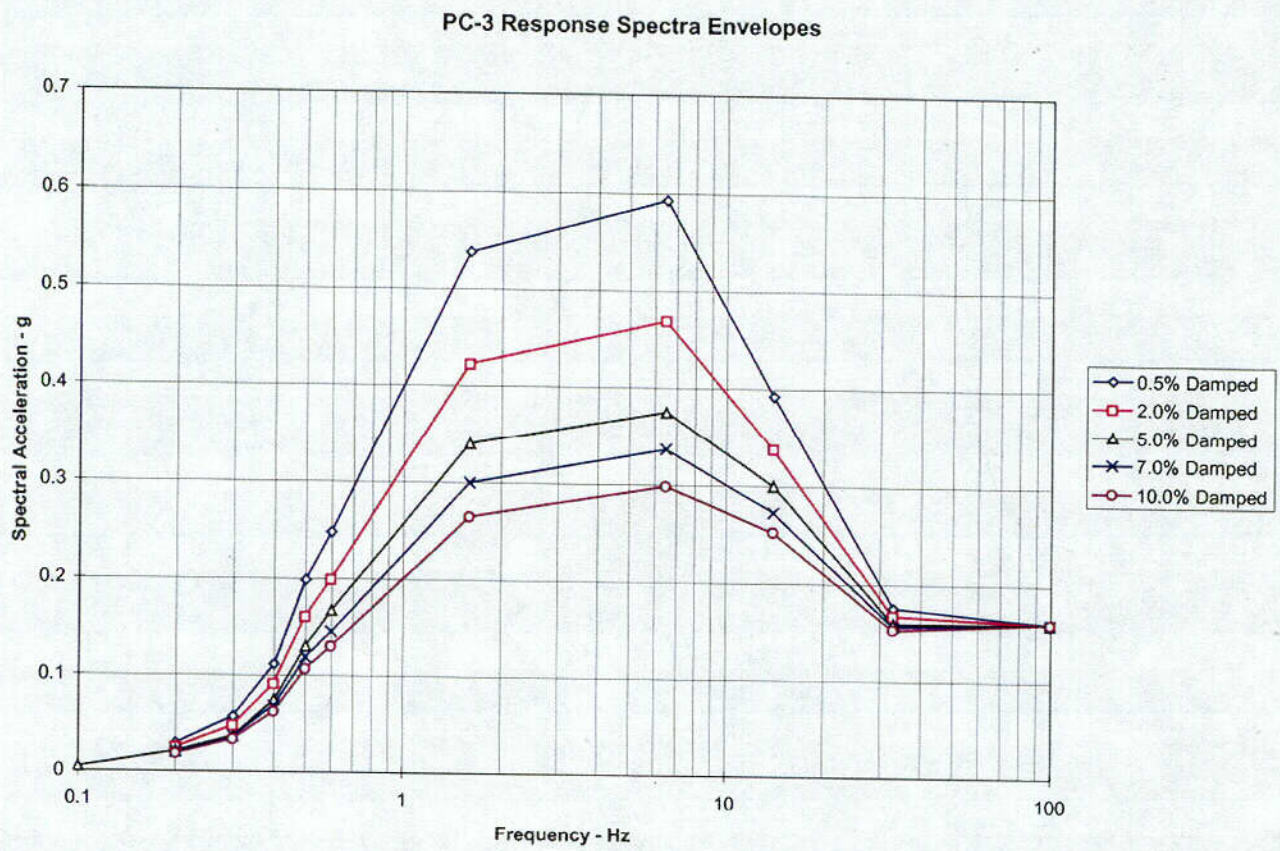


Figure 1.4-71. PC-3 response spectra envelopes.

C44

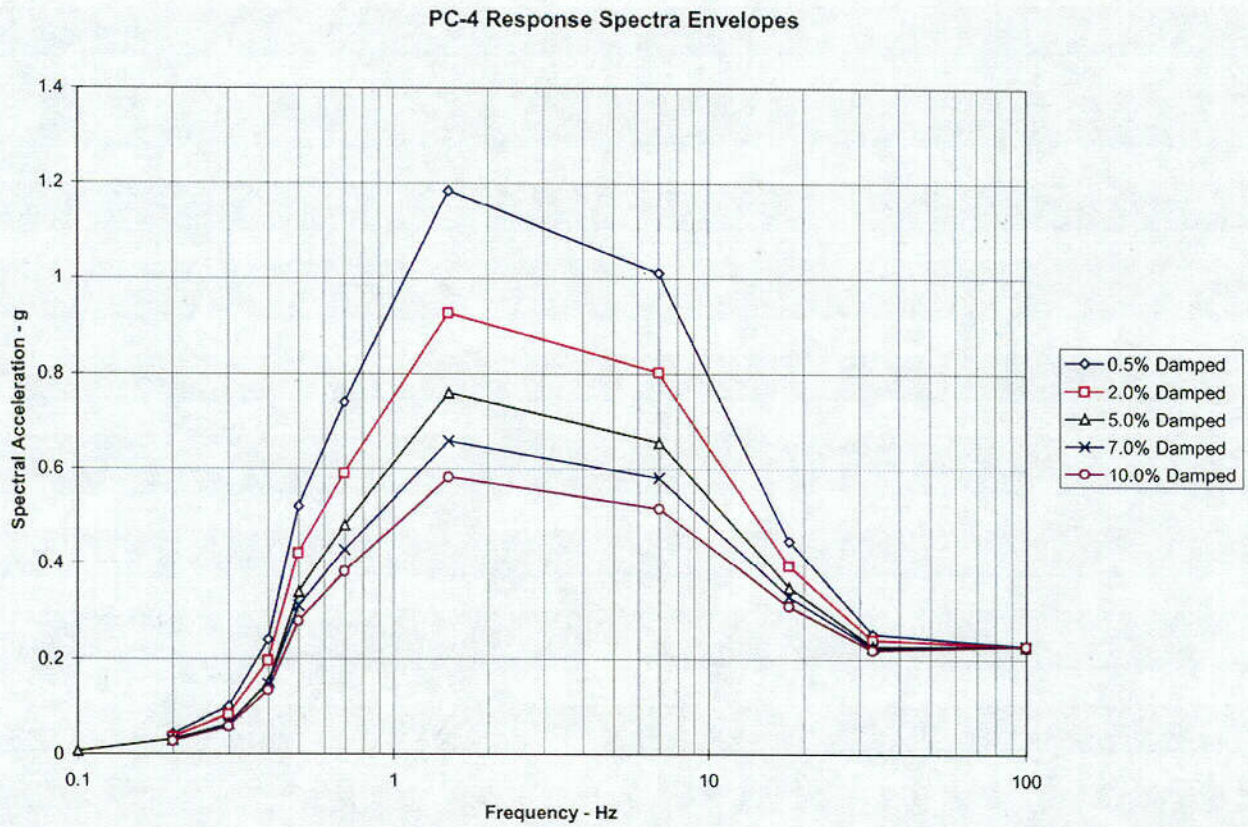


Figure 1.4-72. PC-4 response spectra envelopes.

045

Comparison - PC-3, PC-4, URS/Blume, SRS Interim Spectra (5% damping)

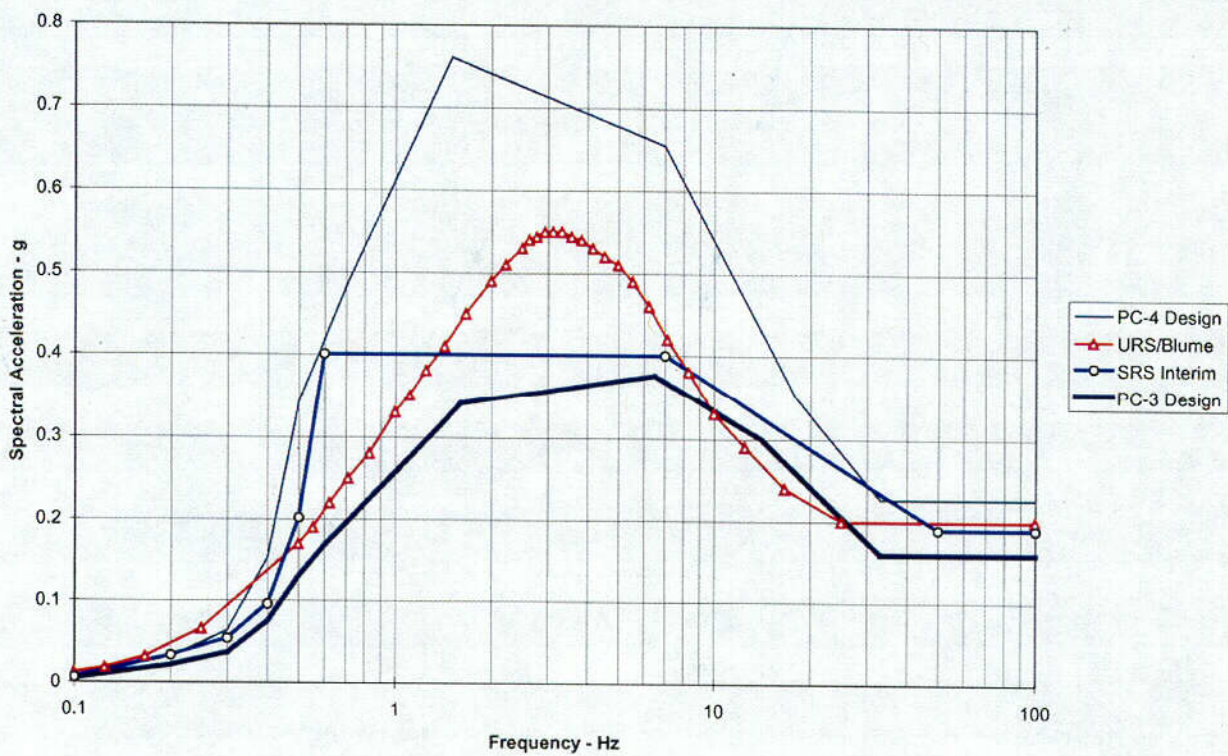


Figure 1.4-73. Comparison – PC-3, PC-4, Blume, SRS Interim spectra (5% damping).

046

Recommended SRS-Specific Soil Surface Hazard (Sv)-Envelope

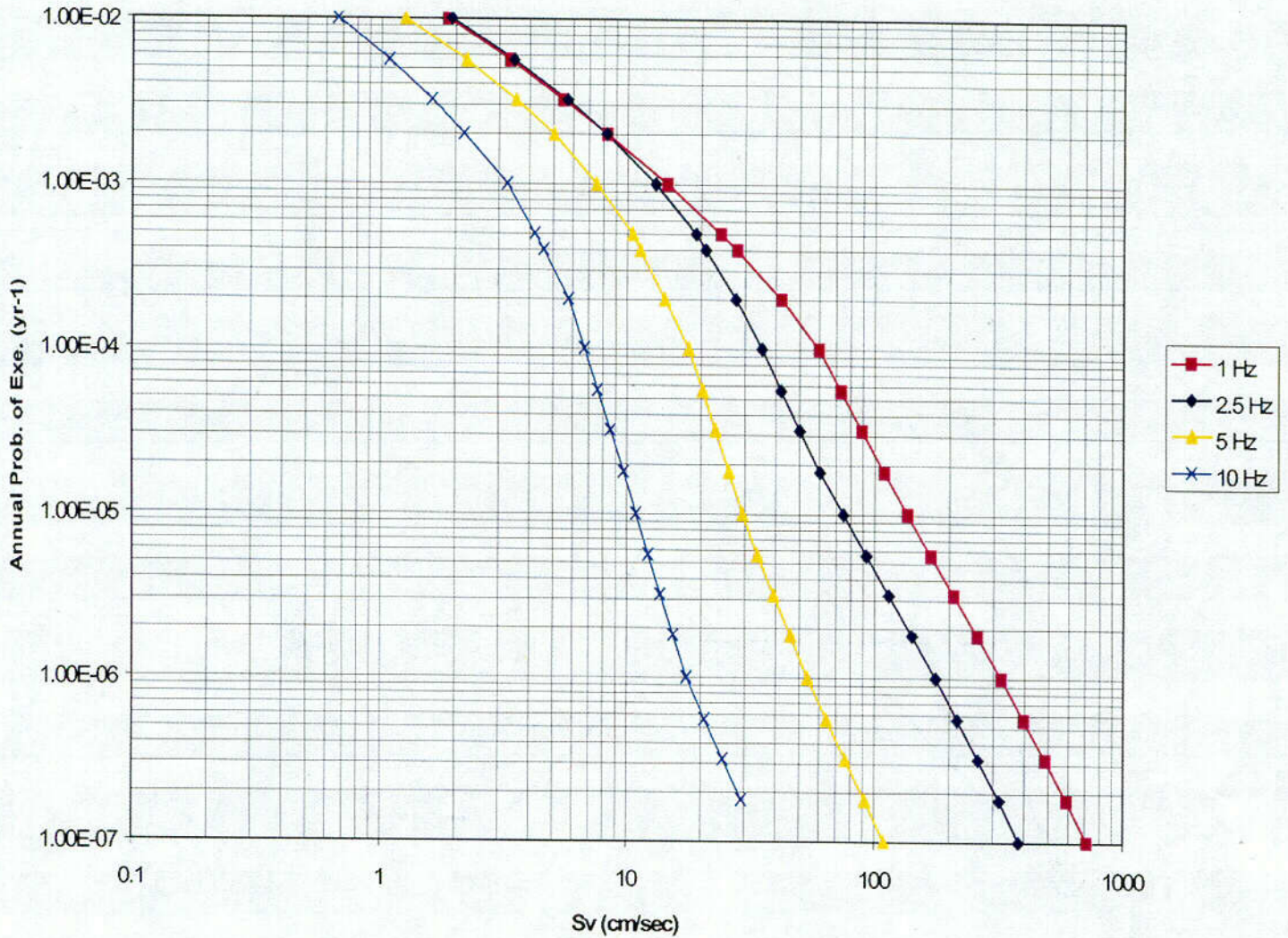


Figure 1.4-73.1. Combined EPRI and LLNL soil surface hazard envelope (probability of exceedence vs. 5% damped spectral velocity) for oscillator frequencies of 1, 2.5, 5, and 10 Hz. fsdf

C47

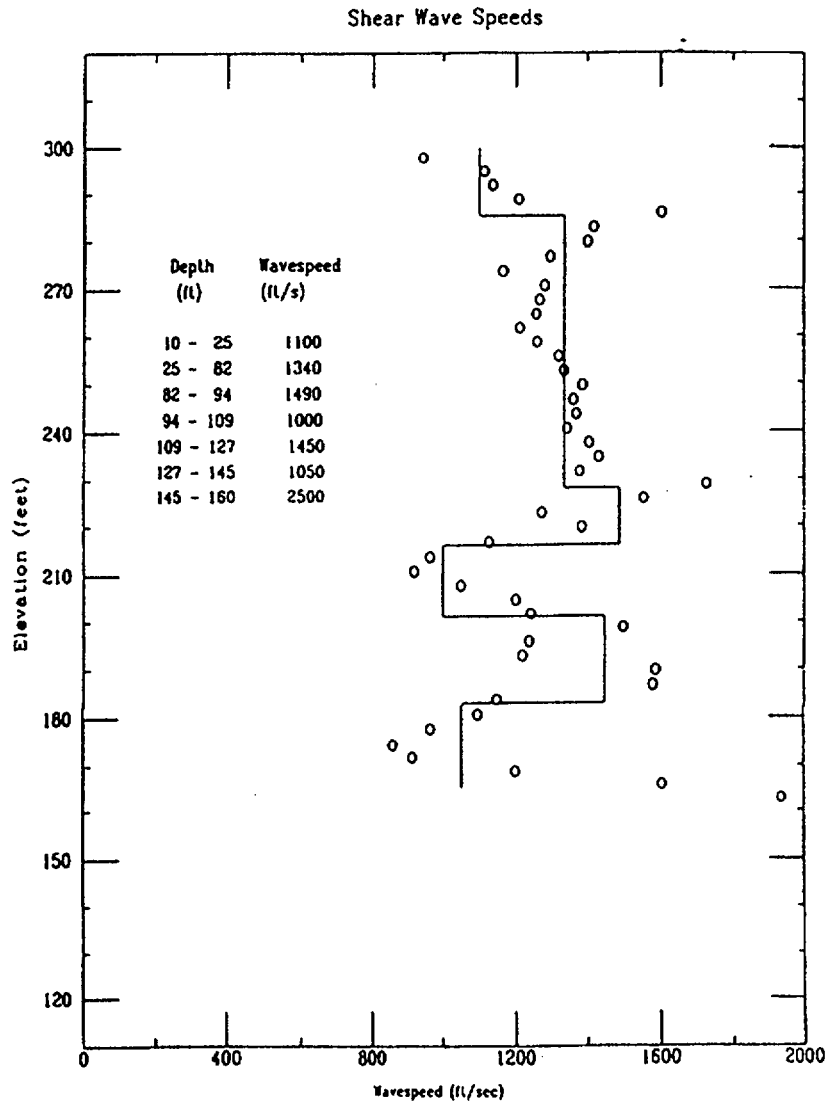


Figure 1.4-74. Example seismic cone penetrometer S-wave interpretation (solid lines). Measurement taken in F-Area.

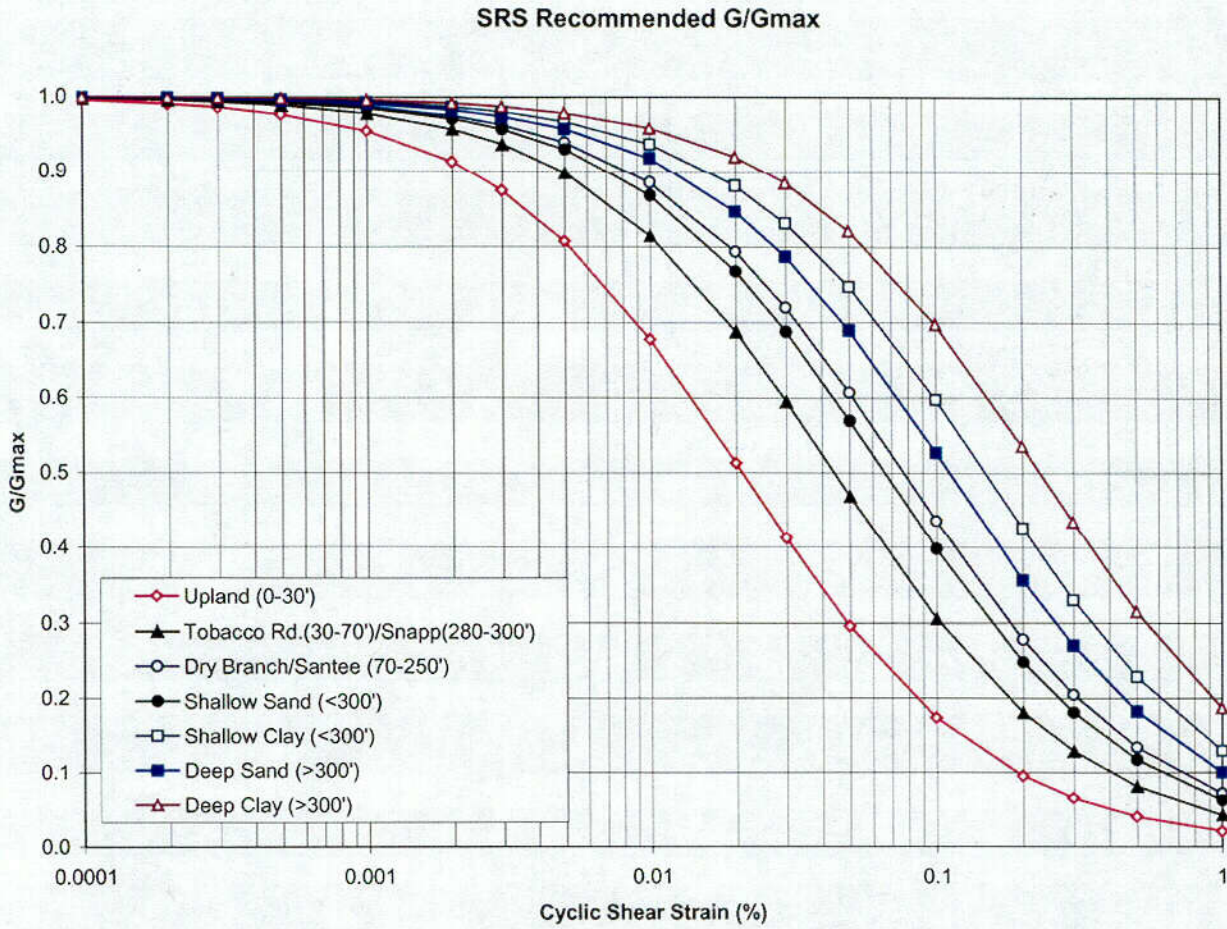


Figure 1.4-75. SRS Recommended G/G_{max} .

C48

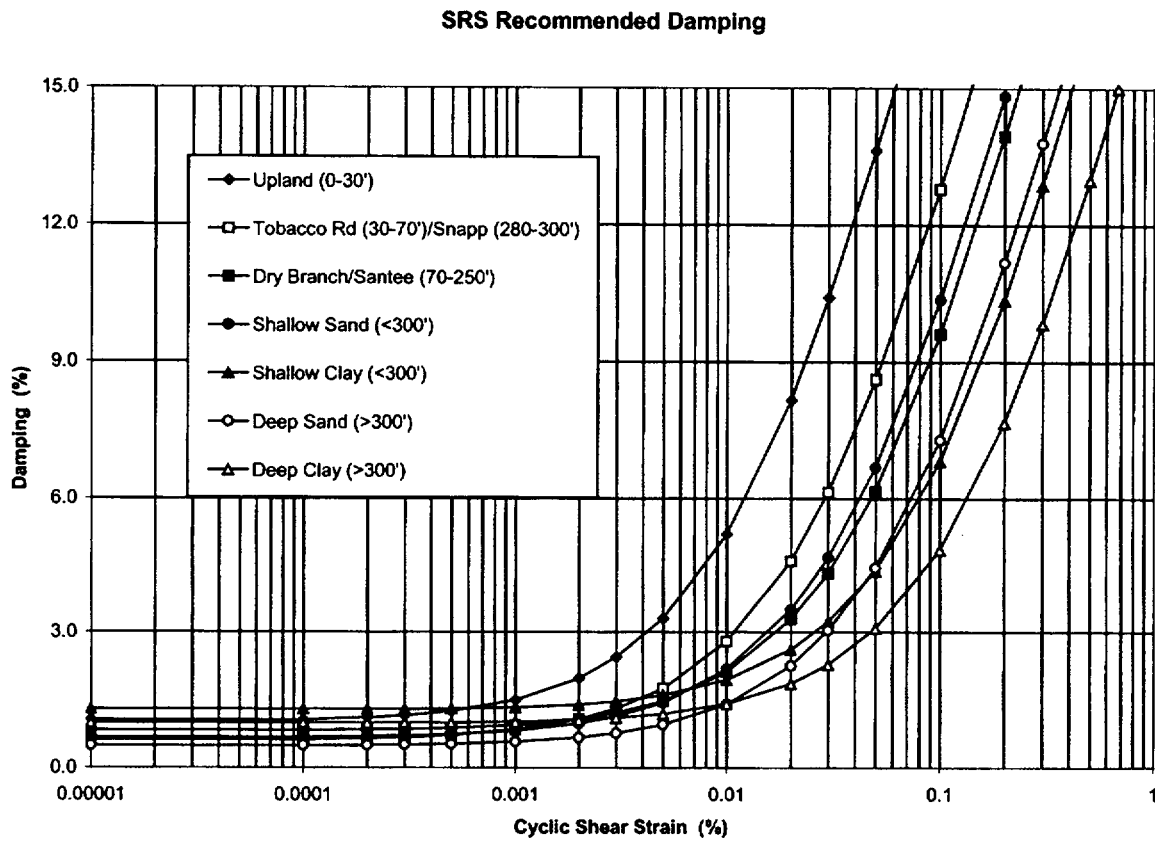


Figure 1.4-76. SRS recommended damping.

Comparison of DOE Revised PC-3 Design Basis Spectrum (Gutierrez, 1999) to PC-3 Design Spectrum (WSRC, 1997)

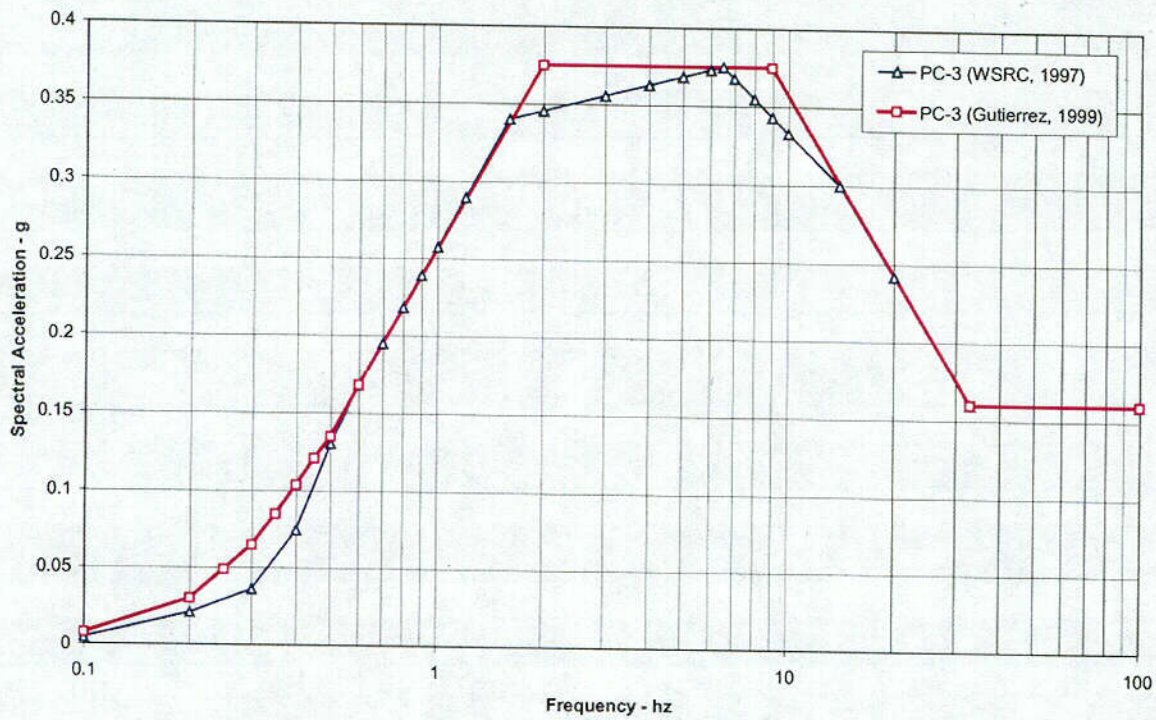


Figure 1.4-77. Revised SRS PC-3 5% damped design response spectrum (Gutierrez, 1999).

249

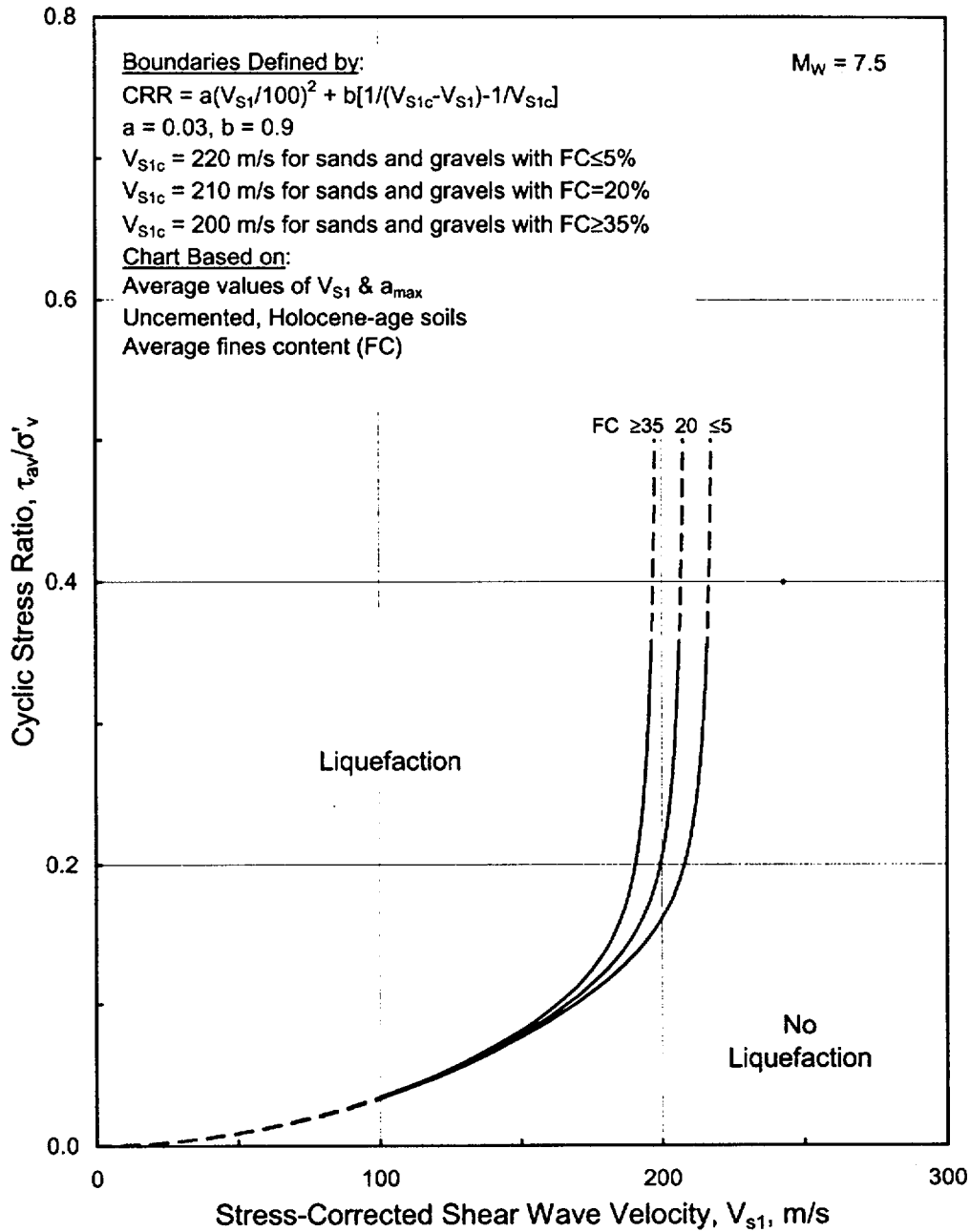


Figure 1.4-78. Recommended Liquefaction Assessment Chart Based on V_{S1} and Cyclic Stress Ratio for Magnitude 7.5 Earthquakes and Uncemented Soils of Holocene Age (NCEER, 1997).

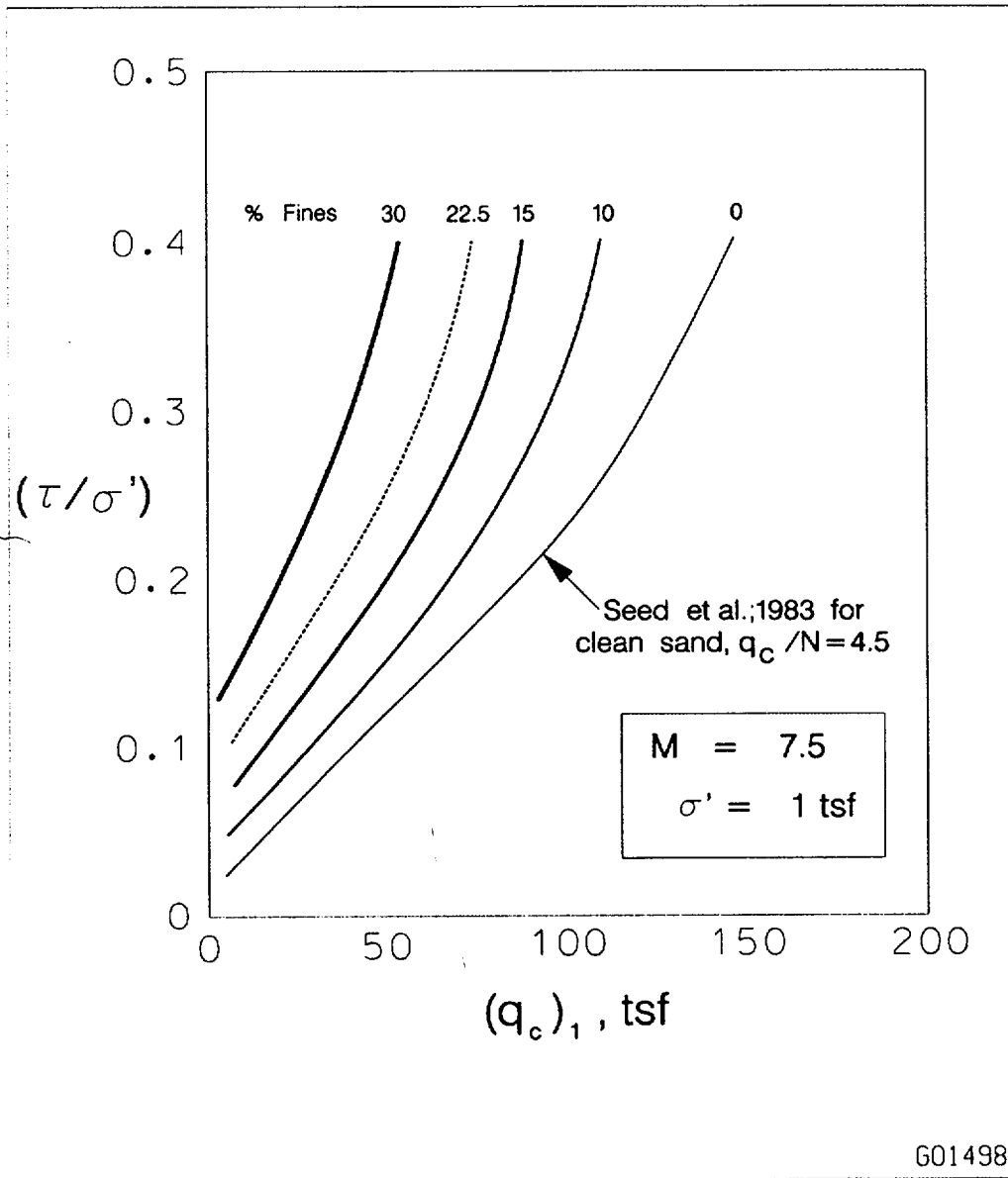


Figure 1.4-79. Correlation Between Normalized CPT Tip Resistance and Cyclic Stress Ratio Required for Initial Liquefaction Due to Magnitude 7.5 Earthquake and SRS Soils (WSRC, 1995).

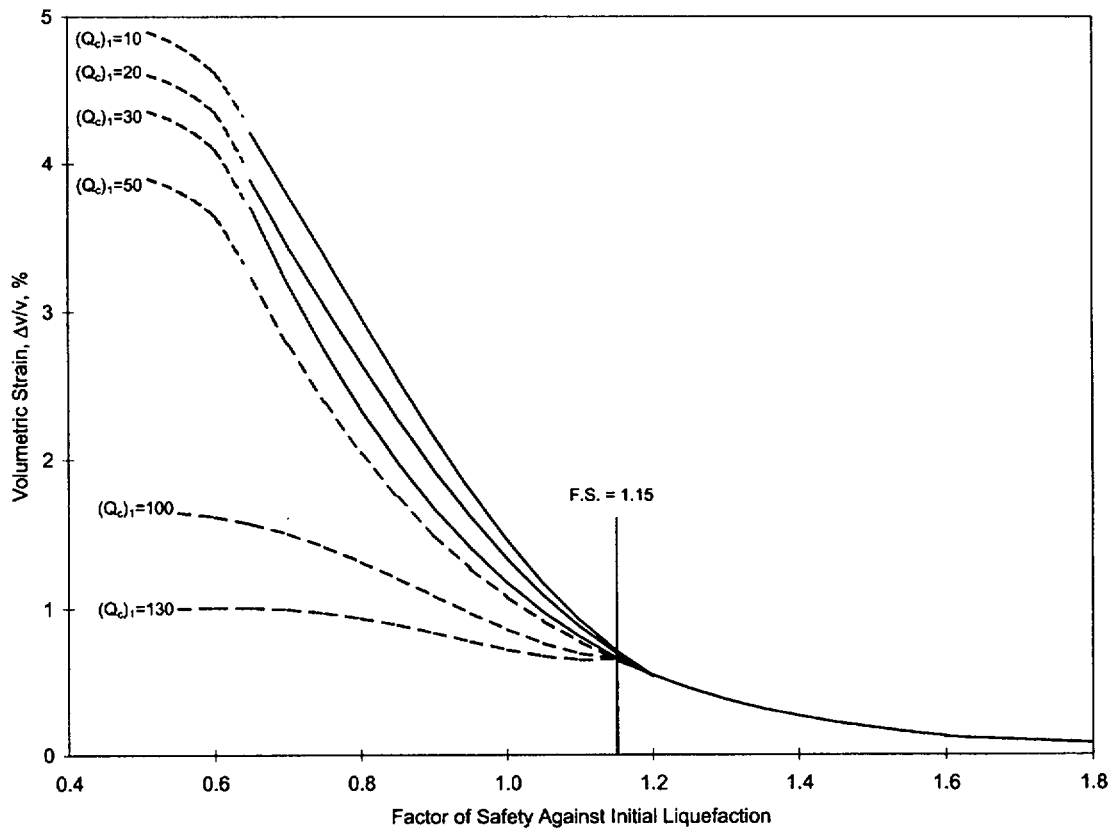


Figure 1.4-80. Volumetric Strain as a Function of Factor of Safety Against Initial Liquefaction for SRS Soils (WSRC, 1995).

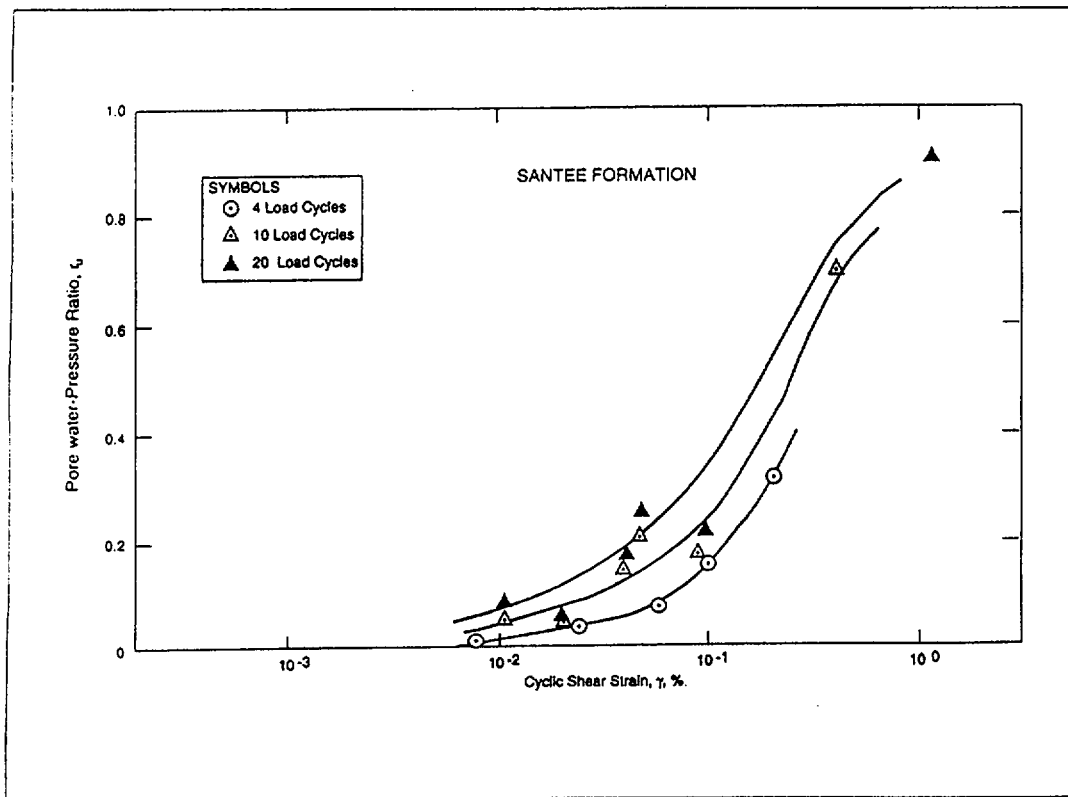


Figure 1.4-81. Pore Pressure Ratio Versus Cyclic Shear Strain for the Santee Formation at the ITP Facility (WSRC, 1995).